Politecnico di Torino

Ingegneria Energetica e Nucleare

A.a. 2023/2024

Sessione di Laurea Novembre 2024

Preceramic polymers for CMC joints: Filler Dispersion Optimization

Relatore: Monica Ferraris

Co-relatore:Aurora Pizzinat

Candidato: Nicolò Tagliafico

Abstract

Ceramic matrix composites are a class of advanced materials with significant potential for various industrial and energy applications. As these sectors push for greater efficiency, leading to higher operational temperatures and, consequently, a need for materials capable of withstanding such extreme conditions. The exceptional properties of CMCs make them ideal for use in such environments where other materials cannot perform reliably. This thesis investigates a strategy for the realization of joints between advanced oxide matrix composites (CMCs) by using a commercial vinyl functionalized polysilazane, Durazane 1800, categorized as a precursor for polymer-derived ceramics (PDCs). The CMCs involved in the study were supplied by the University of Bayreuth, Germany, and consisted in Nextel 610 alumina fibers within an alumina-zirconia matrix. Introducing fillers into the resin is crucial to enhance the strength of the final joint. The goal of this thesis is to create reliable, high-temperature-resistant joints by optimizing the filler dispersion and quantity in the preceramic polymer. The microstructural characterization of the joints, carried out by scanning electron microscopy (SEM), allows the evaluation of the adhesion between the components and the cohesion of the joint material. Two of the fillers' percentages (70wt.% and 80wt.%) showed the best results in term of morphology and mechanical strength of joints. Mechanical tests in a single lap offset configuration were conducted to determine the strength of these joints. A maximum lap-shear strength of about 5 MPa at room temperature was achieved in the 70wt.% filler doped joined samples.

Sintesi

I compositi a matrice ceramica (CMC) sono una classe di materiali avanzati con un significativo potenziale per diverse applicazioni industriali ed energetiche. Poiché questi settori mirano a una maggiore efficienza, ciò comporta l'adozione di temperature operative più elevate, con conseguente necessità di materiali in grado di sopportare tali condizioni estreme. Le proprietà eccezionali dei CMC li rendono ideali per l'uso in ambienti dove altri materiali non possono garantire prestazioni affidabili. Questa tesi esplora una strategia per la realizzazione di giunzioni tra compositi a matrice ossidica (CMC) utilizzando un polisilazano commerciale funzionalizzato con gruppo vinilico, Durazane 1800, classificato come precursore per ceramiche derivate da polimeri (PDC). I CMC utilizzati nello studio sono stati forniti dall'Università di Bayreuth, in Germania, e sono composti da fibre di allumina Nextel 610 in una matrice di allumina-zirconia. L'introduzione di riempitivi nella resina è fondamentale per migliorare la resistenza della giunzione finale. L'obiettivo di questa tesi è quello di creare giunti affidabili e resistenti ad alte temperature ottimizzando la dispersione e la quantità di riempitivi nel polimero pre-ceramico. La caratterizzazione microstrutturale dei giunti, realizzata tramite microscopia elettronica a scansione (SEM), permette di valutare l'adesione tra i componenti e la coesione del materiale del giunto. Due percentuali di riempitivo (70wt.% e 80wt.%) hanno mostrato i migliori risultati in termini di morfologia e resistenza meccanica dei giunti. Sono stati condotti test meccanici in configurazione single lap offset per determinare la resistenza di questi giunti. È stata ottenuta una resistenza massima al taglio di circa 5 MPa a temperatura ambiente nei campioni giuntati con riempitivo al 70wt.%.

Table of contents

Table of acronyms

Acronym	Full form
CMC	Ceramic Matrix Composites
PDC	Polymer Derived Ceramics
SEM	Scanning Electron Microscope
GHG	Greenhouse Gases
EIIS	Energy Intensive Industries
SiC	Silicon Carbide
Ox	Oxide
CTE	Coefficient of Thermal Expansion
Al_2O_3	Aluminum Oxide
Y_2O_3	Yttrium Oxide
CaO	Calcium Oxide
MgO	Magnesium Oxide
ZrO_2	Zirconium Oxide
ARCJoinT	Affordable Robust Ceramic Joining technology
OCMC	Oxide matrix ceramic composite
XRD	X-ray Diffraction
RTM	Resin tranfer molding
AFCOP	Active filler controlled pyrolysis

OFC	Oxide fiber composite
PVA	Poly-Vinyl alcohol
D_{50}	Mean diameter distribution
BSD	Back scattered electron detector
SED	Secondary electron detector
DOE	Department of Energy
NIST	National Institute of Standards and Technology
AMAIGT	Additive Manufacturing of Advanced Indutrial Gas Turbines
CVI	Chemical Vapor Infiltration
PCS	Pre-ceramic Slurry
SiCN	Silicon Carbonitride
NMR	Nuclear Magnetic Resonance
TGA	Thermogravimetric Analysis
FTIR	Fourier Transform Infrared Spectroscopy
SiCBN	Silicon Carbon Boron Nitride
PCP	Pre ceramic Polymer
CW	Continuous wave
UF	Ultra fast
SPS	Spark plasma sintering
HAZ	Heat altered zone
SiO_2	Silica

BN	Boron nitride
TiO_2	Titanium oxide
Si_3N_4	Silicon Nitride
CH_4	Methane
C_6H_6	Benzene
CH_3NH_2	Metilammina
NH_3	Ammonia
H_2	Hydrogen

List of figures

1 Introduction

Greenhouse gases and subsequent temperature rise pose a serious threat to our planet biodiversity. The European green deal offers a roadmap aiming to achieve net zero emissions by 2050, in line with commitments made under the Paris Agreement.
The industrial sector is considered amongst the hardest to decarbonize and alone accounts for about 30% of global GHG emissions and an equivalent share of global energy use. [1]
Energy-intensive industries (EIIs), producing essential materials like steel, cement, and aluminum, are significant contributors to these emissions. Their production processes, such as the reduction of iron ore to iron, rely on fossil fuels and the use of energy-intensive technologies, making the transition to low-carbon alternatives particularly difficult. [2] [1]
To mitigate these emissions, increasing energy efficiency stands out as one of the most straightforward solutions. For many years, energy efficiency has been a crucial strategy for the industry due to its numerous benefits. Over the last four decades there has been a consistent improvement in energy efficiency in energy intensive industries and 'best available technologies' are increasingly approaching technical limits. [1] [3]
Improvements in material, energy, and end-use efficiencies can lead to significant reductions in material demand and, consequently, emissions. [3]

From this perspective, ceramic matrix composites (CMCs) offer a promising solution. They can enhance energy efficiency by allowing processes to operate at higher temperatures while simultaneously replacing steels and superalloys in various applications, thereby reducing the need for their production and substituting them with less energy-intensive alternatives.
In this context, the production of ceramic matrix composites (CMCs) using processes based on polymeric ceramic precursors offers significant advantages. These methods allow for lower processing temperatures compared to traditional ceramic manufacturing methods, which typically require high-energy inputs. By operating at reduced temperatures, energy consumption is minimized, leading to lower greenhouse gas emissions. [4]

1.1. Ceramic matrix composite's role

Ceramic matrix composites (CMCs) represent an advanced class of materials that consists in ceramic fibers embedded in a ceramic matrix. Compared to monolithic ceramics, CMCs exhibit superior damage tolerance due to energy-dissipating mechanisms such as crack deflection, crack splitting, and fiber pull-out. These characteristics contribute to the quasi-plastic behavior of CMCs, making them highly advantageous across various sectors. Notably, they have significant potential for enhancing the efficiency of stationary gas turbines and aero-engines, thanks to their high-temperature and strength capabilities. Compared to conventional nickel-based superalloys, CMCs possess a higher temperature capability, hence CMCs are especially predestined for the use in the hot gas section for cooling air reduction and/or process temperature increase. Furthermore, the density of CMCs is about one third lower than that of metals, benefiting the development of lighter and smaller components. [5] [6]

There are primarily two types of Ceramic Matrix Composite used for the hot sections of turbines and other applications that will be shortly described in the following paragraphs: **SiC fiber-reinforced SiC ceramic matrix composites** (SiC/SiC composites) and **oxide fiber-reinforced oxide ceramic matrix composites** (Ox/Ox composites). The low densities of SiC/SiC composites (2.1–2.8 g/cm³) and Ox/Ox composites (2.5–2.8 g/cm³) are advantageous in comparison to super alloys, resulting in lighter components. Both SiC/SiC and Ox/Ox composites exhibit excellent high-temperature resistance; SiC is durable in the range of 1200 to 1350 °C, while Ox/Ox composites maintain long-term temperature stability at around 1150 °C. [7]

1.2. CMC's applications

The development of CMCs began in 1977 at the University of Bordeaux in France, sparking interest in their potential applications.
In the field of energy production, the start of the *Ceramic stationary turbine* program started in the USA conducted by Solar Turbines, on behalf of the US

department of energy (DoE), with the aim of improving the performance of gas turbine by using ceramic components in the hot gas section. [6]
The efficiency of turbines is often compromised by the excessive cooling air which is mixed with the working fluid, which reduces the power output. By using temperature resistant materials such as CMC the need of cooling can be diminished resulting in better efficiency. [8]
The program was then continued under the name of *Advanced Materials for Mercury 50 gas turbine combustion system* under the supervision of NIST, involving Siemens, Solar Turbines and ATK-COI ceramics. This activity led to the development of the Hybrid oxide CMC. an Ox/Ox is coated with a protective and insulating layer called friable graded insulation (FGI). [6]

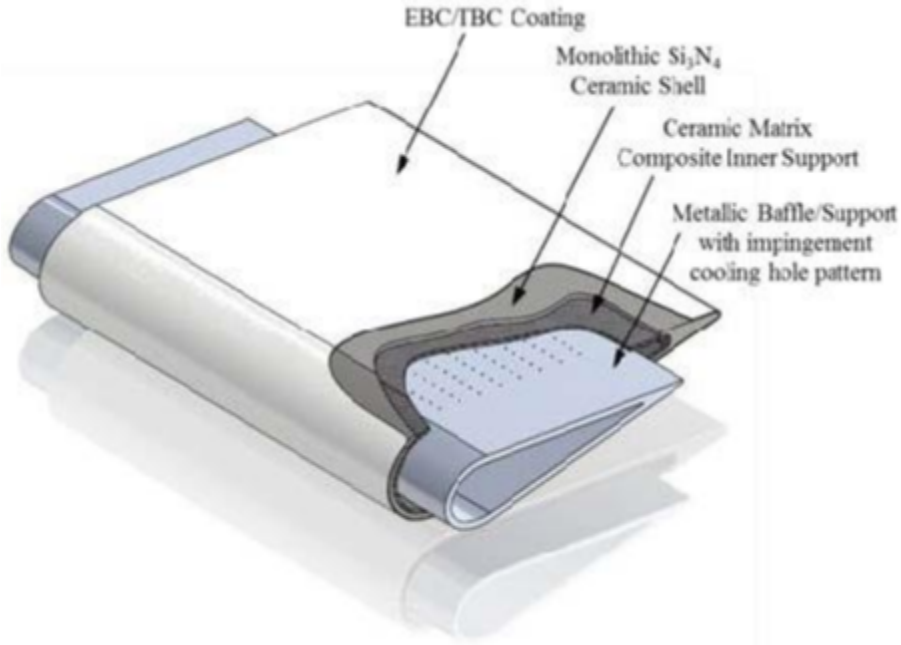

Figure 1—1 Hybrid CMC from a DoE program [6]

Simultaneously, another initiative from DoE in cooperation with General Electric resulted in the Advanced Materials for Advanced Industrial Gas Turbines (AMAIGT). The research by both Solar Turbines and General Electric demonstrated the efficacy of Environmental barrier coatings and supported its future development. [6]
Current programs still under development for turbine applications include *"High Temperature CMC Nozzles for 65% Efficiency"*, *"Hybrid Ceramic-CMC Vane with EBC for Future Coal Derived Syngas Fired 65% Efficient Turbine Combined Cycle"*, *"Additive Manufactured Metallic 3D Ox-Ox CMC Integrated Structures for 65% Combined Cycle Efficient Gas Turbine Components"* to name a few.
Beyond turbine applications, CMCs have various industrial uses. One application involves using ceramic matrix composites (CMCs) as protective jackets for existing

metallic pipes in steam plants. This approach helps extend the life of the pipes, which are often exposed to high temperatures and pressures resulting in creep failure. [9]
Another use are metal alloy burner lances used in steam crackers being substituted by oxide fiber/oxide matrix (OCMC) composites, offering 10 times longer life. Additionally, hybrid OCMC furnace tube (alumina liner, metal insert, outer OCMC sheath) has successfully demonstrated electrical-powered steam cracking (left in fig.2). BASF Ludwigshafen has installed the world's first large-scale electrically heated steam cracker plant, with a potential 90% reduction in CO2 emissions (right in fig.2). [10]

Figure 1—2 Hybrid OCMC furnace tube(left), World first electrically heated steam crack plant (right) [10]

In aerospace, CMCs are widely used in aero-engines, where weight and space are critical factors. The most advanced components made from CMCs in aircraft applications include static parts such as combustor liners, guide vanes, exhaust mixers, and acoustic nozzles, which benefit from the higher operational temperatures facilitated by CMC technology.(pic3)

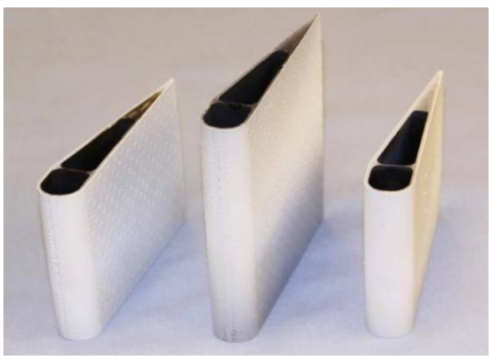

Figure 1—3 Various CMC made engine parts [6]

In terms of ceramic matrix composites (CMCs) for rotating parts, these components are still in an earlier stage of development compared to the others previously discussed. Some test of turbine blades and blisks (component comprising both blades and disk as a single part) were made under test bench but without complete success.
However, in 2015 General Electric Aviation successfully tested the world's first non-static CMC rotating low pressure turbine blades (F414 turbofan demonstrator) made of SiC/SiC. The rotating blades are one-third the weight of nickel alloys usually used for this kind of application; lighter blades generate smaller centrifugal forces allowing also reduction of the size of the supporting parts. With this new propulsion the results are set to deliver a 25% reduction in specific fuel consumption, 30% increase in range and 10% higher maximum thrust compared to fifth generation aircraft. [11]

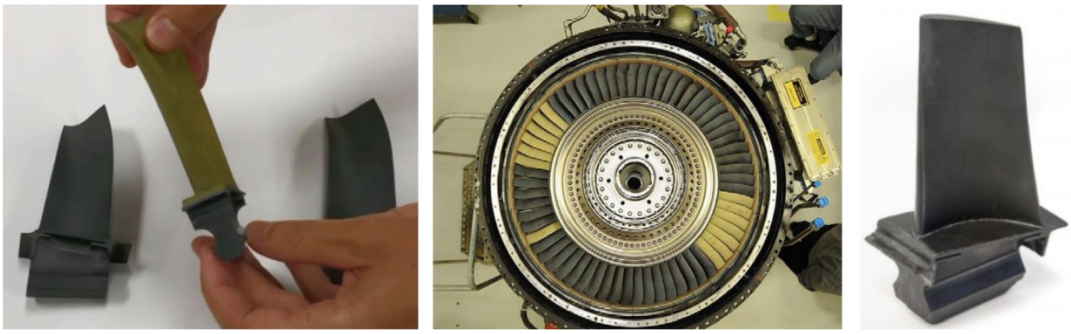

Figure 1—4 Uncooled F414 CMC blades by GE, on center yellow ones are TBE coated [6]

1.3. Objective of the thesis

This introductory section on the properties of ceramic matrices and their current applications highlights the potential benefits of their use across multiple sectors. However, their widespread implementation is still limited by the constraints of

existing joining techniques. This thesis focuses on a novel approach to joining, involving the use of a polymeric ceramic precursor as the joining material. Previous studies on Durazane 1800 and Nextel 610/Alumina-zirconia composite materials (CMS) have shown that the polymer alone is insufficient for achieving a reliable bond between substrates. By doping Durazane 1800 with passive fillers, it becomes possible to enhance the strength and effectiveness of the joining material. The objective of this research is to determine the optimal concentration of passive fillers—comprising Alumina nanopowders and fibers—that, when dispersed in Durazane 1800, will improve the material's morphological final ceramic structure. This will first be evaluated through Scanning Electron Microscope (SEM) analysis. The samples exhibiting the most promising microstructures will then undergo mechanical testing in a single-lap shear configuration to assess their performance.

1.4. Structure of the thesis

The thesis is organized into seven chapters, each building upon the previous one to provide a clear and logical progression from theoretical foundations to experimental analysis. Below is an overview of the chapters and their content:

- **1. Introduction** (Current Chapter): A review of the properties and applications of ceramic matrix composites, focusing on their relevance in various sectors.
- **2. Joining**: An exploration of the importance of joining techniques for ceramic materials, with a review of the most used methods. This chapter also includes a discussion of the first patent related to polymer-derived ceramic (PDC) joints.
- **3.Polymer Derived Ceramics**: A comprehensive literature review on polymer-derived ceramics (PDCs), examining their properties and processing methods. Special attention is put on the role of fillers, on how they modify the final mechanical properties and final structure.
- **4.Materials**: A description of the materials used in the fabrication of the joints, including their key characteristics and relevance to the joining process.
- **5. Experimental activity**: An outline of the experimental procedures used to create the joints, detailing the steps followed in the preparation, processing, and testing of the samples.
- **6.Results and discussion**: A presentation and analysis of the results obtained from the experimental procedures, with a focus on the performance of the joints and material properties.

- **7. Conclusions:** A summary of the key findings, conclusions drawn from the experimental work, and suggestions for future improvements and research directions.

2 Joining

The manufacturing of the products, due to technological limitation or functional needs, is usually relying on joining of some sort. Products are typically assembled using multiple components and joining becomes essential. Most of the time, even when a joint free approach is possible, it becomes a burden from the manufacturing point of view, making the monolithic products unfeasible or impractical.
As previously discussed, there's a growing focus in revolutionizing the processes looking towards an environmentally friendly and energy efficient production. Material joining is a wide area in manufacturing of the components with a high capacity of developing new sustainable methods or more in general optimizing the consumption of energy and of resources by modifying traditional processes.
In particular since 2013 the European commission considered manufacturing and Joining (specifically through the Joining Sub-Platform) as a key enabler for future development of European industry with the scope of developing a competitive, innovative and sustainable Joining competence. [12]
Understanding of joining technologies is therefore a key issue in manufacturing, yet reliable ceramic welding is impossible using standard procedures. The same high-temperature resistance that makes engineered ceramics irreplaceable for many demanding applications poses immense obstacles in joining ceramics. This severely limits the complexity of device geometries. [13]
In the next sections some of the traditional and even few of the most unconventional joining techniques will be addressed.
With regard to joint types, we can consider them under three categories: mechanical, direct, and indirect.

2.1. Mechanical

Mechanical joints are free from chemical rection happening and can be permanent or partially permanent. In this process, no fusion occurs in the joining of materials, and the joint can be easily assembled and disassembled. However, there are certain drawbacks, such as the potential for stress/fatigue in the joints. In particular if the material in consideration is a ceramic or a CMC due to their brittle behavior they could be easily damaged by drilling. Additionally, mechanical fastening adds extra weight and extra space to the joint. [14]

Even if a mechanical joining of CMC by CMC screws/bolts has potential, additionally to the stress concentration we have to take into account the CTE mismatch in case of integration of the CMC with mechanical joints made of a different materials, such as metals, which are commonly used in bolts. In the following pictures an example of an assembled nuclear grade SiC/SiC control road joint segment by using orthogonal shear pins, and C-Clips for mechanical pin retention following assembly. [15]

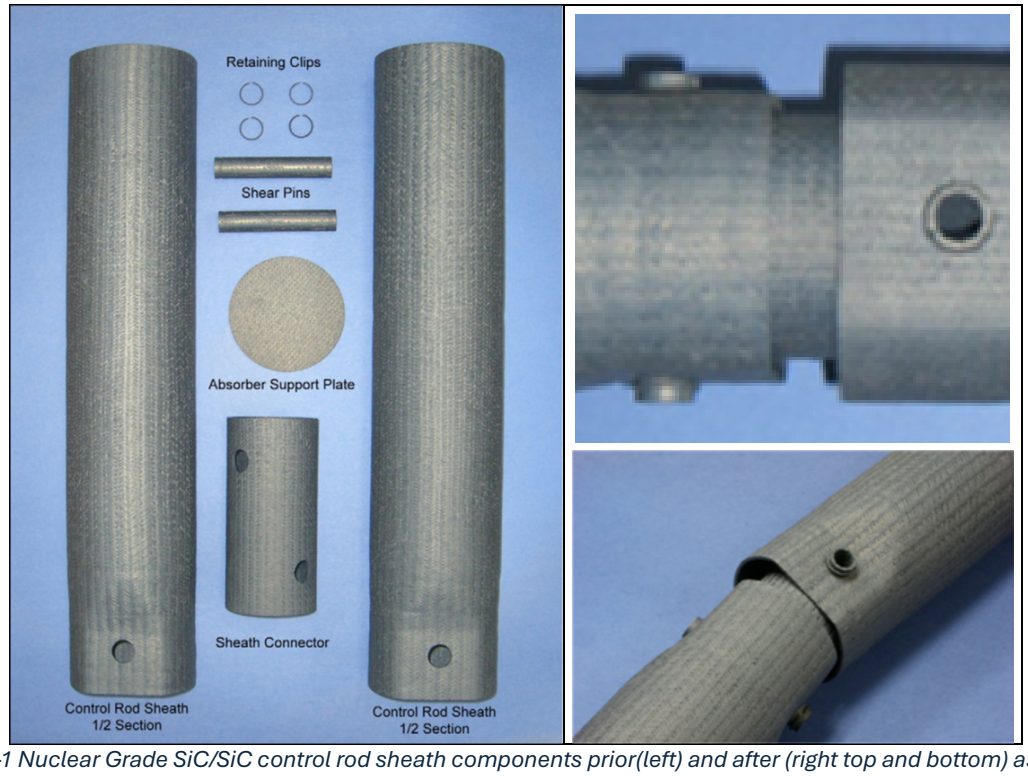

Figure 2-1 Nuclear Grade SiC/SiC control rod sheath components prior(left) and after (right top and bottom) assembly. [15] [16]

A promising approach to improving mechanical joining in CMCs involves combining traditional mechanical techniques with adhesives or other materials such as brazing alloys or glass-ceramics. This method, already successfully used to join

metals and polymers, could be adapted to CMCs, resulting in reliable and hermetic joints. [14]
The potential of this hybrid joint approach was tested by combining the commercial adhesive Graphibond 551RN by Aremco Products after reinforcement by nano and micro-SiC powders to join SiC/SiC composites mechanically machined to have interlocking surfaces. The joint resulted in flexural strength higher than 90MPa(after 1000°C curing in Argon for 1h). [17] [14]

2.2. Direct joining

Under this category are included the methods to create permanent joints without the use of an intermediate as the name suggests and it comprehends basically 2 main methods: welding and solid-state diffusion.

Welding is a process that joins two or more pieces of material by heating them to a molten state and allowing them to cool and solidify together. This creates a permanent bond between the pieces, the heat can be applied under different methods.

Lasers and their controllable energy deposition is already key in additive manufacturing and could be instrumental in efficient ceramic joining. Lasers have been shown to melt ceramics, however, attempts to weld ceramics using powerful continuous-wave (CW) lasers without high-temperature preheating have been unsuccessful because of macroscopic cracking attributed to thermal shock. Instead by using Ultra-fast pulsed (UF) lasers some glasses with lower thermal shock resistance than typical engineered ceramics(alumina, zirconia) have been joined. The problem is the difference in optical properties, with ceramics being translucent to opaque at the laser wavelength. [13]

Penilla *et al. by* focusing the laser on the interface of two ceramic cylinders from the outside and leaving a small gap, to focus light at the interface of the ceramics, the tubes were successfully joined. In the picture below a scheme of the configuration and its results is presented. [13]

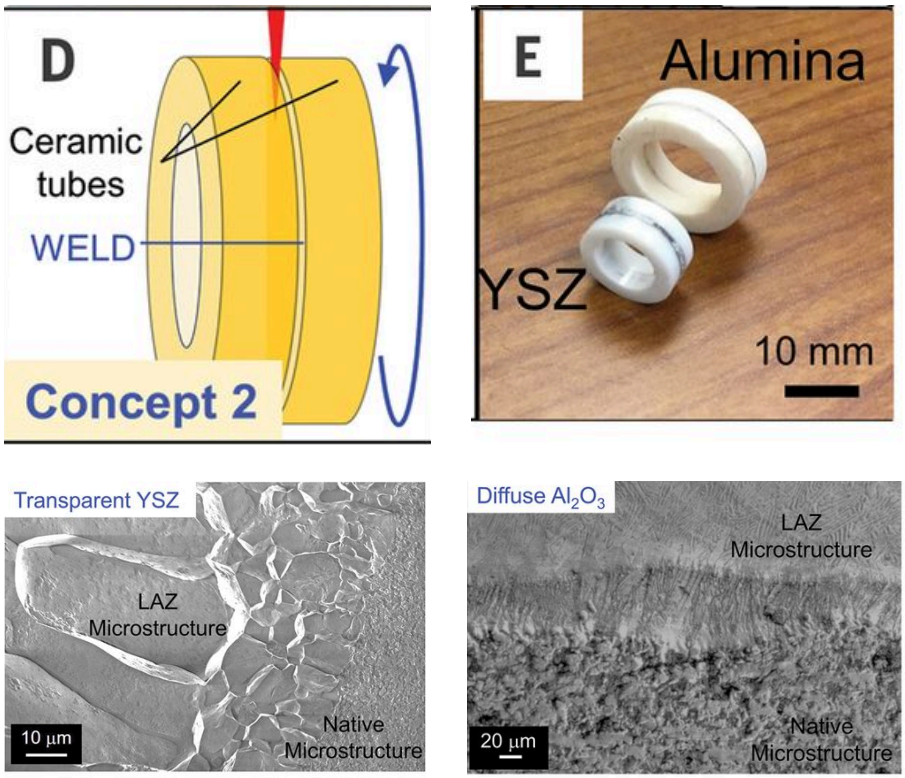

Figure 2-2 Ultrafast laser sintering scheme, finished joint and microstructure by Penilla et al [13].

Other ceramics such as SiC have suitable electrical conductivity for arc welding, but the absence of a melting phase is a big obstacle. As a result, the publications on fusion welding of ceramics are rare, being considered as unconventional welding methods. [18] [19] [20]

Solid-state diffusion is a joining process that involves joining two or more materials by applying pressure and heat while maintaining them in a solid state, below the melting temperature. The process relies on the diffusion of atoms across the interface between the materials to create a metallurgical bond, this kind of method as will be seen in the next paragraphs can also be used by diffusing an interlayer material in the two pieces that need to be joined.

State-of-the art ceramic joining involves high-temperature diffusion bonding. The drawbacks are multiple, the entire assembly is exposed to high temperature for a long time and often requires precise modeling of the shrinking dynamics. Due to these conditions reliable bonding through diffusion is limited to few ceramics and only available for high-cost components. [13]

The most investigated method to realize the solid state diffusion joining is the Spark plasma sintering. Spark Plasma Sintering (SPS) is an advanced technique that utilizes pulsed direct electric current applied through the electrodes in the top and

bottom punches of a conductive graphite die, along with uniaxial pressure, to produce densely sintered materials or in our case of interest to join them, both directly or indirectly (with use of an intermediate). [21]

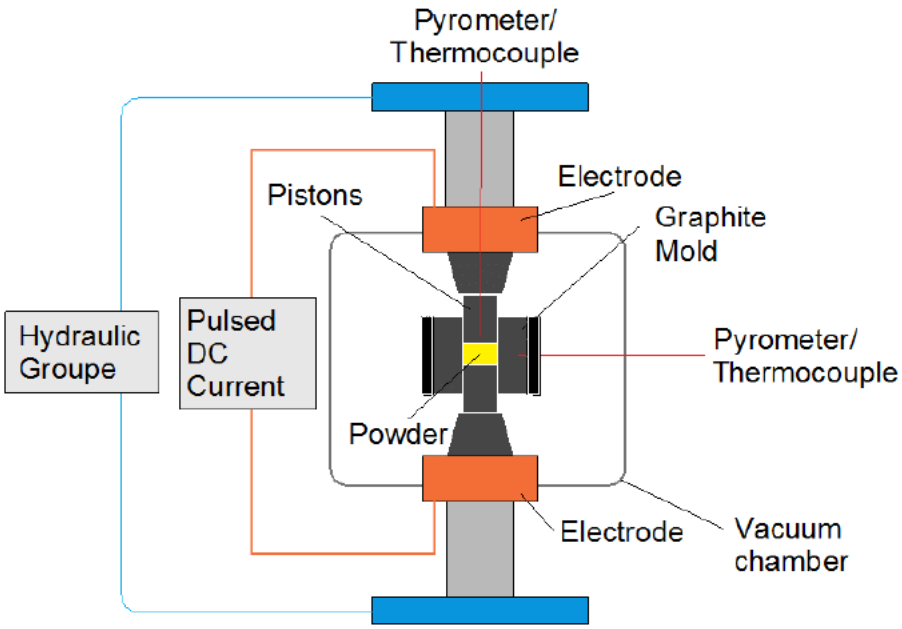

Figure 2-3 Spark plasma sintering scheme [21]

The internal heat generation, so direct heating of the samples leads to significantly higher heating rates with typical values of up to ~1000 °C/min and shorter holding times at sintering temperatures compared to external heating furnaces. [16]

The joining application of this technology was widely used in the recent past for joining of SiC, C_f/SiC and other conductive ceramics resulted in promising result both as direct or indirect (by using a Ti intermediate) joining as shown in the papers "*Joining of alpha-SiC by spark plasma sintering*" by Ferraris and co. or "*Joining of C/SiC composites by spark plasma sintering technique*" to name a few.

An advancement of the Spark plasma technology has been discovered recently, SPS usually takes several minutes of holding time in contrast to the new Flash joining in which its holding time is in the order of seconds.

The flash joining process involves three key stages: the incubation period, flash period, and stable period, as shown in fig.4. During the flash period, the current surges rapidly, causing the electric field power to reach its maximum. The stable period, governed by current control, is defined as the flash joining time. [16]

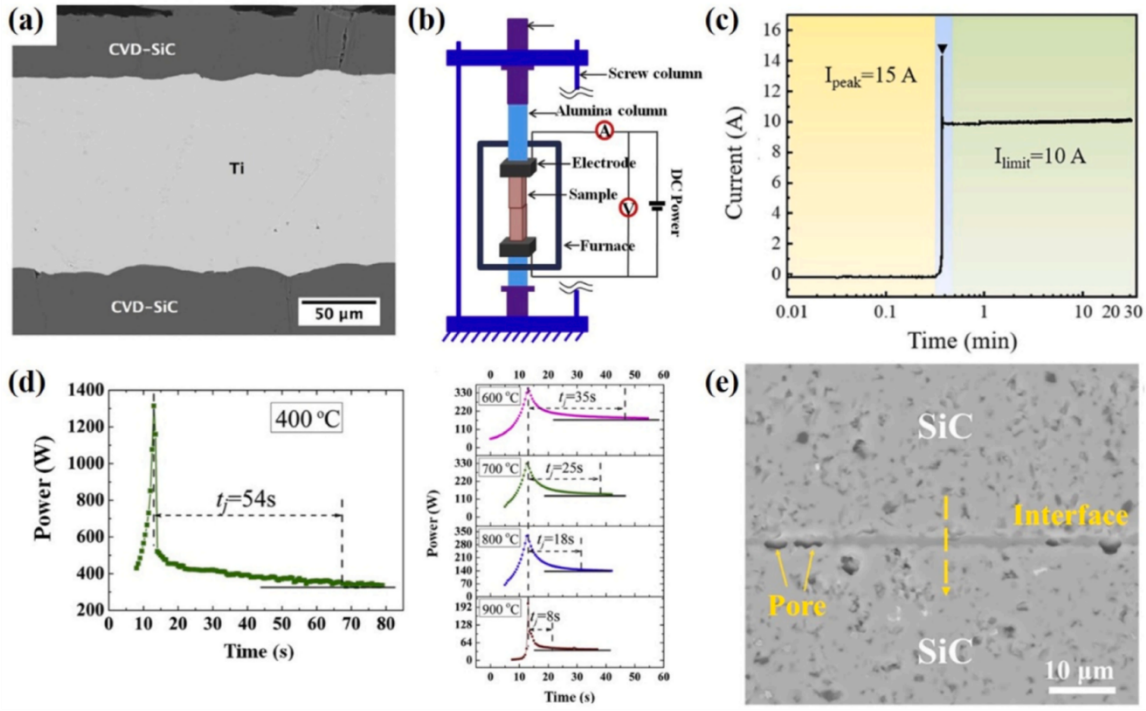

Figure 2-4 (a) SEM image of CVD-SiC/Ti interface; (b) Schematic of flash joining equipment ; (c) Three stages of the flash joining process; (d) Process (e) SEM image of SiC/SiC interface [16]

2.3. Indirect joining

Indirect joining is as suggested by the name a joining technique which relies on the use of an intermediate material which acts as a glue between the two base substrates that we want to join. The "glue" can be a polymer, in this case it is referred to as adhesive joining, or a glass or metal alloy, in this case it is known as brazing.

2.3.1. Brazing

Brazing is the most common way to join dissimilar materials, it is particularly used in case of ceramic to metal joints or CMC joining. The characteristic of the brazing compared to welding is that the intermediate material melting temperature is never above the melting temperature of the base materials. This is both a pro and a burden, it diminishes the HAZ (heat altered zone) but at the same time the thermal resistance of the intermediate will be lower than the "to be joined" ones. This alloy, often in foil or paste form, is placed between the substrates and heated to a temperature above its liquidus point. The process requires careful surface preparation

and precise temperature control. Key considerations for brazing include wettability, reactivity, thermodynamic stability, and the alloy's lower melting point compared to the substrates. [14]

Wettability refers to the ability of the alloy or more in general of the liquid to adhere to the substrate, its theory it's related to the contact angle between the material, the pressure and the atmosphere. Two main static scenarios of wetting are possible: the liquid spreads completely or it sticks forming a cap. The spreading of the liquid is regulated by the parameter Ψ which is related to the specific surface energies of the interfaces: liquid-solid; solid-air; liquid-air which is also indicated by γ (surface tension). Ideally if the surfaces are atomically flat also the other terms could be indicated by the surface tension since in that case there is no difference.

$$\Psi = \hat{G}_{SA} - (\hat{G}_{SL} + \hat{G}_{LA})$$

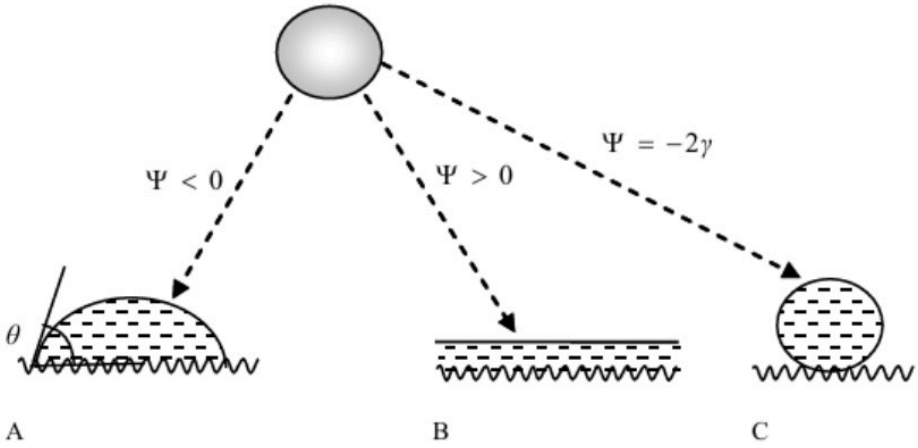

Figure 2-5 A-partial wetting B-total wetting C-complete dewetting

When the angle θ is lower than 90° we can refer to the wetting as good. A good wetting promotes adhesion forces between the material while bad wetting results in a poor joining between the materials. When the term Ψ is higher than 0 then total wetting is observed which is the ideal condition. [22]

In our case, talking about CMC also the qualities of the surface, so porosity and roughness, play a crucial role. In case the wetting of the material is poor - which is very common since due to their polar bond structure, ceramics have a high surface tension that makes them resistant to wetting by traditional metallic melts- the surface of the material must be treated in order to improve it.

Wetting and reactivity go hand in hand with each other, with the use of an active braze a reaction can be triggered to induce surface modification in the CMC and improve the wettability. Usually titanium(Ti, active) or other materials that are used are able to promote the formation of compounds on the CMC surface such as titanium carbides. The surface modification of CMC to improve wettability toward the

brazing alloys, other than by reaction and subsequent creation of metal carbides, can be done by metallization of the CMC surface or the brazing foil itself. [14]

The main drawback of this method is related to the intrinsic lower melting temperature of the brazing alloy in comparison to the CMC or ceramic or metal to be joined. On the other hand, some of the brazing alloys can withstand very high temperature, up to 1230°C [23]. Additionally, the CTE differences between the base material and the brazing alloy must be chosen to be minimal, avoiding excessive residual stresses associated to the cooling after the creation of the joint. Even in the condition where the CTE are closely matched it is possible to further decrease the stresses induced by using slow heating and cooling rates. [14]

Techniques such as the use of multiple layers of different material with gradual change of CTE in order to join pieces with different thermal expansion coefficient, or the use of stiff layers(W,Mo, others) and other ways exist and have been extensively studied by NASA's researcher M.Singh and his colleagues. [24] [25] [14]

2.3.2. Glasses and glass-ceramic

An alternative to metal alloys in indirect joining applications are glasses and glass-ceramics without changing the application method.

Glasses and glass-ceramics are promising materials for joining ceramic matrix composites (CMCs) due to their tailorable properties. These include adjustable characteristic temperatures, coefficient of thermal expansion (CTE), and wettability. Their thermomechanical stability at high temperatures makes them suitable for CMC applications, and they are resistant to oxidation.

Glasses and glass-ceramics can be used as joining materials on their own or as composites with added particles or fibers. The refractoriness of a glassy joining material can be improved through controlled crystallization (glass-ceramic method), resulting in a joint that remains mechanically reliable up to the softening point of the residual amorphous phase. This softening point can be minimized with appropriate heat treatments. [14]

This technique has been used to join the same Oxide/oxide CMC substrates that will be used in the experimental part of this work. Based on Nextel 610™ fibers with 75 wt% alumina – 25 wt% zirconia matrix the substrates were joined and tested to evaluate mechanical stress and creep resistance at high temperatures in the range of 850 to 1000°C. The glass ceramic SiO_2-Al_2O_3-Y_2O_3-CaO-MgO-ZrO_2 resulted in promising results. [26]

2.3.3. Adhesive joining

Adhesive joining is a technique used to join materials together by applying an adhesive substance between the surfaces to be bonded. This adhesive, typically a polymeric resin, undergoes a process of solidification or hardening, either through physical or chemical changes. This process creates a strong and durable bond between the materials, often referred to as adherends.

As for the brazing, the surface of the adherends must be prepared to increase the adhesion, so the wetting is of crucial importance. Adhesives with their intrinsic low mechanical property and low temperature stability compared to the potential of CMC in high temperature environments are not the suited choice most of the time. The low temperature stability can be increased with the modification of the resin by incorporation of ceramic particles, fibers or carbon nanotubes so resulting in enhanced temperature resistance. [14]

An unconventional method for high temperature application of adhesive joining can be seen in polymer derived ceramic, which will be explained in detail in the next chapter. In this case the polymeric compound used has a particular structure that when properly thermally treated lead to the ceramization of the resin and in a fully ceramic joint as a result.

2.3.4. ARCJoinT

Affordable, Robust Ceramic Joining Technology (ARCJoint) is a method invented by M. Singh at NASA Lewis research center back in 1998, initially with the scope of joining Silicon carbide based ceramics and fiber reinforced composites in high temperature applications. [27]

The joining process starts by applying a carbon-based mixture to the joint area, securing the components in place within a fixture, and curing them at 110-120°C for 10 to 20 minutes. This initial step bonds the parts together. Next, silicon or a silicon alloy, in the form of tape, paste, or slurry, is applied around the joint and heated to 1250-1425°C (depending on the infiltrant used) for 10-15 minutes. During this stage, the molten silicon or silicon-refractory metal alloy interacts with the carbon to produce silicon carbide, along with controlled amounts of silicon and other phases based on the alloy composition. The joints formed are able to maintain their

strength up to 1350°C and can join big complex shapes or even be used to repair components damaged during service. [27] [14]

2.3.5. General atomic patented joint

On April 5th, 2012 the patent under the name "High Durability Joints Between Ceramic Articles, and Methods of Making and Using Same" was filed as a European Union patent, submitted by General Atomics, a very significant player in numerous fields such military technology and advanced energy research, with a particular emphasis on cutting-edge innovations in autonomous systems, nuclear energy, and electromagnetic systems.

Due to safety concerns over nuclear fission reactor, the focus is turning in the direction of β-SiC as the structural material in relation to its strength at elevated temperatures and its high resistance to irradiation induced damage. But its usage as a successful fuel clad must ensure retaining the fuel and fission products formed through the fuel cycle so the join too will need to retain the nuclear fuel during the operation. Additionally, it must have well-matched thermal and irradiation induced dimensional change to the articles, as well as chemical compatibility with the fuel, fission products, and coolant. Because of these needs the best option would be to have a join which has the same composition as the articles being joined and thus have substantially the same mechanical strength, thermal expansion coefficient, and other characteristics.

The joint described comprises a ceramic polymorph matrix extending between the first and second articles and including a plurality of inclusions which are distributed among the matrix. The joint is then finished with a sealing layer that may be CVI(chemical vapor infiltration)-derived.

In the following picture a cross section scheme of the join is proposed, the inclusions (104) can be of different type as shown by the diverse shapes and sizes in the figure. In case of absence of inclusion the matrix (103) may otherwise have cracks and voids created during the formation of the joint while, when inclusions are present they occupy and prevent the development of such cracks thus increasing the density of the joint. The sealing layer (105) may penetrate the matrix resulting in zones of increased density compared to the non-infiltrated matrix. Preferably the purity of the sealing, matrix and inclusions should be the same and at least 99% pure.

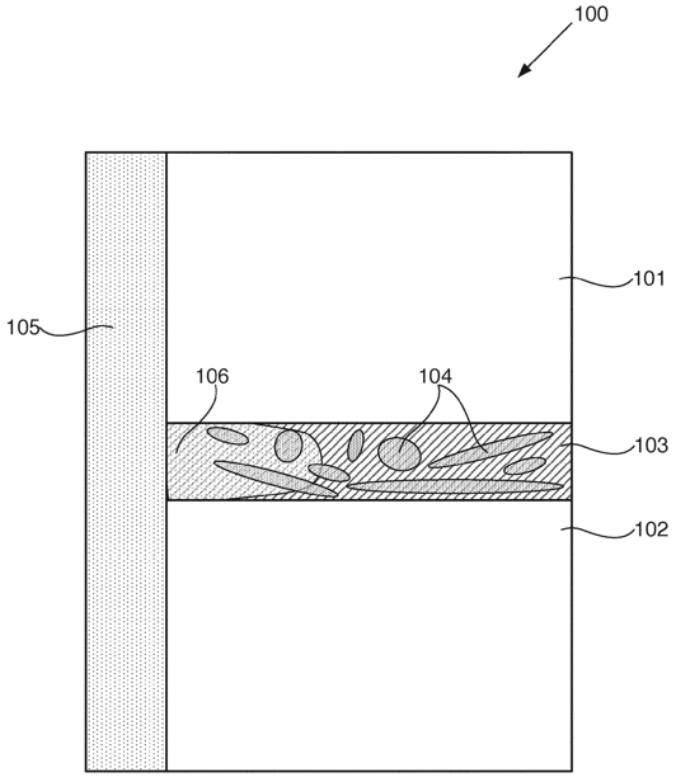

Figure 2-6 Joint parts code indication [28]

A detailed method for preparing these joints is fully described in the patent, and a schematic of the procedure is also presented and shown here in fig.7.

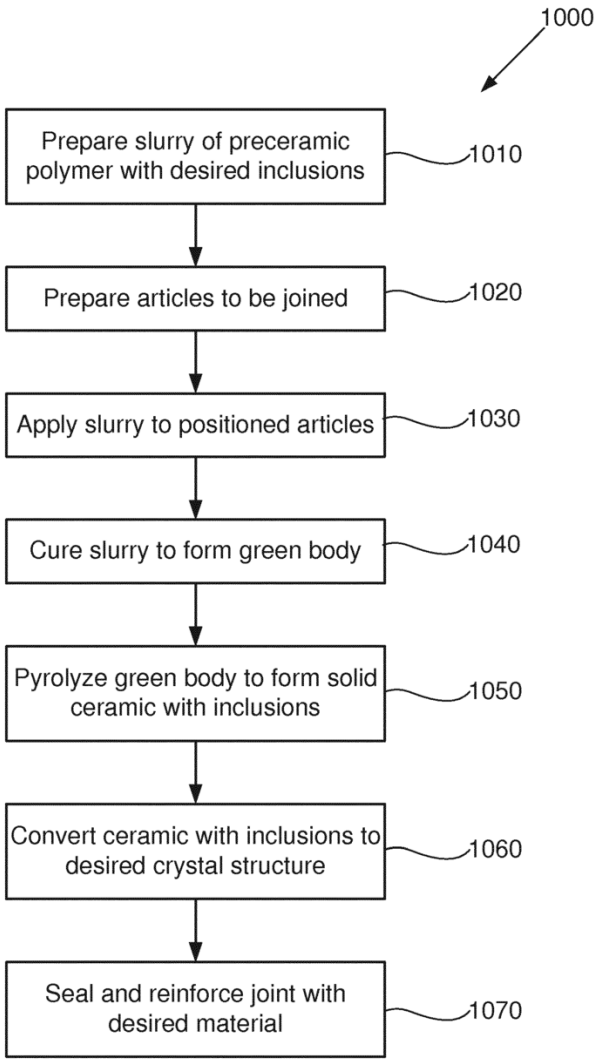

Figure 2-7 Joint formation step of patent [28]

The steps 1050, 1060 are performed preferably in inert atmosphere such as argon or vacuum. To prevent the formation of gas bubbles during the conversion process, the heating rate must be slow, ideally less than 4°C per minute. The thermal conversion of the preceramic polymer of the step 1050 is performed in steps: first monomers are polymerized at low temperature, crosslinking at a higher temperature and then pyrolyzed at even higher temperature all according to the polymer type. The crystallization of the solid amorphous ceramic in step 1060, although it may begin at a certain temperature, is preferably carried out by heating it for an extended period at a significantly higher temperature to ensure complete conversion. The figure 8 shows how the x-ray diffraction (XRD) changes for crystallization at different temperatures, can be noticed that at 1300°C the spectral phase is not as

sharp as the one at 1700°C in which the absence of other crystallization peaks denotes the phase purity. [28]

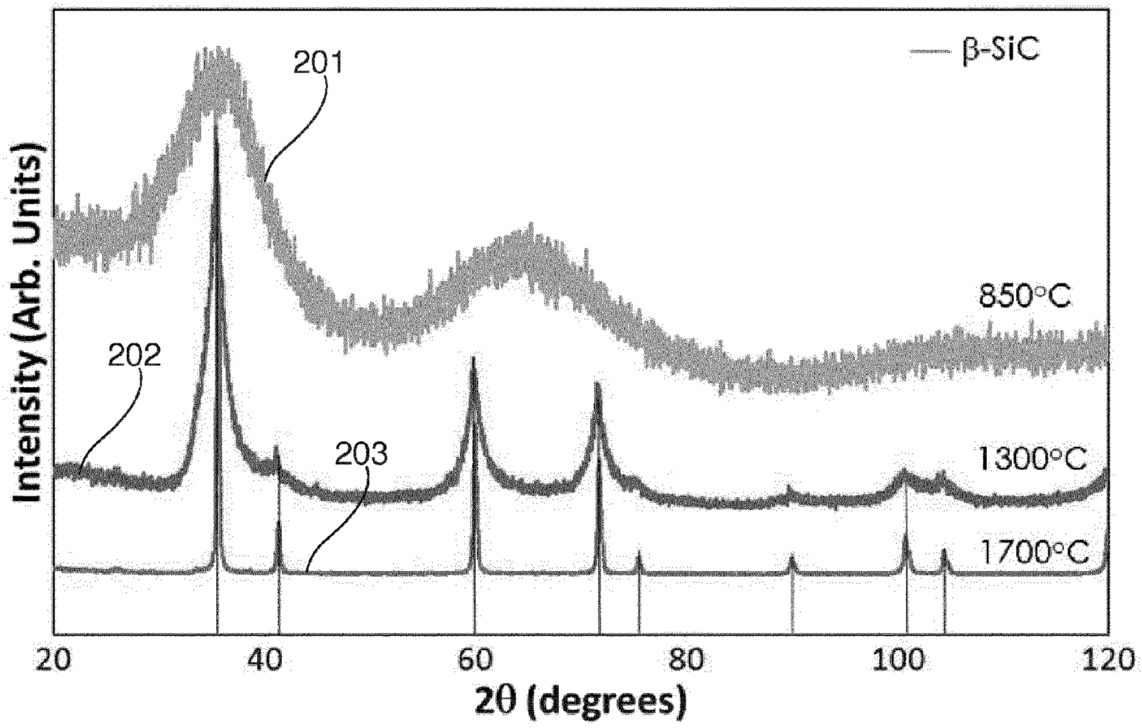

Figure 2-8 XRD at different temperatures

Another curious aspect is about the sealing layer, although it may induce thinking it only has a function in making the joint impermeable it shows a remarkable improvement in both strength and Weibull modulus compared to the joints with only PCS and with both PCS and inclusions (whiskers in this case). In the document It's stated "The hybrid joint had a characteristic apparent shear strength of about 50.7 MPa, about 239% that of the joint prepared using PCS slurry and about 975% that of the joint prepared using PCS alone. The Weibull modulus of the hybrid joint was about 6.7, about 171% that of the joint prepared using PCS slurry and about 353% that of the joint prepared using PCS alone. Accordingly, the joints provided herein have significantly enhanced mechanical properties than those that may be obtained using previously known methods, and indeed **are believed to meet requirements to nuclear applications.**" [28]

3 Polymer Derived Ceramics

Polymer Derived Ceramics are a class of advanced ceramic material synthetized starting from a Preceramic polymer also known as precursor. These polymers represent inorganic or organometallic systems that are converted into ceramics through proper thermal treatment (curing and pyrolysis).

The composition and microstructure of the PDC are a result of the molecular structure of the preceramic polymer. Therefore, the observed differences in the macroscopic properties are also closely related to the variation of composition and solid-state structure of these materials.

Since early 1960s the first investigations on synthesys of nonoxide ceramics starting from silicon-based PDCs, as first reported by Ainger and Herbert, and Chantrell and Popper. In the seventies Verbeek, Winter and Mansmann presented the first practical transformation of polyorganosilicon compounds (polysilazanes, polysiloxanes and polycarbosilanes) into ceramics with the manufacturing of small diameter Si_3N_4 and SiC ceramic fiber suitable for high temperature use. Late in 1970s significant improvements were made in the synthesis process of polymer derived ceramics thanks to the work of Fritz and Raabe. At about the same time Yajima started developing the first process for the synthesis of Silicon carbide (SiC) ceramic material through thermolysis of polycarbosilane. [29] [30]

A scheme of the developed process is shown in the following figure(1).

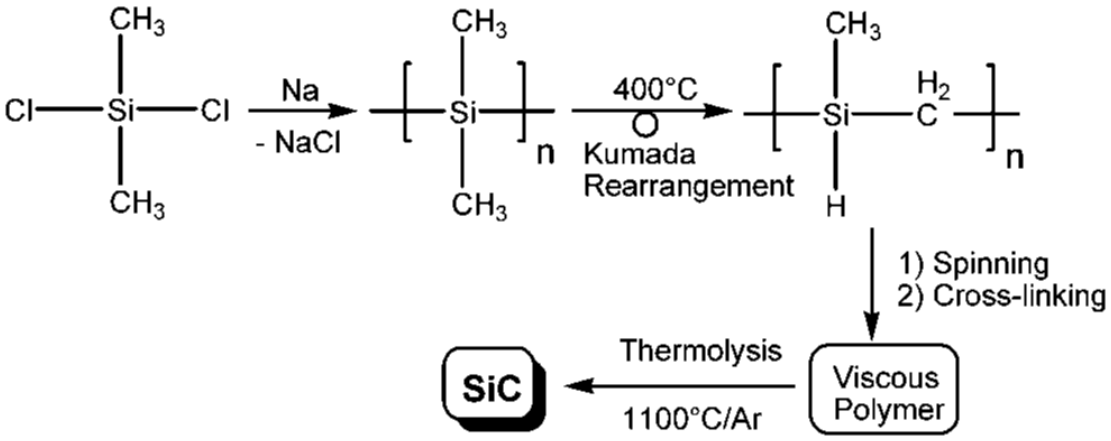

Figure 3-1 Yagima process [29]

Over the years significant advancements were achieved in developing new synthesis methods for preceramic polymers, allowing for better control over their microstructure and processing characteristics. To compete with traditional ceramics, pre-ceramic polymers must either be inexpensive, or their synthesis must be highly selective, producing materials with novel compositions and exceptional or unique properties. [29]

3.1. Preceramic polymer synthesis and classes

The starting materials for these processes include chlorosilanes, hydrosilanes, vinylsilanes, and alkenylsilanes, which facilitate polymerization through elimination, substitution (metathesis), or addition reactions. Chlorosilanes (R_xSiCl_{4-x}, where x = 0–3 and R represents an organic side group) are the most commonly used precursors due to their wide commercial availability and low cost. The synthesis routes for the most representative classes of silicon-based polymers from organochlorosilanes are illustrated in fig.2. [31]

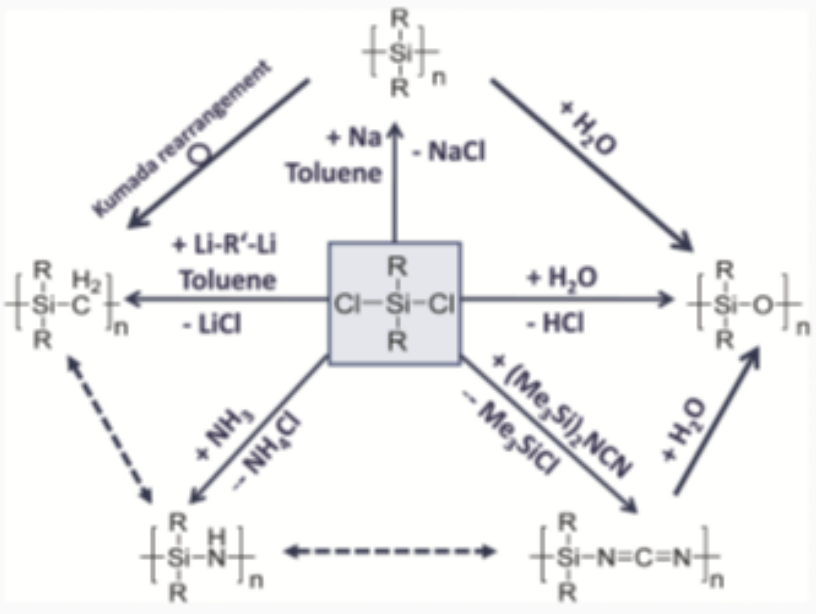

Figure 3-2 Polymerization path from Chloro-organosilicon [31]

Chloro-organosilicon compounds serve as crucial starting materials for synthesizing various silicon-containing polymers, such as polysilanes, polycarbosilanes, polyorganosilazanes, polyborosilazanes, polysilylcarbodiimides, polysilsesquioxanes, polycarbosiloxanes, and other silyl-containing polymers. [31] To have a better understanding of what are the difference in the elements of the different compounds and their structure a scheme is provided in fig.3.

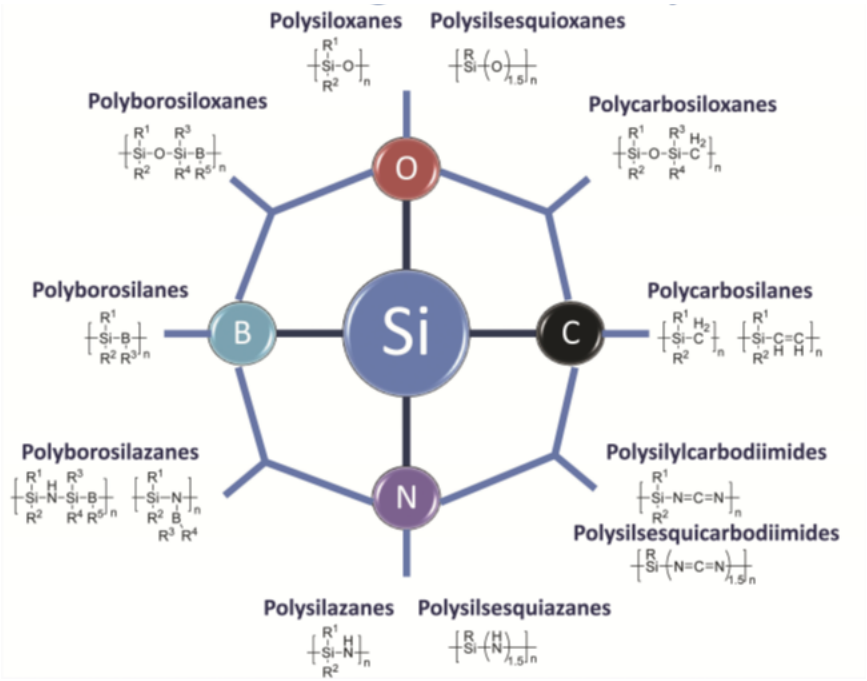

Figure 3-3 Main classes of Si-polymer as precursors for ceramics in the Si-O-C-N-B system

The success in synthesizing silicon-containing PDCs is due to the robust silicon-carbon bonding in the polymeric structure, which prevents carbon from volatilizing as small hydrocarbon molecules during pyrolysis in controlled inert atmospheres. Another important property that the polymer should possess is a high enough molecular weight, again, to prevent volatilization. PDCs can be synthesized at relatively low temperatures, with complete pyrolysis and conversion of the silicon-based polymer to ceramic occurring at or below 1100°C. [31]

Preceramic polymers are usually constituted by a Si-based polymeric chain and side functional groups, an oversimplified general formula for an organosilicon polymer monomeric unit, suitable as a precursor for ceramic synthesis, is shown in fig.4.

Figure 3-4 Simplified molecular structure of organosilicon compounds [31]

At the molecular level the modification of the property of the preceramic can be attributed mainly to two crucial parameters: the group (X) in the polymer backbone and the substituents R1 and R2 attached to the silicon atoms. [31]

To the group(X) can be attributed the highest importance as it determines the class of the final polymer, e.g. with X=NH the class is polyorganisilazanes instead with X=CH2 it's polyorganocarbosilanes, for further possible combination refer to fig3. By instead altering the side chain functional groups R1 and R2 attached to the silicon atoms, the chemical and thermal stability, as well as the solubility of the polymer, can be adjusted. This modification also affects their electronic, optical, and rheological properties. Typically, hydrogen, or aliphatic or aromatic organic side groups R are attached to the silicon atoms. The solubility, thermal stability, and viscosity of the polymer, which vary with temperature, are important characteristics for further processing. Additionally, the organic substituents as side groups R influence the carbon content in the resulting ceramic. [31]

The group in the polymer backbone based on the molecule attached to it give rise to different classes as previously said. The following paragraph will explain more in detail about each main class and their applications.

3.1.1. Polysiloxane

The most important synthesis route for the realization of polysiloxanes consists on the reaction of chloro(organo)silanes with water, as schematized in fig5.

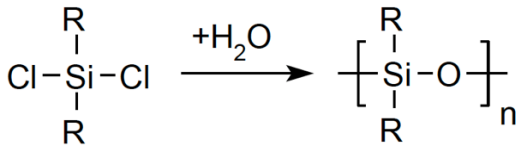

Figure 3-5 Chloroganosilane reaction to polysiloxane

Alternative synthesis methods have been explored for producing polysiloxanes. Two key approaches include the polycondensation of functionalized linear silanes and the ring-opening polymerization of cyclic silaethers. These methods result in silicon-rich polysiloxanes that merge the properties of conventional polysiloxanes with those of polysilanes. [31]

In addition to linear and cyclic polymers, an important subclass is polysilsesquioxanes, which follow the general formula $-[RSi-O_{1.5}]_n-$. This unique category of siloxanes is defined by a highly branched molecular structure, which can manifest in various configurations, such as random, ladder, or cage structures, as illustrated in fig6.

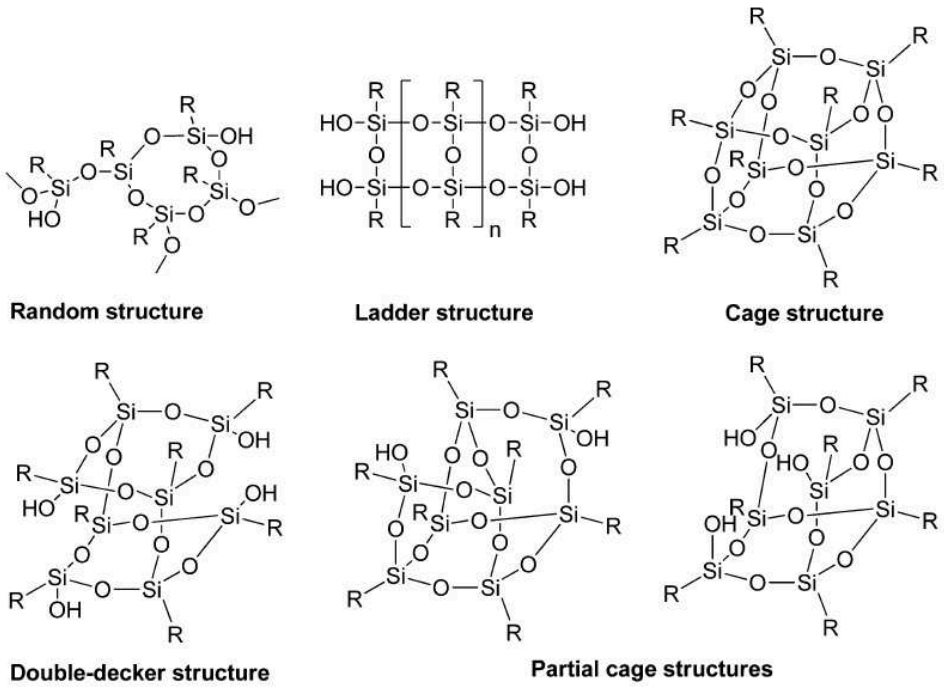

Figure 3-6 Possible structures of polyssilesquioxanes [31]

Due to their significant branching, these polymers are often referred to as silicon resins. Typically solid at room temperature, they are known for their high ceramic yields when subjected to pyrolysis. In non-oxidizing environments, pyrolyzed polysiloxanes produce an amorphous silicon oxycarbide residue. This network, composed of both Si–O and Si–C bonds, forms at relatively low temperatures—a process that is unattainable through more conventional techniques. The final ceramic material appears black due to the presence of free carbon. [31]

Polysiloxanes are among the most widely used polymers. Beyond their role as ceramic precursors, they are commonly employed in their polymeric form as sealants, lubricants, adhesives, and gaskets across various industries, including aerospace, semiconductors, and personal care. Prior to ceramization, they are typically odorless, colorless, water-resistant, chemically stable, electrically insulating, and able to withstand high temperatures. [29]

3.1.2. Polysilazane

Polysilazanes are polymers characterized by a main backbone constituted by alternate silicon and nitrogen atoms. They are typically produced through ammonolysis reactions, where chlorosilanes react with ammonia or other amines.

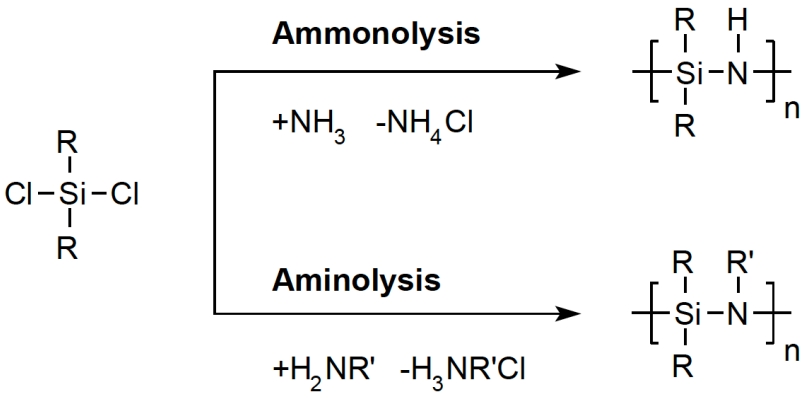

Figure 3-7 Routes for Polysilazane syntesis [29]

However, the resulting products often consist of volatile oligomers and low molecular weight polymers, leading to low ceramic yields. To address this issue, researchers have focused on modifying silazane oligomers into non-volatile precursors by attaching suitable side-chain groups to the silicon atoms. Durazane 1800, a well-

known commercial polysilazane precursor and the one that will be employed in the experimental part of the thesis, employs vinyl groups for this purpose.

In general, they provide better performances than siloxane. Commercially available polysilazanes are primarily used to realize high-temperature SiN or SiCN ceramic coatings or components, but more common as coatings in polymeric state.

3.1.3. Polysilanes

Polysilanes are a class of silicon-based polymers that consist of a backbone of silicon atoms linked together by single bonds, with organic side groups (usually alkyl or aryl groups) attached to the silicon atoms.
Figure 8 reports the typical synthesis reaction for polysilanes production. Kipping first proposed this reaction in 1921, and it is still one of the most popular synthetic pathways for the synthesis of polysilanes today. [32]

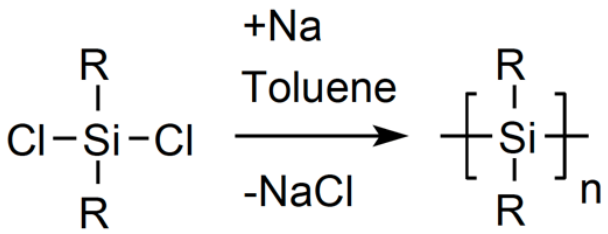

Figure 3-8 Chlorosilane to Polysilane [31]

Polysilanes and polycarbosilanes are being utilized more frequently as precursors for silicon carbide ceramics(high performance SiC fibers such as Nicalon™ by Nippon Carbon Co.) and as functional materials including photoresists, semiconductors, and hole-transporting materials (necessary for perovskite solar cells, OLED,etc.) [33] [34] [35]

3.1.4. Polycarbosilanes

Polycarbosilanes, which feature a Si-C backbone, contain branched side groups such as methylene, vinylidene, and phenylene, making them more structurally complex than polysilanes. Apart from the Si-C bond also Si-Si bond could be present together with hyperbranched structures, this could lead to modification to both the Si:C ratio and to the final ceramic yield. Thus modification of the synthesis structure leads to many different structures and features. The most common synthesis route for these polymers involves the thermal decomposition of polysilanes under

pressure via the Kumada mechanism(fig.9). However, this process can be hazardous due to the buildup of gaseous byproducts (e.g., methane, trimethylsilane (Me_3SiH), silane (SiH_4)), which may lead to a dangerous pressure increase within the autoclave. Alternatively, polycarbosilanes can be synthesized at ambient pressure through the pyrolysis of polydimethylsilane in a nitrogen atmosphere, but there is the need of a catalyst. This class of organosilicon polymers is widely utilized in the production of silicon carbide (SiC) components, including fibers, composites, powders, and other advanced non-oxide ceramic structures. [36] [37] [38]

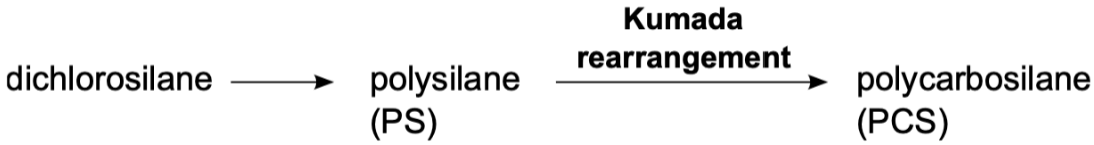

Figure 3-9 Sythesis of polycarbosilanes from dichlorosilane [38]

3.2. Processing of preceramic polymers

Shaping and Cross-Linking the polymeric precursor are the first steps in the creation of the ceramic components. One of the advantages of PCPs is their viscoelastic behavior rising from their polymeric nature. Shaping due to this intrinsic characteristic precursor can be made with a large variety of techniques for forming, many of which are either unique to polymers or significantly easier to apply compared to ceramic powders or pastes. [31]

Various plastic forming technologies, such as resin transfer molding (RTM), warm pressing, fiber drawing, extrusion, and injection molding, can be applied to preceramic polymers as shown in fig10. For instance, spinning thin fibers is easily achievable, and the rheological properties of the precursor can be tailored by modifying its molecular architecture. This often results in components with finer details compared to those produced using powder-based systems. [31]

Moreover, preceramic polymers can exist in liquid (cross linkable) or solid form, depending on their molecular architecture and weight. If solid, they can be dissolved in various organic solvents or melted at low temperatures (usually below 150°C). A necessary property of the PDC is that the part needs to retain its form after the shaping, it needs to be transformed to a thermoset polymer. The thermoset part must be able to keep the shape also at higher temperatures since during its ceramization process ideally what we want is just a change in the material not in its form. [31]

Compared to fabrication methods of ceramics from powder, in this case the machining of the parts can be done in the polymeric state so avoiding the issues that are associated to a ceramic material such as tool wearing and brittle fracture. [39]

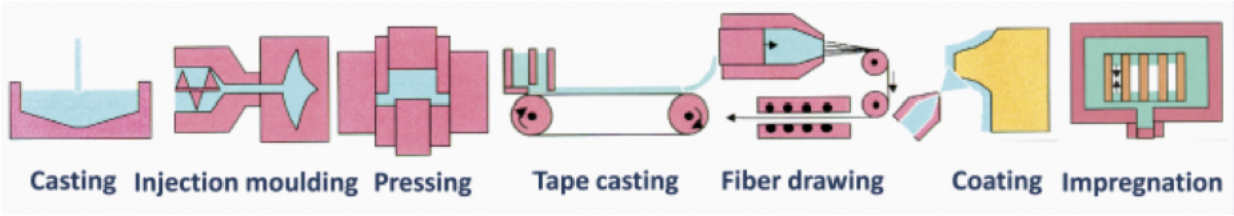

Figure 3-10 Plastic sector derived shaping techniques

The degrees of freedom also regarding the possible microstructure and functionalities are higher than the typical ceramics, e.g. siloxanes can be saturated with supercritical CO_2 to fabricate microcellular plastics and then treated to get highly porous foams. Not only micro or even nanostructure (wires, belts and tubes) but taking advantage of the transient porosity (will be seen in detail in the focus chapter about pyrolysis) superior adsorbent materials can be made. [40]

In literature publications about other and, in recent years, more advanced techniques have been developed for the shaping of the precursor, e.g. additive manufacturing. Some of the methods are listed in fig11. [31]

Shaping technique	References
Casting/freeze casting	Melcher and colleagues[193–196]
Impregnation/infiltration	Satoa and colleagues[197–199]
Tape casting	Cromme *et al.*[200]
Coating (spraying, dip- or spin-coating, chemical vapor deposition)	Goerke and colleagues[201–203]
Pressing (cold/warm—uniaxial, cold—isostatic)	Haug and colleagues[204–206]
Injection molding	Zhang and colleagues[207,208]
Extrusion	Mutsuddy and colleagues[209–211]
Fiber drawing	Bunsell and colleagues[212,213]
Blowing/foaming	Zeschky and colleagues[111,188,214]
Machining	da Rocha *et al.*[185]
Joining	Colombo and colleagues[186,215,216]
Rapid prototyping	Friedel *et al.*[217]
Ink jetting	Mott and colleagues[218,219]
Electro-hydrodynamic-spraying/spinning	Nangrejo and colleagues[220–224]
Aerosol spraying	Xiao and colleagues[225,226]
Self-assembly	Garcia and colleagues[227–229]
Microcomponent processing (UV/X-ray lithography, nano-/microcasting, replication, microextrusion, embossing/forging)	Hanemann and colleagues[230–240]
Microfluidics processing	Ye *et al.*[241]
Emulsion processing	Bakumov *et al.*[242]
Formation of nanostructures (tubes, fibers, wires, cables, belts, coils), directly by pyrolysis	Otoishi and colleagues[190,195,243–249]

Figure 3-11 List of techniques from literature, references can be found in [31]

It is important to note that when a significant amount of filler particles is added to the preceramic polymer, cross-linking may not be required. The solid additives

often provide enough support (limiting the flow) to the polymeric matrix, helping to retain the shape of the part during heating. The addition of fillers significantly impacts the rheology of the preceramic polymer. [41]

3.3. Fillers

The polymer-to-ceramic conversion involves gas release, isotropic volume shrinkage (20–30% linear shrinkage), and the formation of both micro and macro porosity. This process often results in significant defects, such as cracks or pores, making the direct conversion of a preceramic part into a dense ceramic nearly impossible, unless the part's dimensions are typically below a few hundred micrometers, as seen in fibers, coatings, or foams. [31]

To fabricate bulk components of size limited only by the dimensions of the pyrolysis furnace, the main strategy employed has been the introduction of fillers. Fillers of various types (polymeric, metallic, ceramic) and shapes/dimensions (nano- or microsized powders, platelets, nanotubes, nanofibers, chopped or long fibers) can be incorporated into a preceramic polymer before shaping. [31]

In addition or as alternative pathway to the use of fillers, other strategies have been employed to reduce shrinkage and cracking. These include the direct pyrolysis of specially-made scaffolds infiltrated by a liquid preceramic polymer, as well as the warm-pressing of partially cross-linked polymer powders. [42] [31]

These fillers can be categorized into four basic types based on their behavior during heat treatment: passive, active, glass (meltable), or sacrificial fillers. The picture(fig.12) below shows a visual idea of the different behavior of the fillers [30]

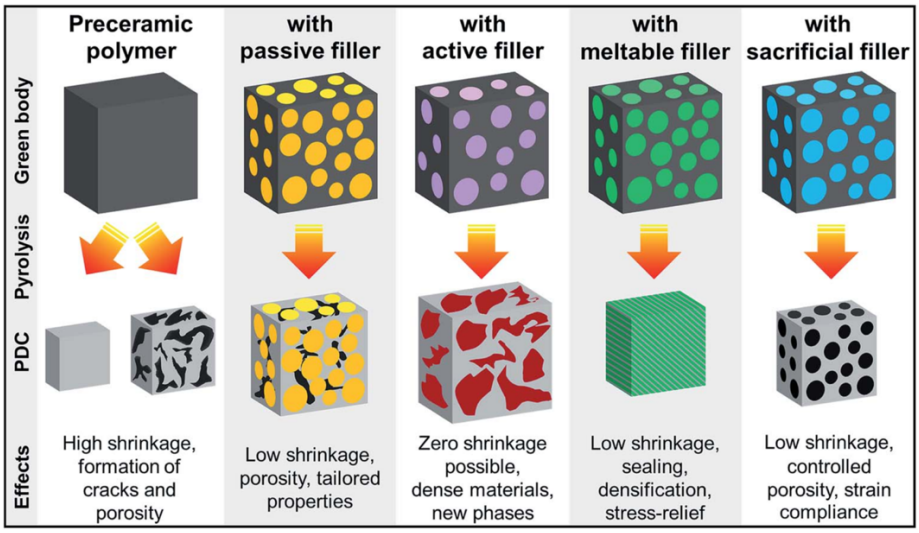

Figure 3-12 Types of filler and their effect [30]

Combining various polymer precursors with different inert and reactive fillers, including particles or fibers, enables the design of a wide range of microstructures and materials, as shown in fig13. Composite materials created from reactive filler-containing polymer mixtures feature a three-dimensional interconnecting network of the filler reaction phase (carbide, nitride, oxide, etc.) embedded in a nanostructured polymer-derived Si-O-C-N matrix. Additionally, the specific properties of the fillers can impart unique functionalities to the final composite materials(e.g. increased eletron conductivity, enhanced oxidation stability, etc.). [43]

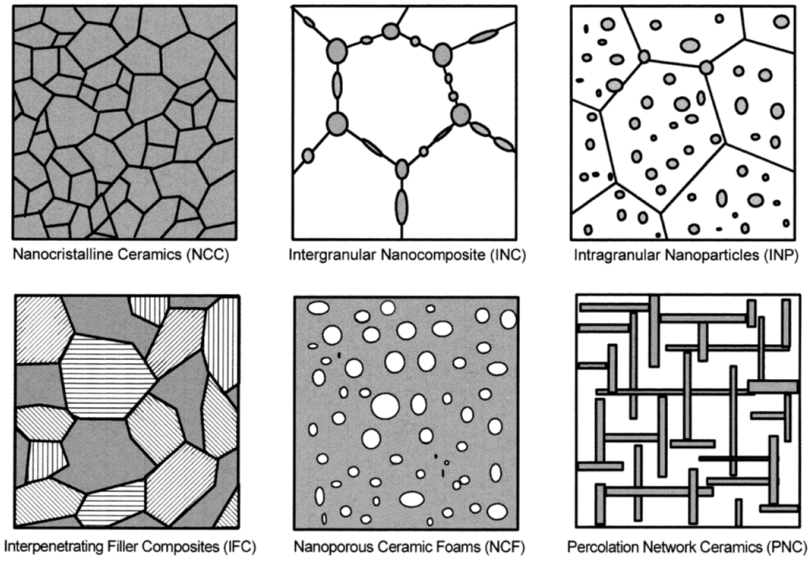

Figure 3-13 Possible microstructure of PDC [43]

The mechanical properties of polymer-derived amorphous or nanocrystalline materials primarily depend on the amount of residual porosity. Fracture toughness, Young's modulus, thermal shock resistance, and fatigue strength can be improved by dispersing filler particles or fibers in the polymer-derived matrices. Even at low volume percentage of dispersed particles can lead to the crack-tip bridging toughening mechanism. Generally, the mechanical properties increase with the filler volume fraction up to a maximum at approximately 40-50 vol.%, followed by a significant decrease at higher filler fractions due to increased porosity formation, the trend in shown in fig14 (a). [43]

The filler additionally can precipitate creating a network that can result in nonlinear property changes, such as an electrical insulator-to-conductor transition when a percolation threshold is exceeded (see fig14 (b)). [43]

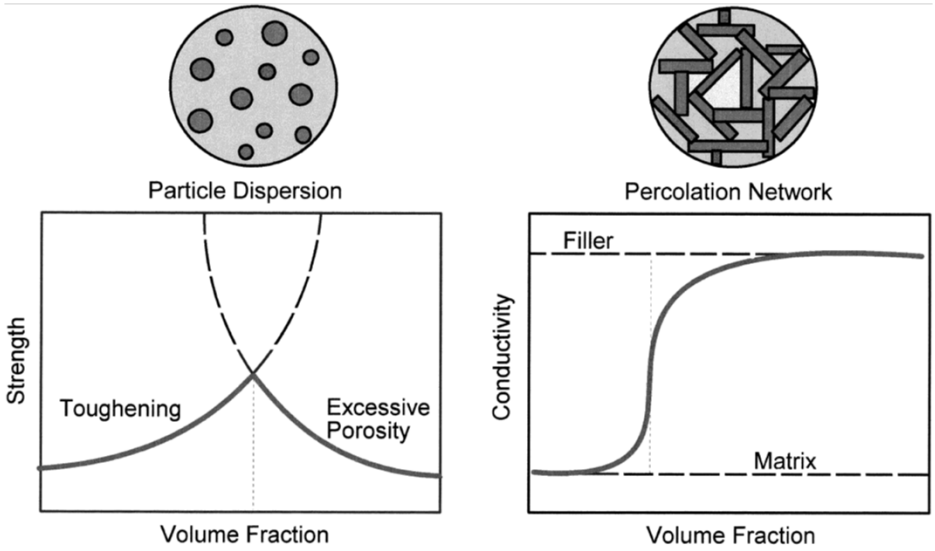

Figure 3-14 Volume fraction variation effect on (a) mechanical prop. (b)Conductivity [43]

3.3.1. Passive:

Passive fillers are inert components that preserve their original properties, such as composition, mass, and particle size, throughout the manufacturing and application processes, excluding thermal expansion. Their primary role in Polymer-Derived Ceramics (PDC) is to mitigate the shrinkage by reducing the volume fraction of the shrinking phase of the preceramic polymer during the pyrolysis step. This reduction helps to minimize total weight loss, shrinkage, and crack formation. Additionally, they facilitate the escape of gaseous species by creating more efficient pathways for their release. [30] [31] [43]

This kind of filler has been used in many applications, one of them is to substantially improve the maximum coating thickness. The strategy has been utilized for a considerable period, with initial research dating back to 1993, titled "Ex-polymer SiC Coatings with Al2O3 Particulates as Filler Materials" by M. Labrousse et al. [44]

Despite its long history, it remains an active research topic. A recent study by Rajendra K. and colleagues investigated the variation in critical thickness of the coatings when yttria (Y_2O_3) was used as an inert filler in the polymer-derived ceramics (PDC). The study examined volumetric contents ranging from 45% to 93% of yttria added to a SiC polymer-derived precursor. The objective was to enhance the critical thickness of the coating, resulting in a dense and crack-free final product. The accompanying figure (15) illustrates the increase in critical thickness for coatings composed of 45%, 77%, and 93% yttria. [45]

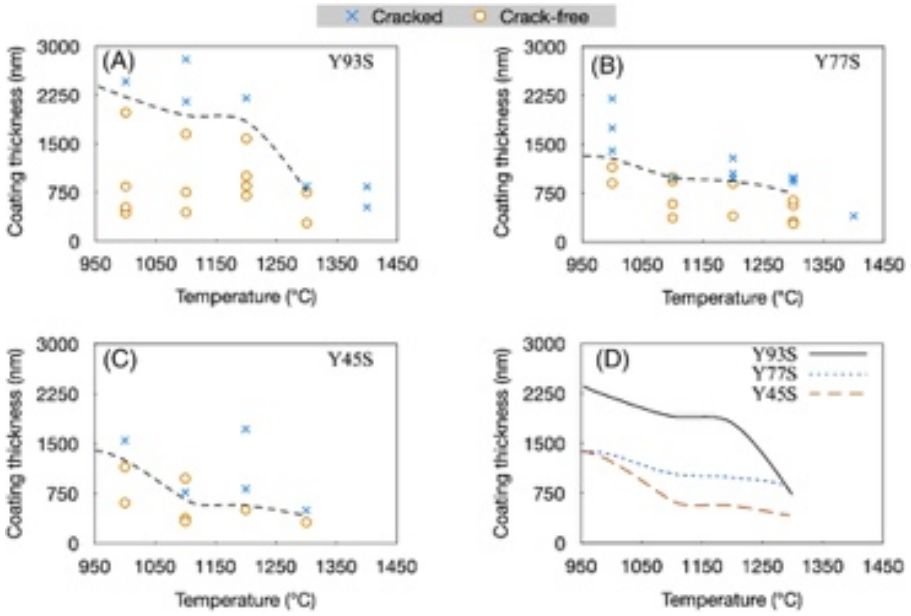

Figure 3-15 Critical thickness for different volume percentage of dispersed filler [45]

The inert behavior of certain fillers is contingent upon specific conditions, such as an oxygen-free environment or lower temperatures, which are frequently unattainable in PDC processing. The rigorous conditions of pyrolysis often lead to the degradation of organic polymers, the melting of glass components, and the oxidation of metallic elements. Given these challenges, ceramic materials, including SiC, Si_3N_4, ZrO_2, TiO_2, BN, Al_2O_3, and SiO_2, are predominantly utilized as passive fillers. These ceramics exhibit exceptional thermal stability, high melting points, and robust oxidation resistance, enabling them to maintain their inert characteristics across a broad temperature spectrum without requiring protective atmospheres. [30]

The passive nature of these fillers permits the incorporation of high filler loadings into coating systems, providing opportunities to fine-tune the properties of the final ceramic product. Even though this strategy may completely avoid the macroscopic shrinkage of the coatings caused by precursor densification during ceramization, residual porosity will always remain in the coatings when medium to high volume fractions of passive filler are used. Furthermore, the amount of porosity increases with increasing volume fraction of filler, especially if the fillers have a narrow particle size distribution. Despite the reduction of macroscopic shrinkage, crack formation may still occur due to localized stresses (e.g., around filler particles), particularly in thicker coatings. [30]

3.3.2. Active:

Active fillers are those that engage in chemical reactions during the coating process. These reactions can occur with the precursor, with gaseous byproducts from pyrolysis, or with the pyrolysis atmosphere, leading to the formation of new phases.

Active fillers can progressively increase their volume during the pyrolysis step following the reaction with the decomposition products of the PDC, due to this increase the polymer shrinkage is compensated. This technique, known as active-filler-controlled pyrolysis (AFCOP), leverages volume-expanding fillers to address shrinkage challenges in PDCs, in the figure 16 a visual exemplification of the process is shown in function of the reaction time of the filler for a siloxane filled with 40vol% of Boron. [46] [30]

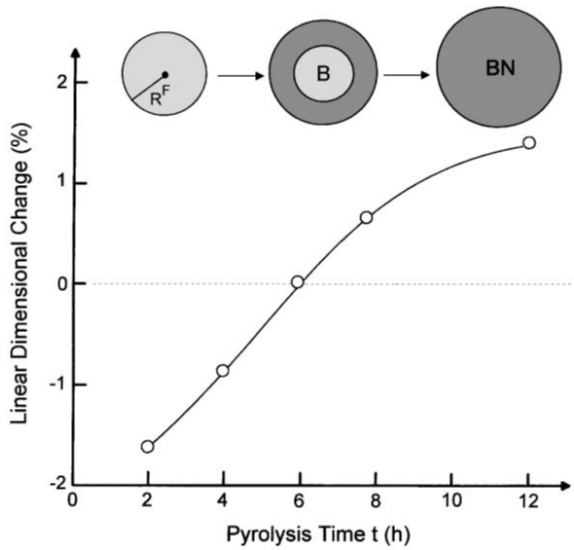

Figure 3-16 Siloxane boron filled (40vol%) pyrolysis [46]

Particle size of the filler takes an important part in the reaction, decreasing particle size, the reaction time of the filler is reduced. Consequently, within a given reaction time, a higher proportion of smaller particles undergo transformation compared to larger particles. This results in a greater overall reduction in shrinkage.

The tailoring of the filler properties to the PDC can lead to low or even a net zero shrinkage during the ceramization process as reported by Peter Greil in "Near Net Shape Manufacturing of Polymer Derived Ceramics". Although, to achieve zero shrinkage, it is obtainable only by leaving a certain amount of residual porosity in the final part. As already discussed porosity means lower mechanical properties, in the next figure some experimental data are shown where the correlation between shrinkage and porosity for a polymethylsiloxane(white circle) and polyphenylsiloxane(black circle) are visualized. [46]

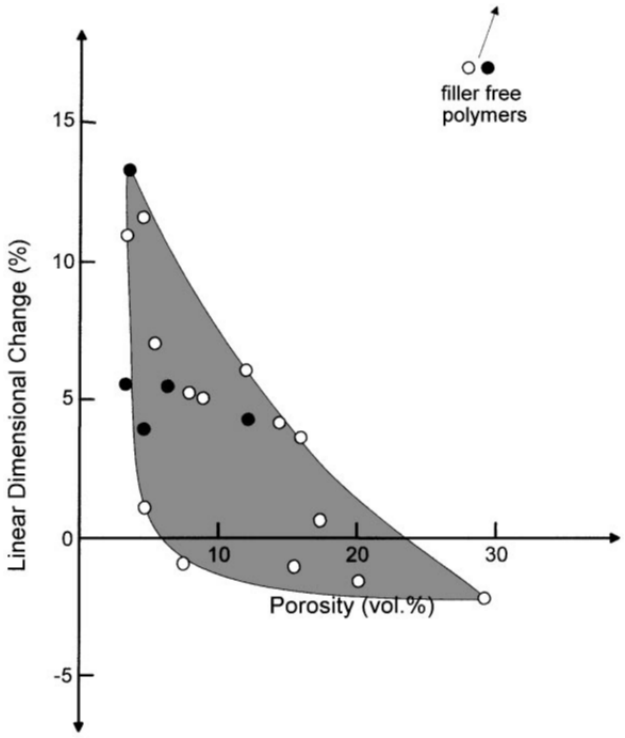

Figure 3-17 Shrinkage versus porosity of various poly(siloxane)/active filler systems pyrolyzed at 1200–1400°C [46]

3.3.3. Meltable filler:

The third category of fillers used in PDC coating systems consists of meltable materials, typically glasses. When subjected to pyrolysis and high temperatures, these glasses can melt or soften, which helps to seal porosity and densify the layer, thereby enhancing its protective performance against oxidation and corrosion. Additionally, by softening at high temperatures, they lower the Young's modulus of the coating or the joining material, allowing for the relaxation of thermomechanical stresses caused by thermal expansion mismatches between the substrate and the filler/ceramic material, as well as between the fillers and the precursor matrix. If an

inappropriate type of glass is used, pyrolysis at high temperatures can lead to an excessive decrease in the viscosity of the melted glass, or even cause the glass to crystallize or decompose. [30]

In contrast, if the temperature is not sufficient, it could result in unsuccessful softening or melting, leading to the glass merely acting as a passive filler. [30]

3.3.4. Sacrificial filler:

They are typically organic compounds that are incorporated into the Polymeric precursor. Following application and cross-linking, these fillers are removed through thermal decomposition or solvent dissolution, creating porosity within the coating. This porosity can be tailored in terms of shape, quantity, size, and distribution by selecting fillers with specific particle characteristics. In addition, the generated porosity due to sacrificial fillers contribute to the stress management by reducing the coating's effective elastic modulus, enhancing its strain compliance. [30]

3.4. Curing

After the processing of the polymer with fillers and the shaping the next step in the chain is the crosslinking. In order to have a highly cross-linked precursor a certain latent reactivity is required, the quality of the preceramic and the final ceramic is strongly influenced by this step. Precursors are usually composed by low molecular weight polymers, if a low level of crosslinking is achieved it would result in volatilization and depolymerization in the thermal steps following the curing. [47]

This step is crucial in creating the solid PDC structures. It involves converting a low viscosity, moldable organic precursor into a hard, non-meltable thermoset. This transformation ensures that the desired shape is maintained during subsequent processing steps. The hardening process, as known as cross-linking, is typically accomplished through heating in an oxidizing environment in the range of 100 to 250°C, chlorosilane cross-linking, or exposure to radiation such as microwaves, electrons, or gamma rays. The thermal curing is the most used method to achieve the crosslinking, preceramic polymers containing functional groups such as Si-H, Si-OH, and Si-vinyl can undergo spontaneous crosslinking below 200°C through hydrosilylation(addition) or condensation reactions, causing the formation of 3D polymeric networks. While traditional air-atmosphere curing of PCPs readily produces SiO_2 ceramics, this method is unsuitable for non-oxide ceramics. The incorporation

of up to 15 wt% oxygen can affect the thermal stability and compromise the overall performance of non-oxide ceramic materials. [47]

By introducing an appropriate catalyst or radical initiator, the thermal curing temperatures can be lowered, resulting in a higher ceramic yield due to decreased oligomer evaporation. The curing process can produce gaseous byproducts which can form bubbles within the polymer. These bubbles may be beneficial for creating porous materials but can be detrimental if a dense, pore-free ceramic is the desired outcome. [48] [49]

Effective cross-linking reactions yield highly branched polymeric structures with increased molecular weight, consequently minimizing the presence of oligomers and low molecular weight chains susceptible to volatilization at elevated temperatures. This ultimately enhances the final ceramic yield. 48] [49]

3.5. Polymeric to ceramic conversion

Following cross-linking, if additional heat treatments are conducted, typically at temperatures exceeding 300°C, pyrolysis starts, an organic-to-inorganic conversion is induced, transforming the thermoset polymer into an amorphous ceramic. Above 400°C, an open-pore network forms, further increase of temperature results in transient porosity, diminishing upon heating to 800-1000°C. For most precursors, the ceramic transformation is complete below 1100°C, while for some, the required temperature may be much higher. The amorphous network is constituted by different covalent bonds, the most common and important being Si-C, Si-O, Si-N and C-C. [31] [43] [29]

The pyrolysis mechanism involved in the polymer-to-ceramic conversion is typically complex. This process entails structural rearrangements and radical reactions that lead to the breaking of chemical bonds (such as Si–H, Si–C, and C–H), the release of organic functional groups (like CH_4, C_6H_6, CH_3NH_2, NH_3, and H_2), and the formation of an inorganic network. In an oxidizing environment, CO and CO_2 may also be released. [31] [46] [43]

The environment is an essential part in determining the final structures in ceramic. Due to its importance the reaction mechanisms during pyrolysis in different atmospheres have been investigated using techniques such as solid-state nuclear magnetic resonance (NMR), Fourier transform infrared spectroscopy (FTIR), Raman spectroscopy, and thermogravimetric analysis (TGA) combined with mass spectroscopy. [47]

To create non-oxide ceramics such as silicon carbide (SiC), silicon nitride (Si_3N_4), silicon carbon nitride (SiCN), silicon boron carbide (SiBC), or silicon boron carbon nitride (SiCBN), preceramic polymers are pyrolyzed in an inert atmosphere of argon or nitrogen. Conversely, silicate ceramics are formed when preceramic polymers are pyrolyzed in air with the addition of active metal oxide fillers. This method, particularly involving polysiloxanes and polysilsesquioxanes, is widely employed in the production of oxide ceramics. [30]

In order to have a quality indicator of the Polymer precursor and the thermal treatment applied to it is common to relate the final transformed ceramic weight to its polymer initial weight. This parameter or better this efficiency is called "ceramic yield" (α_c) of a PDC.

$$\alpha_c = m_c/m_p$$

The ceramic yield is typically in the order of 70 to 90%, with some reaching 105 wt% under specific conditions. in the last decades substantial effort have been made in order to modify the chemistry of the polymers and its processing in order to enhance the conversion to ceramic. [30] [31] [50]

Total weight loss is a cumulative effect of various processes occurring at different temperature ranges. The polymer's structure and composition significantly influence the final ceramic yield. Low molecular weight components, such as oligomers, can drastically reduce yield through vaporization and degradation during pyrolysis. As previously said effective cross-linking is crucial for producing a stable, non-meltable material and increasing the final ceramic amount. Organic side groups play a pivotal role in both cross-linking and the overall thermal decomposition process. [29]

The Pyrolysis step, causing most weight loss through bond cleavage and gas release, is a critical stage. Subsequent dehydrogenation and carbothermal reduction contribute to weight loss but are less significant. The weight loss trend is investigated by thermogravimetric analysis, in the next picture(fig18) can be seen that during the pyrolysis happens most of the mass loss. This step in the ceramization is also the main challenge in the creation of flawless parts, the gas release associated to the thermal treatment causes crack formation and shrinkage. [51] [30]

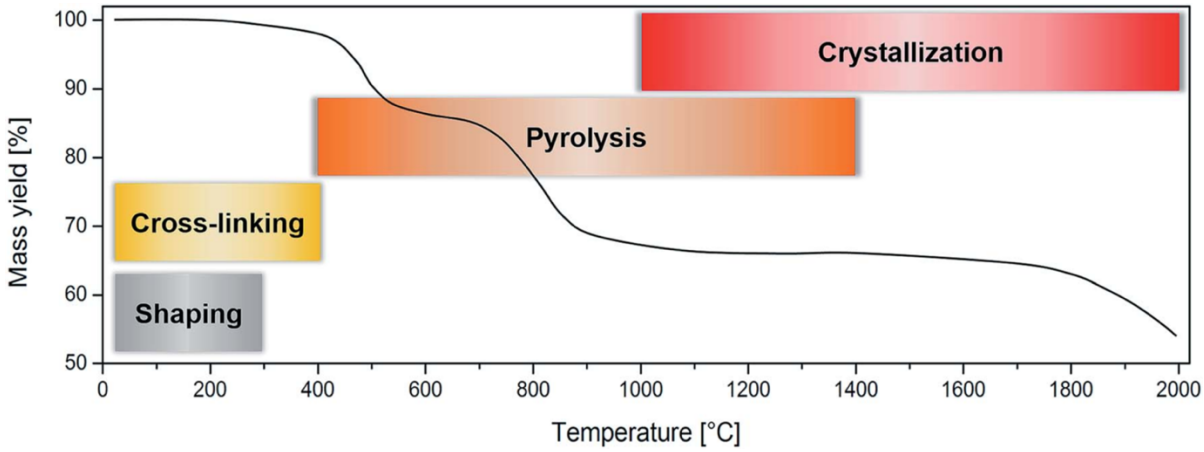

Figure 3-18 TGA analysis of a polycarbosilane in inert atmosphere [30]

During the polymer-to-ceramic transformation, in addition to the mass loss a significant reduction in volume occurs causing a major density increase (from approximately 1 g/cm³ to over 2 g/cm³)(fig19) This volumetric shrinkage, often reaching 40% linear contraction, can cause substantial shape distortion. Additionally, the release of gases during the early stages of ceramic formation leads to porosity. While some of these pores disappear due to material shrinkage, residual porosity can persist in the final product. [52] [30]

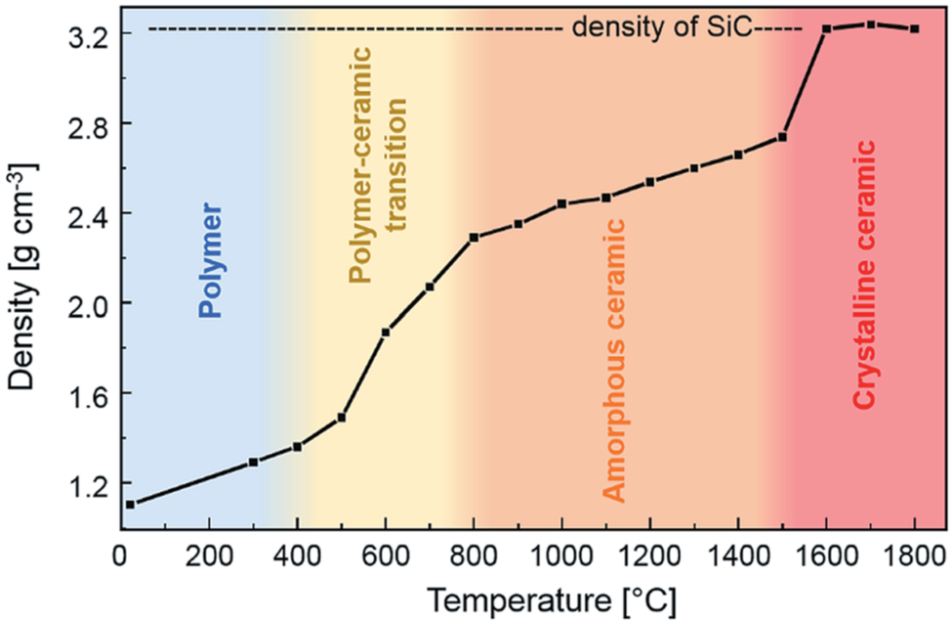

Figure 3-19 Density increase related to shrinkage of a polycarbosilane [30]

The shrinkage during the conversion can lead to significant stresses, in particular when different parts of a component shrink at different rates. This can induce significant internal stresses and, due to the rigid nature of ceramics, cracks may form,

compromising the structural integrity of the component, and in severe cases, leading to complete failure. [30]

In small dimension parts, in the order of hundreds of micrometers and smaller such as fibers, this behavior might be mitigated by viscous flow or diffusion process. Extensive research has focused on scaling up ceramic component dimensions to expand PDC applications, at the moment the introduction of different types of fillers has been so far the most widely explored possibility, as explored in the processing of the polymer in the previous chapter. [52]

3.6. Crystallization

During the ceramization process of PCPs, important parameters such as heating rate, reaction atmosphere, reaction temperature, and dwell time influence the phase composition and microstructure of the final ceramics. They influence the extent of crystallization, carbothermal reduction reactions, and filler reactions within the material. [31]

Generally, the heat treatment of the polymer derived ceramics ends at about 1100°C depending on the type of PDC since for many applications, crystallization is unnecessary or even undesirable, and processing is stopped once the amorphous ceramic is achieved. While most PDCs, especially those containing oxygen, tend to crystallize at temperatures as low as 1000–1200 °C, some materials can resist crystallization even at temperatures up to 1700 °C. [43] [53]

Further heating of the ceramic in the range of 1200-1800°C start gradually crystallizing the material causing several structural rearrangements. These changes are due to the rupture of chemical bonds that together with the atomic rearrangement causes the separation of ceramic and carbon phases to then form a multiphase ceramic system. The latter promotes nucleation, with increasing time and temperature the nuclei growth is sustained. The amorphous to crystalline transition is usually coupled with gas release due to the decomposition reaction of the process. [30] [54]

To sum up the processes in fig.20 a visual scheme of the material structures present at the different steps

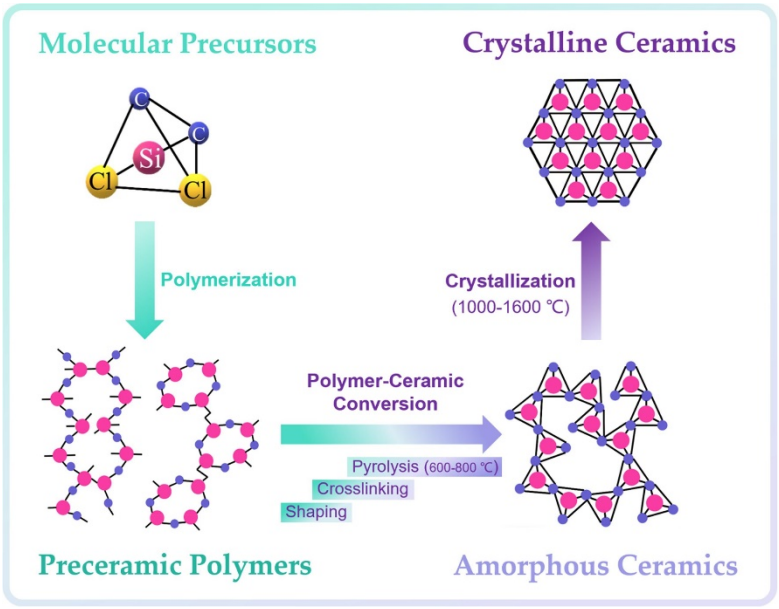

Figure 3-20 Material structure transformation visualized [55]

4 Materials

During this chapter a brief overview about the provided materials, that were used during the experimental part this work, and their properties will be provided.

The materials comprehend the oxide fiber oxide matrix CMCs, the Durazane 1800 which is a commercial polymeric precursor, the alumina nanopowder and the Nextel alumina fibers.

4.1. Ox/Ox Ceramic matrix composite

The focus of the present work is the joining of oxide fiber composite (OFC) using the polymer derived ceramic approach, with the objective of having a joint as strong as the base material.

The base material in this case is part of a relatively new class of compounds for high temperature applications. Like all ceramic matrix composite the behavior is pseudo-ductile in comparison to the brittle nature of just ceramic materials. This is mostly explained by the weak matrix concept. The porous matrix dissipated crack energy and additionally the weak bonding between matrix and fibers, instead of transferring the crack from the matrix right to the fiber, deflects the crack parallel to the fiber. [56]

The most used fibers to produce the OFC are Nextel™610 high purity α-alumina fibers, they have a maximum temperature application under load in the range of 1000°C, above that they are prone to degradation and consequently decrease of mechanical properties, but they will be treated more in detail later in the thesis.

These fibers are used together with a matrix of alumina and zirconia by the Department of Ceramic Materials Engineering of University of Bayreuth to provide the CMCs used in this thesis experimental work. [57]

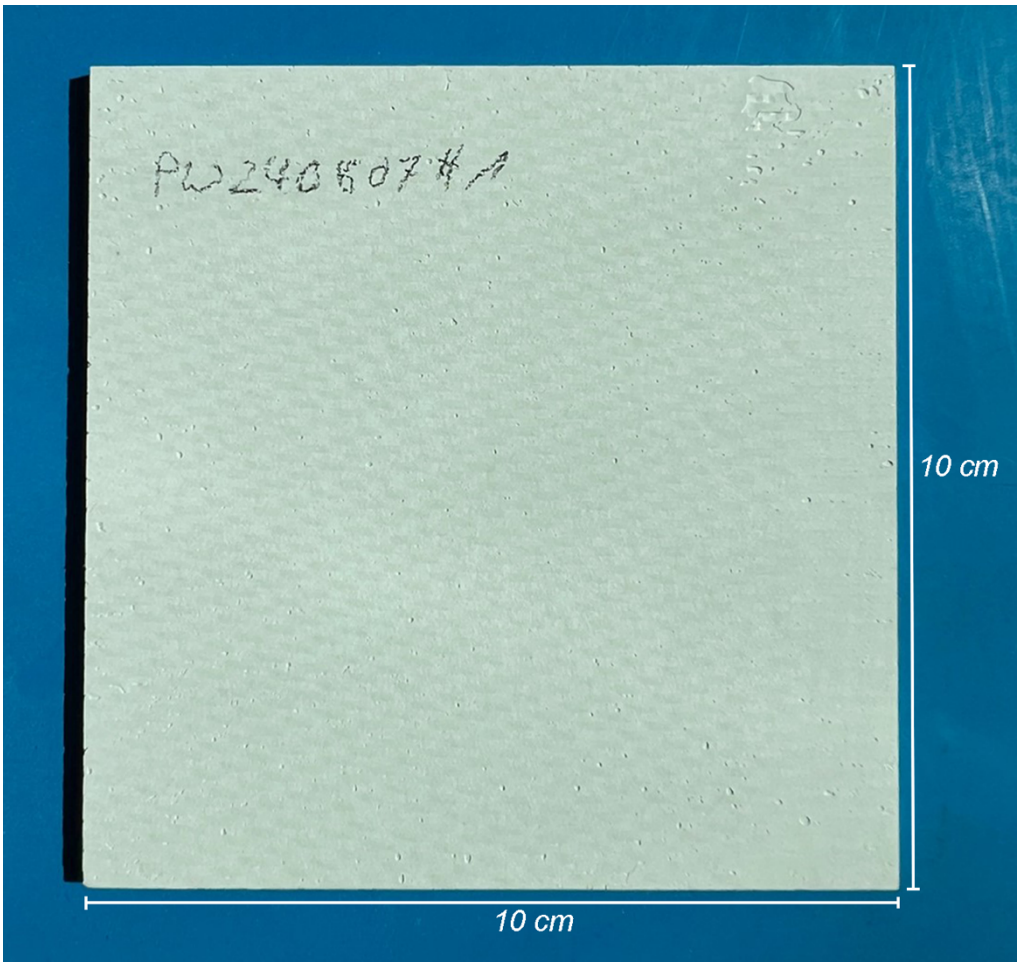

Figure 4-1 Oxide CMC quoted

The use of alumina and zirconia as matrix material is only one of the possibilities that are proposed in the literature for OFC. This choice is quite advantageous due to the matching CTE of the two materials and they both form thermodynamically stable and coexistent phases. Additionally, the porosity increase related to the grain growth of alumina particles is inhibited by zirconia, therefore preventing the decrease in mechanical properties. [57]

The process to produce the substrates starts with preparing the slurry. The solid content of the slurry is of 66.3 wt.% and comprised of sintering sluggish alumina powder (CT 3000 SG, Almatis, OYAK, Turkey) and 30 wt.% sintering-active powders, namely 3YSZ powder (TZ-3Y-E, Tosoh, Japan) and alumina powder (TM-DAR, Taimicron, Japan). The liquid phase is composed of the dispersant plus glycerol and water.

The infiltration of the fabric made of fibers with the slurry is followed by its placement between two release films and the slurry content defined by using a doctor blade with a gap of 800 μm. Every composite created is composed by 4 prepregs

that were laminated using a cold roll laminator. After the lamination the composite is dried and then sintered in a furnace at 1225°C for 2h in air in order to obtain the final product. A complete flow of the process with each entering and exiting compound is shown in fig2.

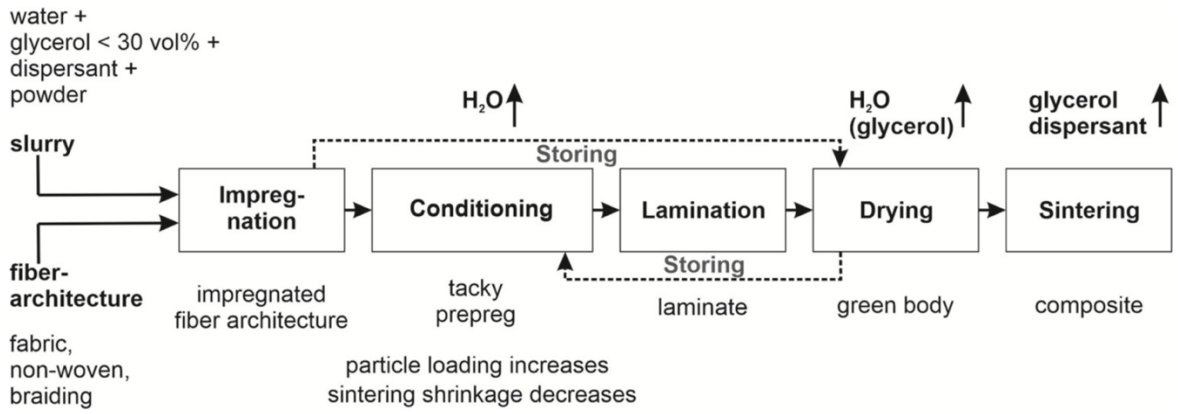

Figure 4-2 Prepreg process for OX/OX by Bayreuth university 57]

In the paper named "Novel prepreg manufacturing process for oxide fiber composites" by G. Puchas, S. Möckel, W. Krenkel the process of production of the prepreg is improved by testing how the variation of glycerol content affects the water sorption/desorption behavior of the slurries and by varying the conditioning route. An optimal value of 26 wt.% of the glycerol allowed to obtain the fabrication of the OFC in less than 36 hours thus proving the advantages related to the high reproducibility of the process, which also has potential to upscaling to an industrial scale. [57]

4.2. Durazane 1800

In this research activity the polymeric precursor is the Durazane 1800, a commercially available vinyl functionalized polysilazane resin from the german brand Merck. This resin other than the use as a polymeric ceramic precursor can be employed as a coating binder as it shows good adhesion,hardness, hydrophobicity and barrier properties. [58]

When used as a precursor, the pyrolyzed ceramic material shows excellent high-temperature stability, capable of enduring peak temperatures of up to 1000 °C, with a high ceramic yield of 80-90% depending on the atmosphere used, as determined by TGA. 58]

As the scope of the analysis the joining in oxidizing atmospheres, the Durazane will be thermally treated in air.

The structure of the Durazane 1800, which at ambient temperature is a low viscosity liquid(10-40 cP at 20 °C, density 0.950-1.050 g/cm3 at 25 °C), consists in a silicon and nitrogen backbone. It is schematized in a simplified way in the following picture(3a), (b) and (c) show the possible structures of the final molecule when groups are attached to it, usually being hydrogen, methyl and vinyl groups. [59]

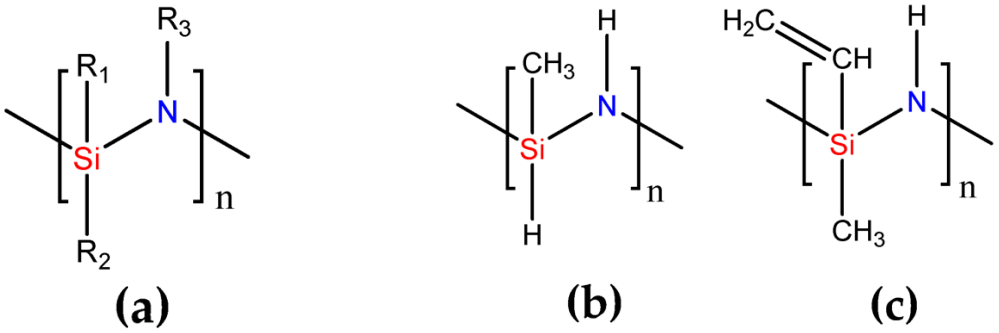

Figure 4-3 Durazane molecular structure a)backbone| b and c with groups 59]

The first step in the conversion of the polymer into a ceramic is the crosslinking. As discussed in the chapter that focused on the PDC, the correct and effective crosslinking leads to higher ceramic yields. The curing step, where the crosslinking happens, in this analysis is carried out in air.

The reactions that take place are different compared to the other atmospheres, in the ambient one the crosslinking reactions are mostly hydrolysis and polycondensation reactions, so basically the ≡Si–NH–Si≡ group reacts with a water or an oxygen molecule under formation of silanol groups, which subsequently polymerize to polysiloxane via polycondensation. [60]

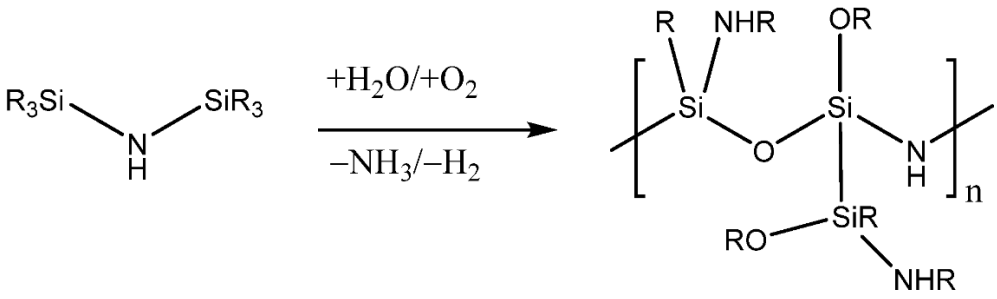

Figure 4-4 Hydrolysis and polycondensation reaction of Durazane 1800 [60]

As reported in the technical data of the product from Merck curing can be aided by using radical initiators which can reduce the temperature and/or the time of the process. The standard curing time without aids consists in a curing time of 4h at 180°C, this are also the setting that are used in the thermal treatment of this current thesis activity.

The next step is the pyrolysis of the cured polymer, it starts at temperatures above 400°C and goes on up to 1200°C, at this point further mass loss is negligible. In the following picture is depicted the trend of the mass loss related to the varying temperature with most of the loss occurring at sub 900°C. As reported by Motz et al. the mass change of Durazane 1800 is caused by the release of volatile oligomers, ammonia, hydrogen and methane, while the incorporation of oxygen occurs to form Si-O-Si bridges and result in a ceramic with an elemental composition of approximately $SiC_{1.15}$ $N_{0.68}$ $O_{0.42}$ after pyrolysis at 1000°C in air. [61] [62]

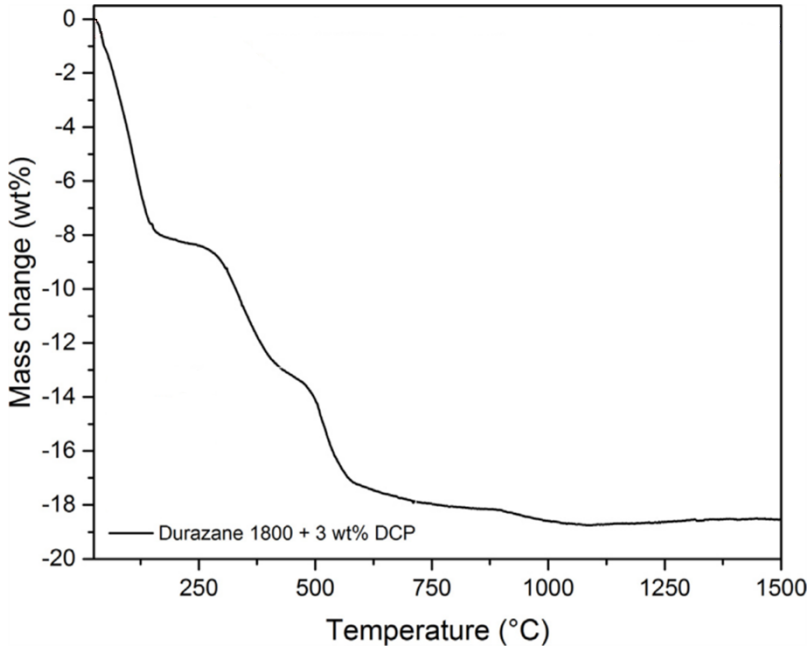

*Figure 4-5 TGA of durazane 1800 plus 3 wt% of DCP (curing agent) in air [*61]

4.2.1. Silazane adhesion mechanism

Silazanes mechanism of adhesion is for most of the surfaces due to chemical bonds involving the creation of oxygen bridges between surface and the silazane polymeric chain. Three primary mechanisms contribute to the formation of oxygen bridges between the silazane polymer and the substrate surface, as they are depicted in the following image. 63]

While these reactions can occur both at the interface and within the joining material, the limited availability of water molecules within the coating suggests that the initial adsorption of water on the substrate surface plays a crucial role in the formation of oxygen bridges. [63] The latter is the reason why before applying the polymeric precursor in the experimental part of the work some drops of water were deposited on the cleaned substrate.

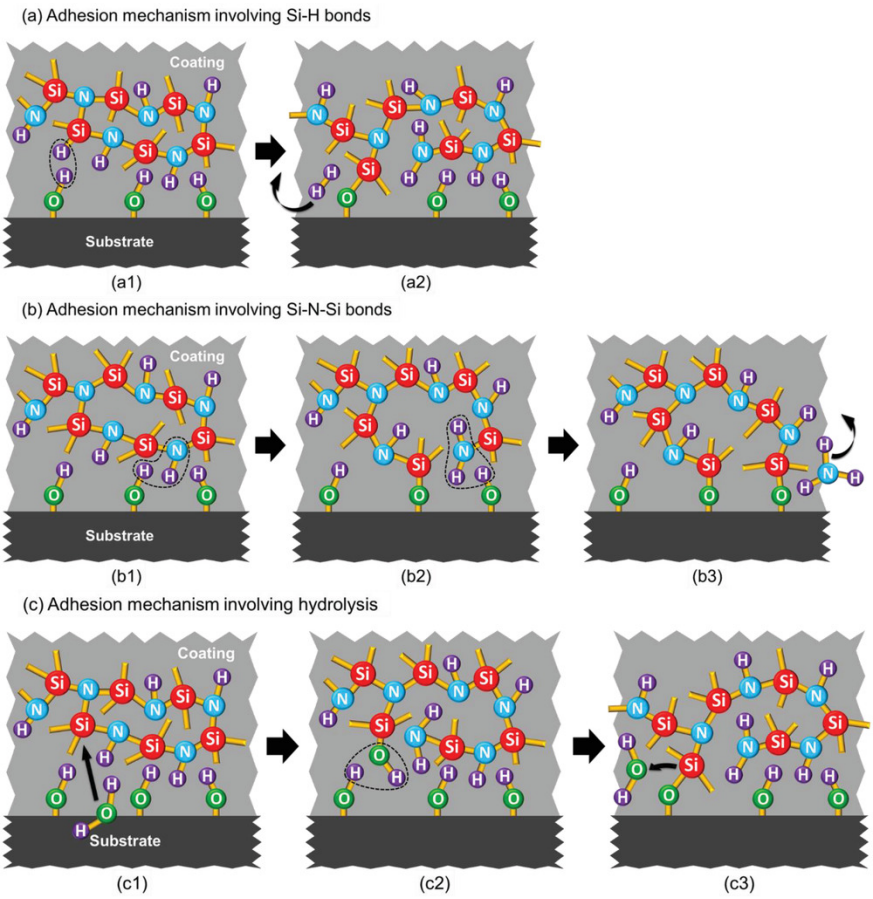

Figure 4-6 Silazane adhesion mechanism 63]

4.3. Fillers

The Durazane 1800 before use was processed by incorporating nanopowders and fibers with both being the same utilized in the CMC oxide fabrication.

4.3.1. Alumina powder

The nanopowders used as passive fillers, which do not engage in reactions during the pyrolysis of the polymeric precursors, are from Almatis, global leader in the production of high-quality alumina. More in detail the name of the ones used is "CT3000 SG" and they are characterized by high purity(99.7% Al_2O_3), a mono-modal size distribution with a mean particle size of D_{50}=0.55 µm, and typical specific surface area of 7.5 m^2/g. [64]

4.3.2. Oxide fibers

The fibers used are 3M Nextel 610, produced by the typical sol-gel spinning process. They are structural grade ceramic fibers based on a fine-grained single-phase composition of α-Al_2O_3.

However, because it is essentially single phased, the strength rapidly decreases at higher temperatures (about 1100°C) due to grain growth as shown in figure 7, in which they are compared to the Nextel 720 type which has a mullite structure able to sustain higher temperatures. [65]

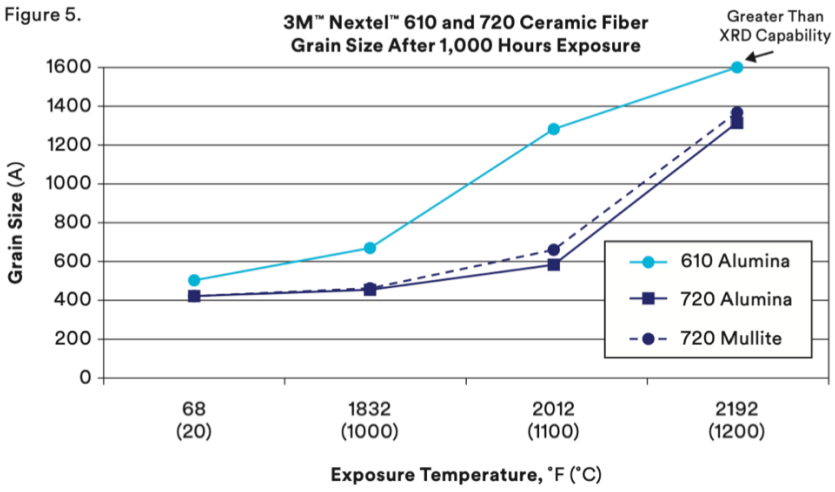

Figure 4-7 Grain size growth with increasing temperature 65]

At room temperature the tensile modulus of the fiber is 370GPa while its tensile strength is 2800 MPa.

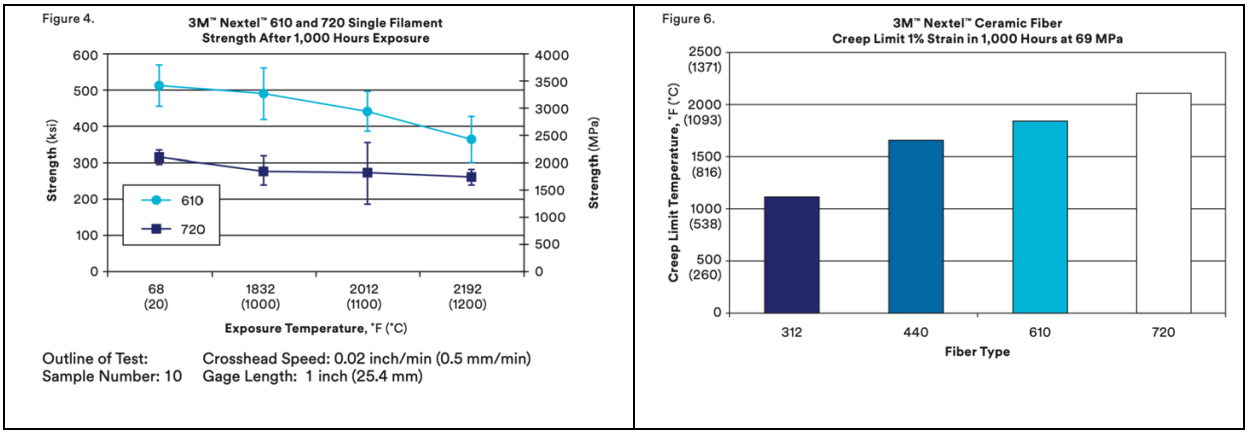

Figure 4-8 Strength and Creep limit after 1000 hours exposure 65]

The fibers as received are covered by sizing, a processing aid to provide lubricity and binding action to have both protection and easier handling. The Nextel 610 uses a sizing composed of polyvinyl alcohol (PVA) and additives (plasticizers, lubricants, etc.), that are designed for easy removal by heat cleaning. They appear white to off-white or yellowish (shown in picture 9) both before and after sizing removal, but usually a pigment is inserted in sizing to aid the identification.

The removal of the polymeric sizing is done by heat cleaning, keeping the fibers at a soak temperature of 700°C for a different amount of time depending on the furnace and the quantity of material inside. [65]

Figure 4-9 Visual appearance of the Nextel 610 fiber fabric [66]

5 Experimental part

This chapter provides a detailed description of the experimental methods used to fabricate the joints, outlining each stage of sample preparation, processing of the polymer, and testing.

5.1. Preparation of the substrates:

As addressed in the previous sections the dimensions of the substrates provided by the University of Bayreuth are quite large. In order to adapt them to the activity's needs different sizes from the original tablet were obtained.

For the first step of the experimental activity the target size of the substrate is 15x10mm, these dimensions were achieved by cutting the original tablet using the Brilliant 220 cutting machine. For the second stage, in which the substrates were subjected to mechanical testing the machine required bigger dimensions, so additionally 25x25mm substrates were produced. The Brilliant 220 is a precision wet abrasive cut-off machine, in case of the Al_2O_3/ZrO_2 CMC the machine should be equipped with diamond cutting wheels.

The cutting can be easily tailored to the material which needs to be processed, in this case all the substrates were cut under the same conditions which will be reported under the following table.

Nextel 610/Al_2O_3-ZrO_2	Mode	Blade [RPM]	Speed[mm/s]
	horizontal	3200	0.07

Figure 5-1 Brilliant 220 cutting machine

5.1.1. Polishing

Following the cutting process, all the pieces were measured by using a digital Caliber to ensure the dimensions were correct. If not, the error would be usually lower than a millimeter so refined by using the Polishing machine, eliminating the need for further cutting.

The actual polishing of the surface of the dimensionally accurate substrates was then carried out by using the Struers LaboPol-2. SiC paper with a coarse P320 grit was employed as polishing material. The grit selection was determined by preliminary experiments conducted by previous graduate students and doctoral researchers as it optimizes the material removal without damaging it.

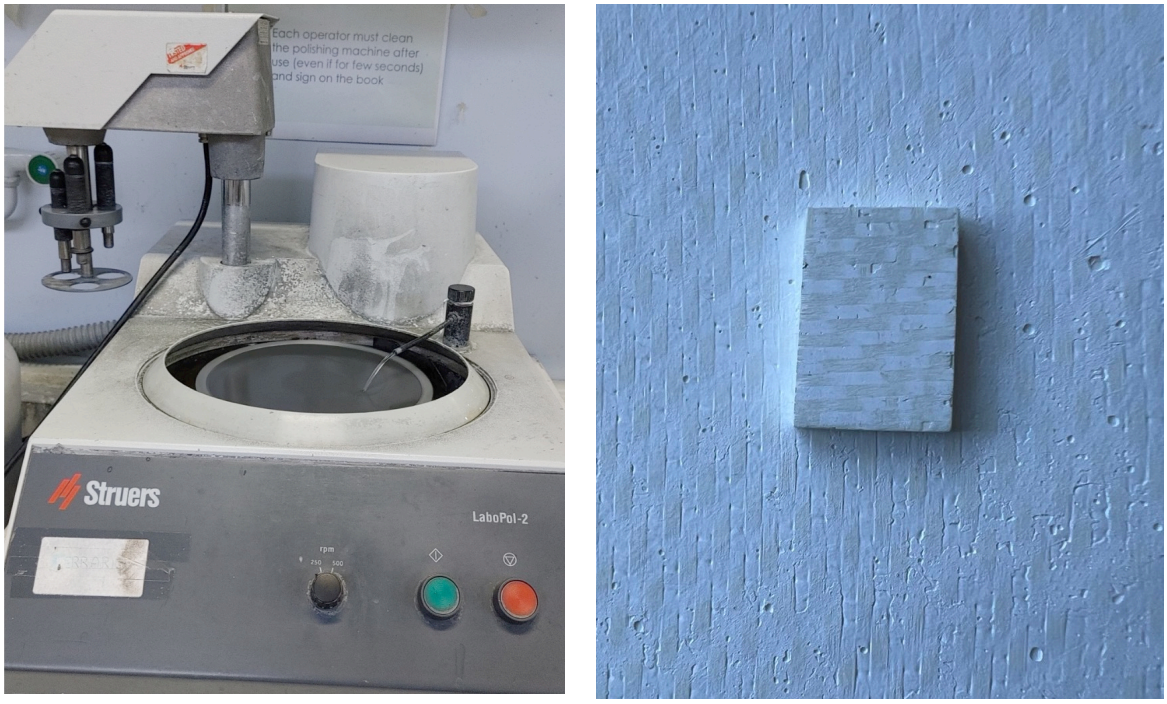

Figure 5-2 a) Labo-pol 2 b) polished substrate in front, unpolished in the back

The polishing activity was performed at low speed, 250RPM, for a sufficient time to visibly expose the fibers thus enhancing the infiltration of the polymeric precursor in successive steps.

5.1.2. Cleaning process

Right after the polishing process, the cut substrates were dried and placed into a beaker filled with ethanol. Once all the necessary substrates were polished the beaker was inserted into the ULTRASONIC CLEANER PROCLEAN 4.5S ULSONIX.

This ultrasonic cleaning machine by performing a 10-minute cycle at 40°C, frees the substrates from dust particles, grease and other contaminants. This step is particularly crucial due to the high porosity (28%) of the substrates, as all of its active sites need to be free from dust and other contaminants to facilitate strong bonding with the preceramic polymer.

5.2. Filler dispersion

Differently from other preceramic polymers, which are usually stored while in solution with solvents, Durazane 1800 can be used directly from the bottle, eliminating the need for additional processing steps before application.

To enhance the performance of the precursor, the incorporation of fillers has proven to be an effective if not the best solution, up until now, to reduce shrinkage, porosity, and other issues discussed in the PDC chapter.

By using the ULTRA-TURRAX IKA T10 Basic disperser, different quantities of Alumina nanopowders from Almatis (CT3000 SG , D50=0.55 µm) were dispersed. Featuring a maximum possible viscosity dispersing capability of the machine of 5000 mPa·s even high wt.% of aluminum oxide could be dispersed. Additionally, fibers were incorporated into the filler dispersed Durazane 1800.

Weighing of the Aluminum oxide nanopowders and oxide fiber was a critical preparatory step.The weight of the preceramic polymer determined the amount of filler to be added, so it was also the first to be weighted. Given the toxicity of Durazane, both weighing and dispersion were conducted under complete exhaust fume hood. The Durazane 1800 (4-5 mg) was dispensed into a cylindrical container, filling it approximately halfway. Using weighing boats, the appropriate amounts of powder and fibers were accurately measured.

The dispersion process was then carried out by gradual addition of small amounts of the alumina powder into the Durazane 1800, using a laboratory spoon. The machine was then turned on to initiate the dispersion process. The ULTRA-TURRAX rotation speed was kept consistently low, typically between levels 3 and 4. Once the initial small amount of Alumina powder was fully dispersed, the process was repeated by adding more powder until the entire weighed quantity was incorporated into the Durazane 1800.

Figure 5-3 ULTRA-TURRAX IKA T10 Basic and 80% filled resin

Initially, the fibers were dispersed before the powders. However, a part of the fibers at the end of the process was sticking into the machine. By adding them at the end and manually disrupting the fiber textile structure, the correct dispersion of the fibers was ensured. This problem was likely also solved due to the increased viscosity of the particle-filled Durazane 1800. At the end of the process the instrument was cleaned with acetone as indicated by the Merck spreadsheet information on the polymer removal.

A total of 5 different weight percentages of aluminum oxide were dispersed and investigated to identify the optimal value While the initial plan included varying the fiber weight percentage, this was ultimately limited to a constant 1 wt.% due to concerns about damaging the delicate dispersing machine. In the following table the values in weight are reported for all the filled resin, the "r." indicates the real measured values while the "exp"(for experimental) indicates the calculated ideal values.

FIBRE 1%

Nanoparticles wt.%	50%	60%	70%	80%	90%
Barattolo a vuoto [g]	8.493	5,481	5.414	8.492	8.493

Durazane 1800 [g]	4.909	4.179	4.063	4.134	4.387
exp nanoparticles [g]	2.4545	2.5074	2.844	3.307	3.947
exp fiber [g]	0.04909	0.04179	0.0406	0.041	0.043
r. nanoparticles [g]	2.501	2.51	2.842	3.308	3.944
r. fibers [g]	0.0491	0.045	0.041	0.042	0.043

Table 1 Durazane 1800 with fillers values

5.3. Shaping and Thermal Processes

Once the resin is ready and the substrates are cleaned the shaping and curing are performed.

For each resin filled with different percentages both a coating and a joining were prepared. The procedure consisted in the wetting of the surface of the substrate with a droplet of distilled water which was then partially dried, this simple escamotage again investigated by previous graduate students and PhD was revealed to enhance the adhesion of the resin to the surface.

After ensuring the adsorption of water in the substrate, the excess was dried, the resin was applied to the substrate and then flattened with a spatula. For the coating nothing else was done while the 2 joined substrates were pushed together by applying a little weight on top, due to the low viscosity of the resin the thickness of the joining material become very thin, as we will see later in the order of 100 microns.

These samples were used to investigate the best microstructure related to the filler quantity, with the scope to achieve the best joining results. While simple overlapping was sufficient for the microstructure analysis, for mechanical test instead an offset between the 2 substrates was needed. In order to do so without relying too much on the precision of the user, a block of foam glass was carved in order to precisely have the substrates locking into it with a certain offset. This procedure was specifically employed for the specimen which were going to be subjected to mechanical testing.

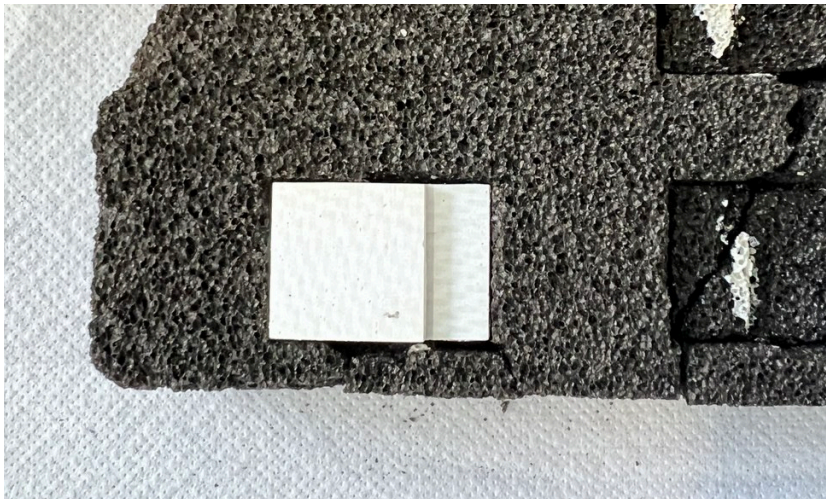

Figure 5-4 CMC offset in the foamglass carved slot

The next step involved the crosslinking or curing of the resin. Merck, the producer of Durazane 1800 advised a residence time of 4h at 180°C. This process was performed in the Binder ED 23, a drying and heating chamber with natural convection. All thermal processes were performed in air.

Since the importance of crosslinking is very high, to ensure the temperature displayed on the oven is accurate, a thermocouple temperature verification was performed. The shown temperature corresponding to actual 180°C, was 205°C on the oven.

Visual inspection of the cured samples was necessary to ensure no contamination happened during the dispersion of the particles. In a few instances the samples appeared to have a dark grey color which is instead supposed to be off-white. As it is shown in the picture below, the color of the top row, which corresponds to the 70wt.% samples, is completely different from the others. When this happened, the entire dispersion had to be done again from the beginning.

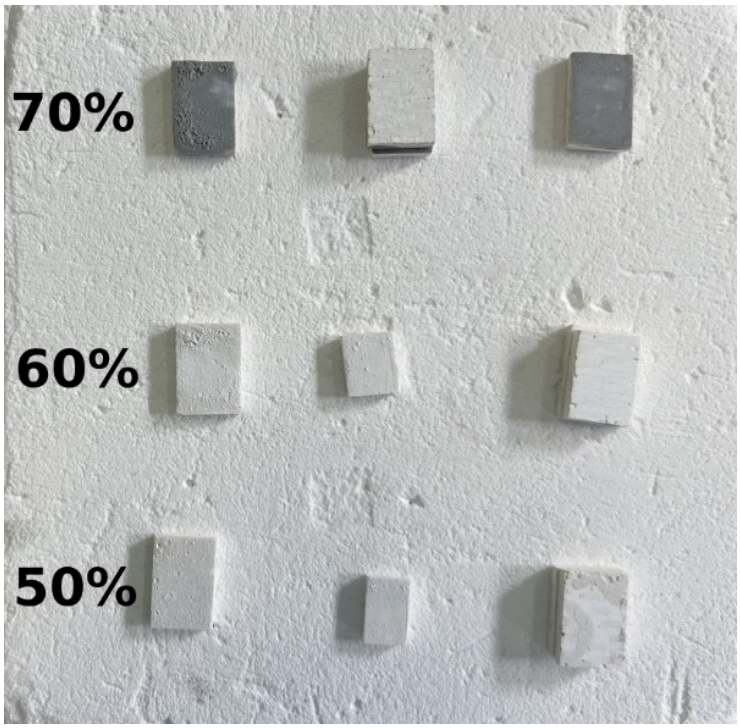

Figure 5-5 Pyrolyzed samples, top row contaminated

After the curing was effectively concluded the pyrolysis step was next. The furnace in which the thermal treatment was conducted was the Carbolite CWF 1300. Due to breakdown of the furnace few of the samples were produced in a different furnace, but in both cases the calibration curve was strictly followed in order to have consistent results.

In the following graph the thermal process which was performed is illustrated. It is known from literature that the majority of the reactions and weight loss happen between 400 and 800 degrees Celsius, to reduce at the minimum the stresses and possible cracking the heating rate is lower within the two values.

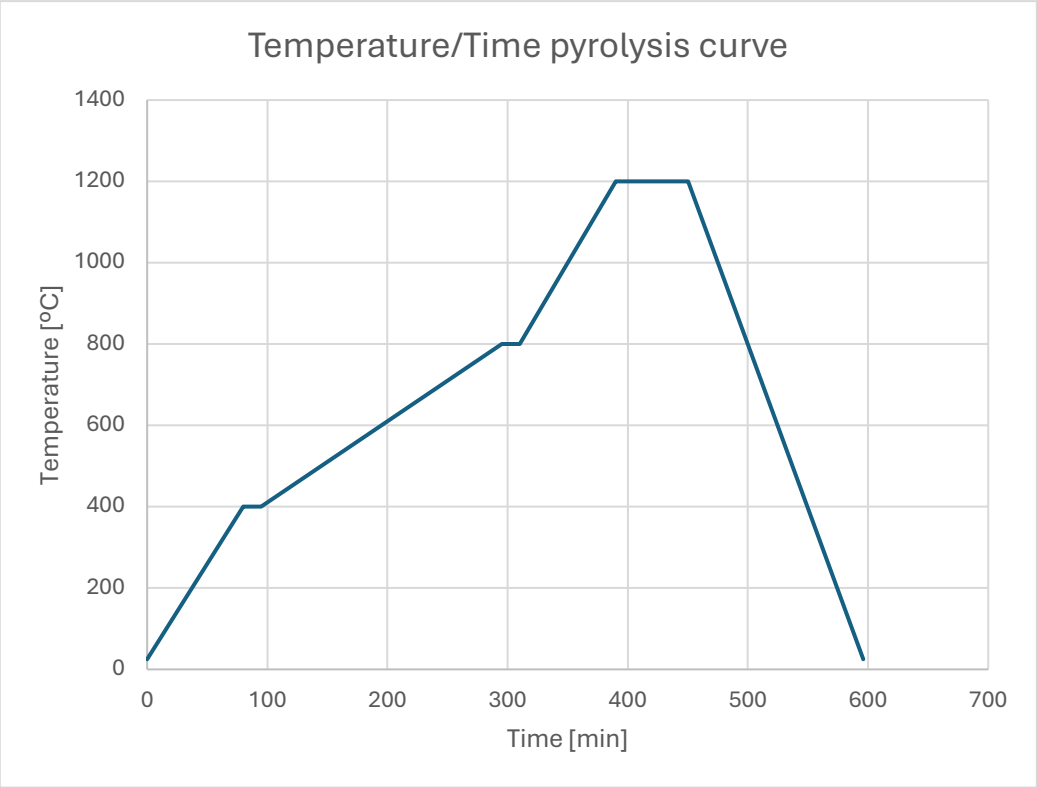

	Heating rate [°C/min]	T set point[°C]	Holding time [min]
step 1	5	400	15
step 2	2	800	15
step 3	5	1200	60
cooling	8	25	

Table 2 Thermal treatment steps

5.4. Analysis

Once the samples were ready two kind of analysis were performed: microscopic analysis of the structure in both coatings and the joining interface, as well as mechanical testing.

The joints observed were cut in half in longitudinal direction in order to observe an internal section, more representative of how the actual situation. Resistance to cutting served as a preliminary indicator of successful joining.

5.4.1. Scanning Electron Microscope (SEM)

The microscopic analysis was done by using the JEOL JCM-6000 PLUS which is a Scanning electron microscope.

A scanning electron microscope (SEM) operates by directing a focused electron beam across a sample's surface while capturing the resulting signals with dedicated detectors. Electrons are produced and accelerated at different specified accelerating voltages (in case of the JEOL 5-10-15 kV). The interaction between the electron beam and the sample's atoms generates various signals that reveal details about the sample's surface topography and composition. These images are displayed in real-time on an external monitor, where software synchronizes the beam's position with the intensity of electrons detected. Common detectors used for high-resolution imaging include the secondary electron detector (SED) and the backscattered electron detector (BSD). For surface composition analysis, energy dispersive X-ray spectroscopy (EDS) detectors are employed. The specific configuration of a SEM influences its resolution and available imaging modes.

SEM can analyze a wide array of solid materials directly. However, insulating samples such the oxide CMC used in this activity need to be sputter-coated with a thin metal layer, like gold or platinum, to reduce charging effects.

The material of choice for the sputtering in this case was platinum as it shows better material compatibility and stability with the OCMC, a cycle of 20 seconds of platinum sputtering was done for every sample observed at the microscope.

5.4.2. Mechanical testing

With the objective of concluding the research of the optimal weight percentage of filler dispersion on the Durazane 1800, a final mechanical testing was conducted on the two samples that exhibited the most promising microstructure.

The instrument in which the tests were performed was the Zwick Roell Z050. The machine can perform a big variety of tests and has a maximum test capability of 250kN. The high range of possible speeds, from 0.00005 to 3000 mm/min makes it ideal to all type of material testing.

Since the objective of the joining of this kind of material is to work at very high temperatures, the dimensions of the test samples were changed to fit the specimen grip able to resist to high temperature test. The high temperature tests were restricted to cases in which the ambient temperature ones had a positive outcome.

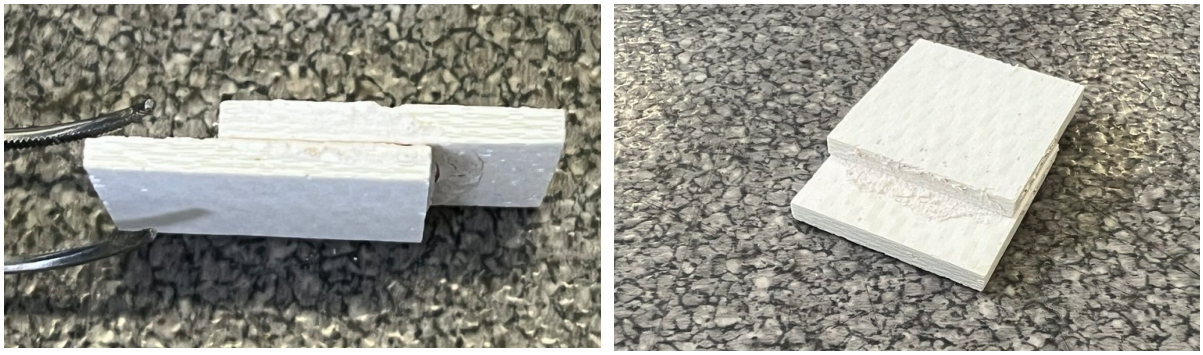

Figure 5-6 Test samples

The specimen grip, called "reversal cage" was designed for test samples with shape and dimensions as shown in the following picture. Due to a different design thickness of the substrates compared to the one required by the grip, it was seen that by increasing the thickness using another piece of OCMC the target thickness was obtained. By using a commercial adhesive, the additional substrates were glued to the test sample, a gap was intentionally left to exclude any participation of the substrate in the test.

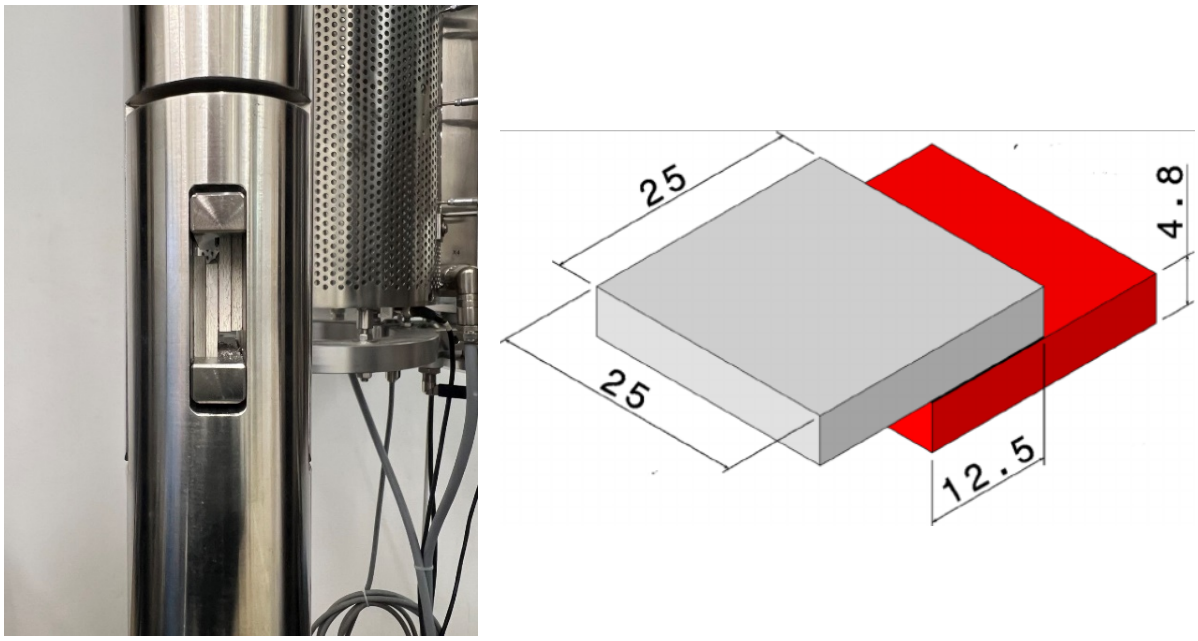

Figure 5-7 On left the specimen grip with sample pre-test, on right the design dimension for the specimen [67]

This specimen grip is subjected to a tensile force by the testing machine, doing so the height of the zone in which the sample is placed undergoes a reduction, inducing compressive stress on the specimen. The test speed was set to 1mm/min.

6 Results and discussion

Obtaining joints by using polymer derived ceramic has quite few complications compared to the theoretical prediction. From previous experiments its was acknowledged that using only the polymer precursor without the addition of any kind of filler can lead to poor results. The Durazane 1800 is engineered for use as a coating, the wettability and adhesion test were successful on the Oxide CMC with infiltration of the matrix due to low viscosity, similar to water. This preliminary study on adhesion was conducted only up to curing step. When the same pure Durazane was tested in a joint configuration the result was the detaching of the pieces, but not due to adhesion. Cohesion forces weren't strong enough even when still only in the thermoset polymeric phase. As known from literature by dispersing an amount of filler in the resin we could be able to get an increase in strength.

An insufficient amount of filler would mean a low increase in strength, instead a value which is too high would lead to an inadequate link between the filler and the resin, leading to detachment of the powder and fragility, in the end resulting again in lower strength.

The value of filler incorporated is essential to determine the maximum strength possible from the PDC. Ideally, the volume of filler added should match the volume loss during pyrolysis. However, accurately correlating mass loss from thermogravimetric analysis to volume loss was proved challenging due to material transformations and density changes during the thermal process.

Therefore, for the rest of the experiment a more conventional trial and error was adopted. The pivot point was a starting mixture with 60wt.% concentration in filler, which already demonstrated to keep the joint together, from this point other 4 concentration (50, 70, 80,90 wt.%) were investigated. In table 1 all the weight values for each concentration can be found.

For each concentration both coating and joint were created, followed by their characterization, so analysis of the morphological properties and the structure of the ceramic material. Analysis of the coating at the Scanning electron microscope was performed to assess the cohesion properties of the PDC in top view configuration, for what concern the joints as previously said a longitudinal section (after cut) was analyzed to better understand the adhesion and bridging between the substrates.

Starting from the lowest filler concentration(50 wt%) the topview showed a relatively smooth surface, the visible porosity was quite low. Although where present, it was the reason of the crack formation and propagation. At the lower magnification and indicated in the picture some fibers are visible, as it can be seen they work as supposed to by deflecting the crack.

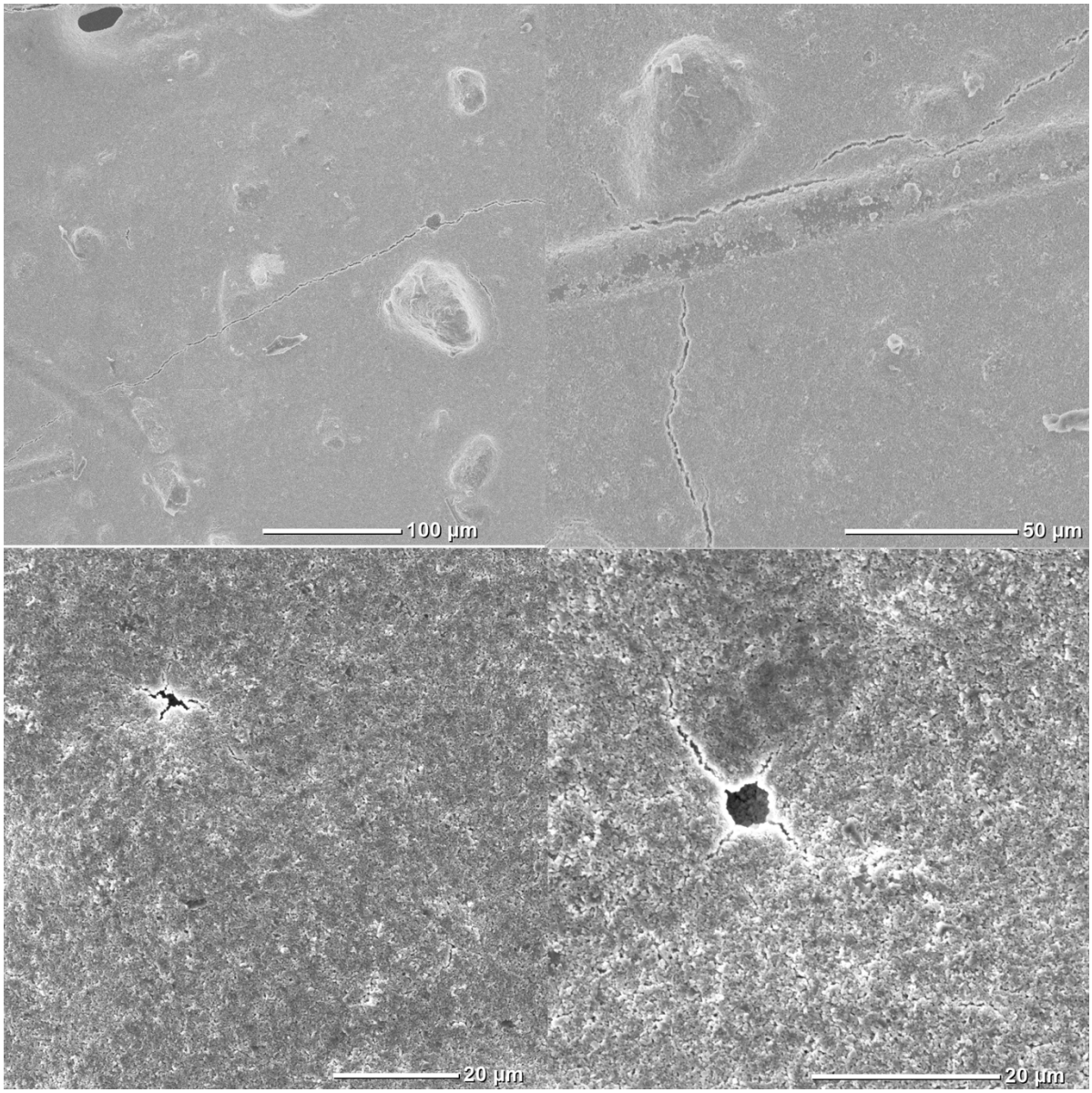

Figure 6-1 50wt.% coating samples at increasing magnification

Examining the images at higher magnifications, can be observed that the larger pores visible at lower magnifications (top row) can initiate smaller cracks. Nevertheless, these cracks are often arrested by the surrounding matrix. Overall, the structure appears quite compact.

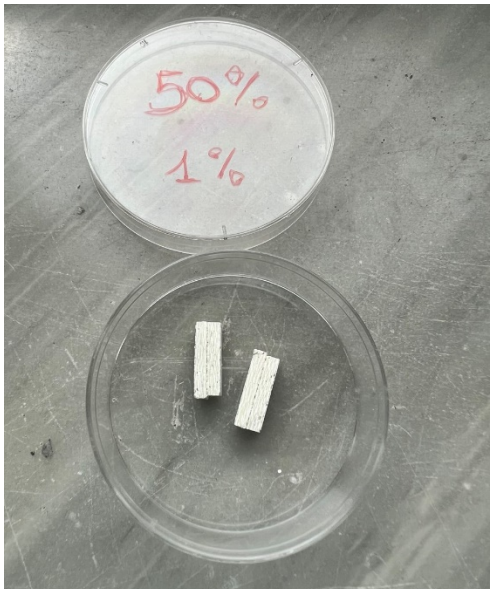

Figure 6-2 50wt.% samples right after cut

Moving to the joint, different pictures at low magnification(20x) were made in order to capture in its entirety the longitudinal section. By using a software the images were combined together, the final picture is reported below.

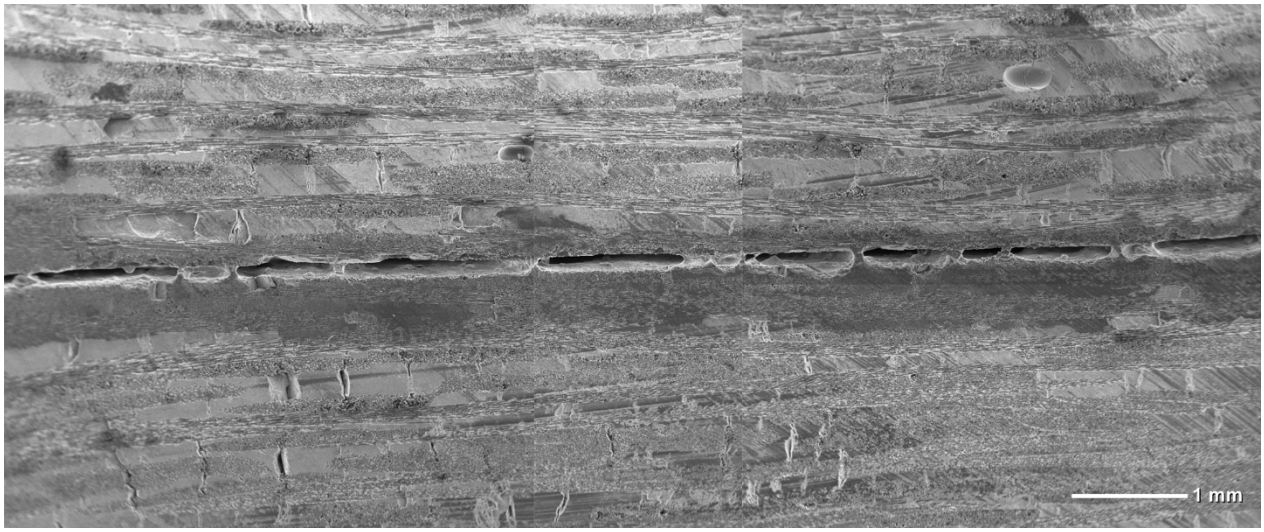

Figure 6-3 50wt.% full joint cross section

Unfortunately, the images indicate that only in few points of reduced width there if full connection between the two samples. This limited bonding would lead to low mechanical strength, as the stress would be concentrated in a much smaller area than the overall joint area.

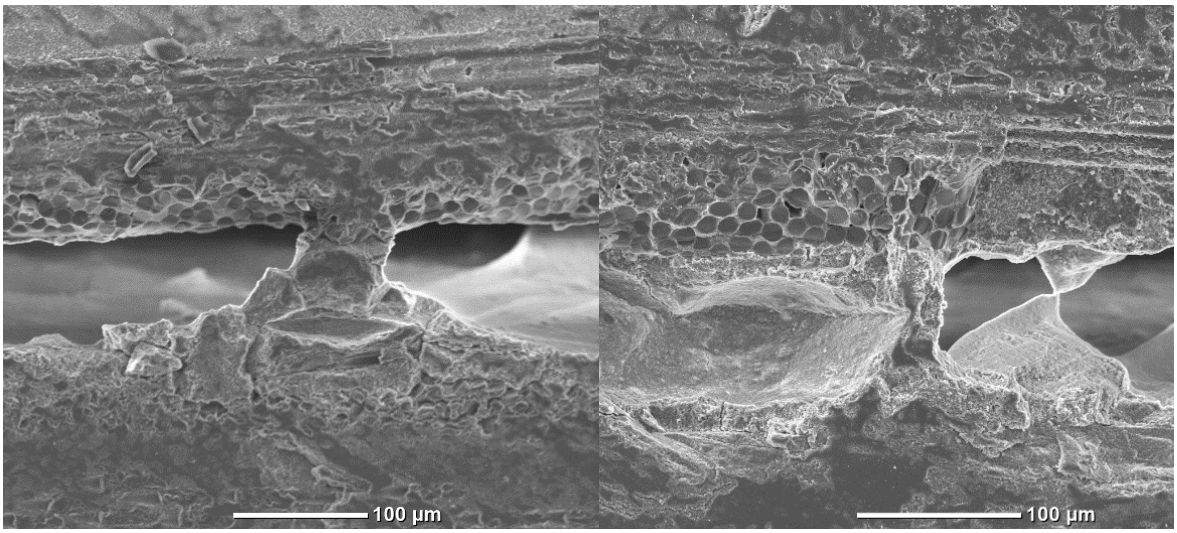

Figure 6-4 Magnified 50wt.% joint

When magnified, focusing on the continues structure bewteen the different substrates we can notice that a proper wetting and adhesion to the exposed fibers is present. Although in the middle region, at equal distance between the substrates a narrowing is typically present so further reduction of the active resistant area. Additionally, significant voids are evident between the substrates, especially in the background.

Moving to the 60wt.% samples, in the coating as shown in the following images a little difference from the previous can be noticed as the cracks from the porosity formed less frequently and with lower propagation. Some bigger structures are present, probably due to agglomeration of powders and can be attributed to ineffective dispersion.

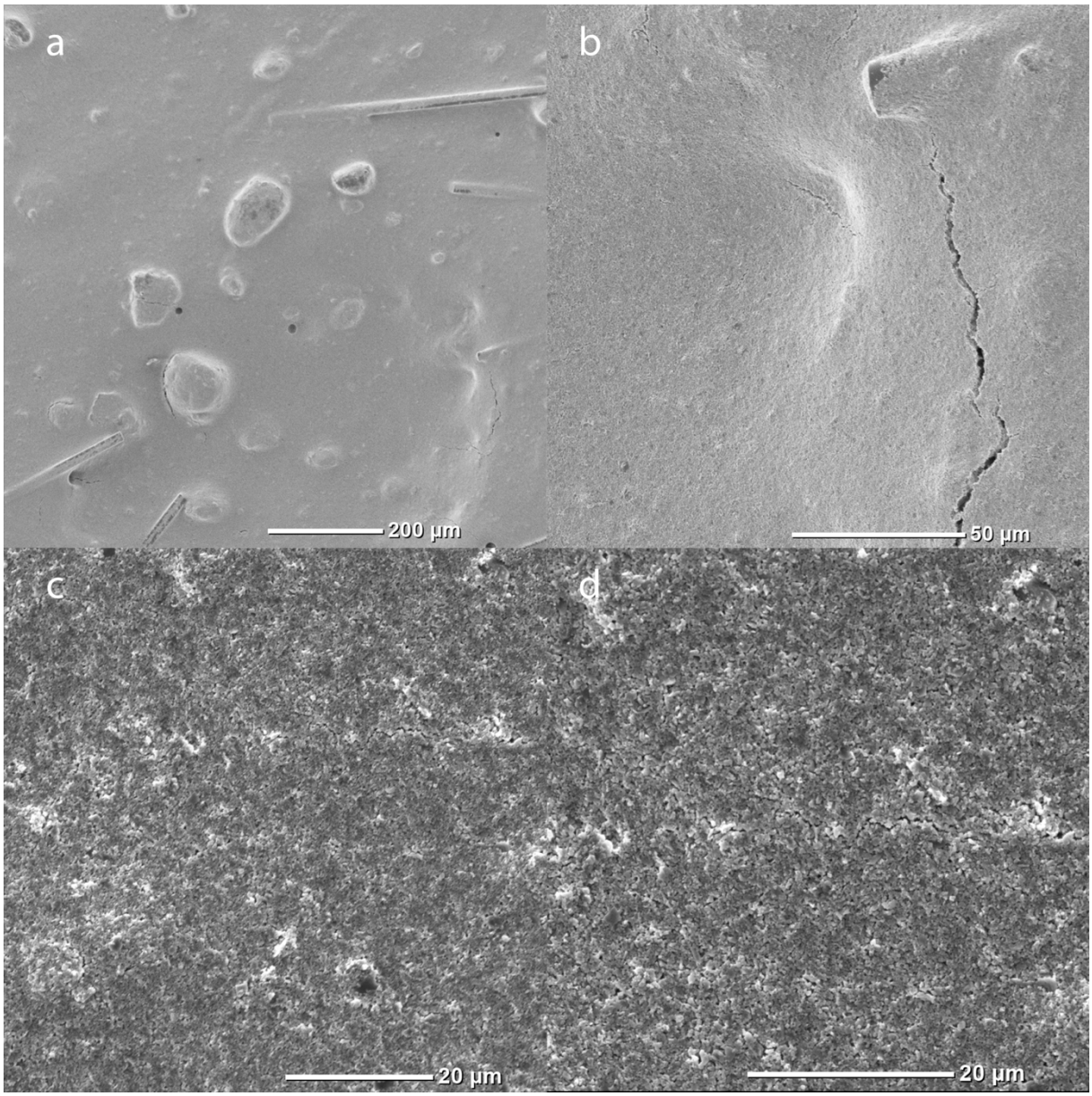

Figure 6-5 60wt.% coating samples at increasing magnification

The thickness of the coating is not uniform, in the zone higher in thickness(down right in fig.5a) a concentration in the presence of cracks is noticed as expected, in the following pictures a magnification of that cracked zones(left x1500, rigth x2400) is shown. Again, also in this wt.%, on the second magnification a fiber blocking the crack propagation is visible.

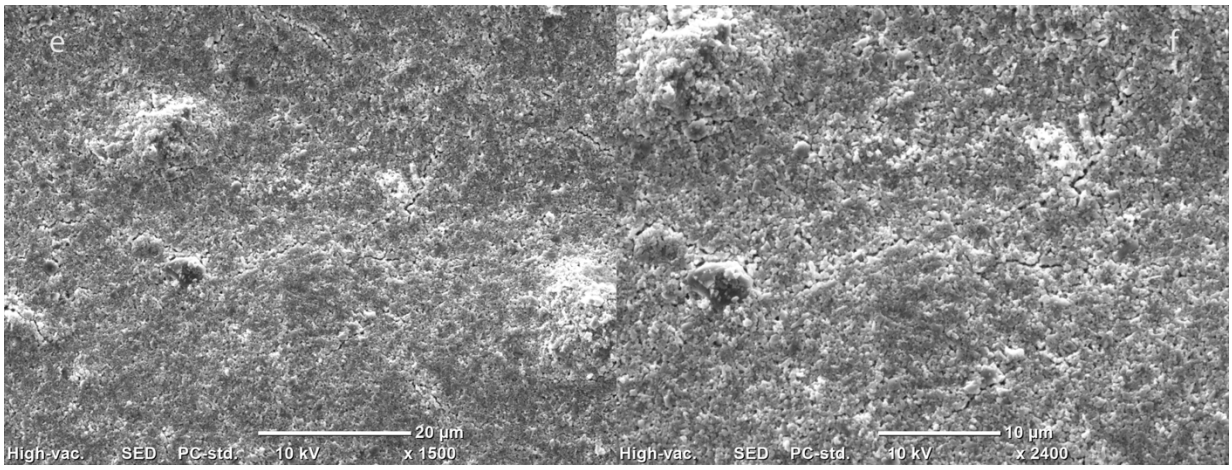

Figure 6-6 50% cracked zone magnification

Photo d and e have the same magnification, on photo f the zone magnified is the one with increased thickness, the probability to find cracking is therefore higher as it can be seen. On photo f (x2400) the crack is easily seen.

In case of the joint, when proceeding with its longitudinal cut, half of the 60wt.% cut joint didn't held together due to poor handling. The other half instead resisted, and its images will be shown shortly.

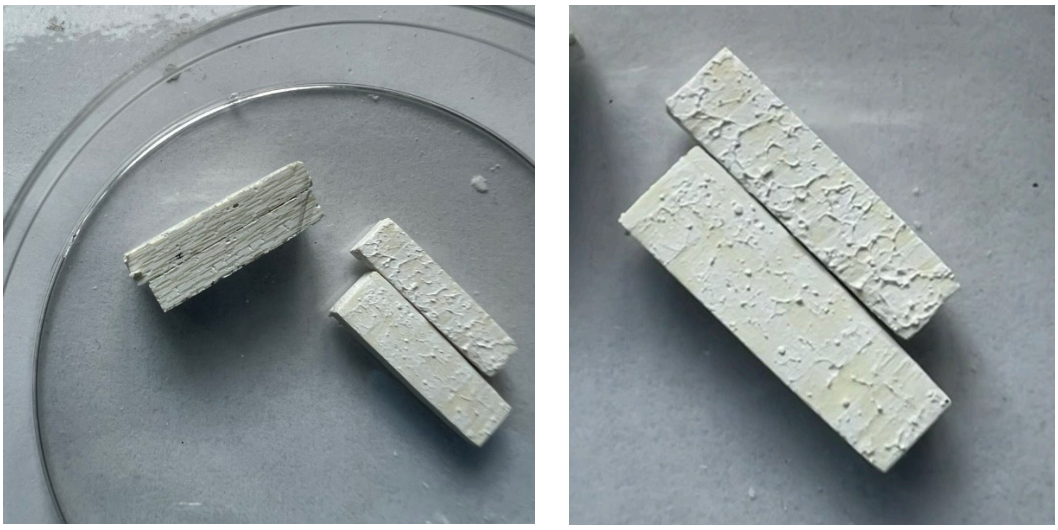

Figure 6-7 60wt. % after cut

Compared to the previous case, more continuity is observed between the two substrates. Although a lot of void spaces are still present, and apart from few zones in which the bridging of the two substrates is quite thick, the rest is composed by the typical hourglass shape (with the narrowing in the middle region) also observed in the lower filler content.

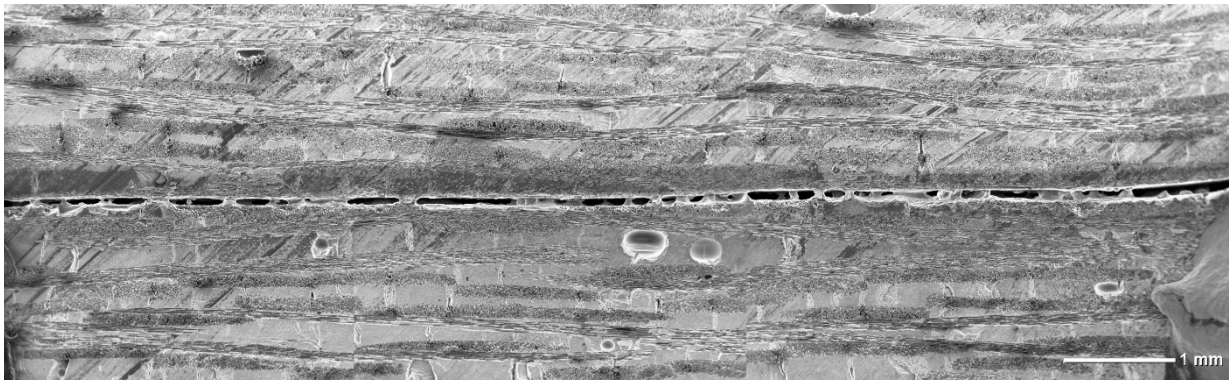

Figure 6-8 Full 60% joint

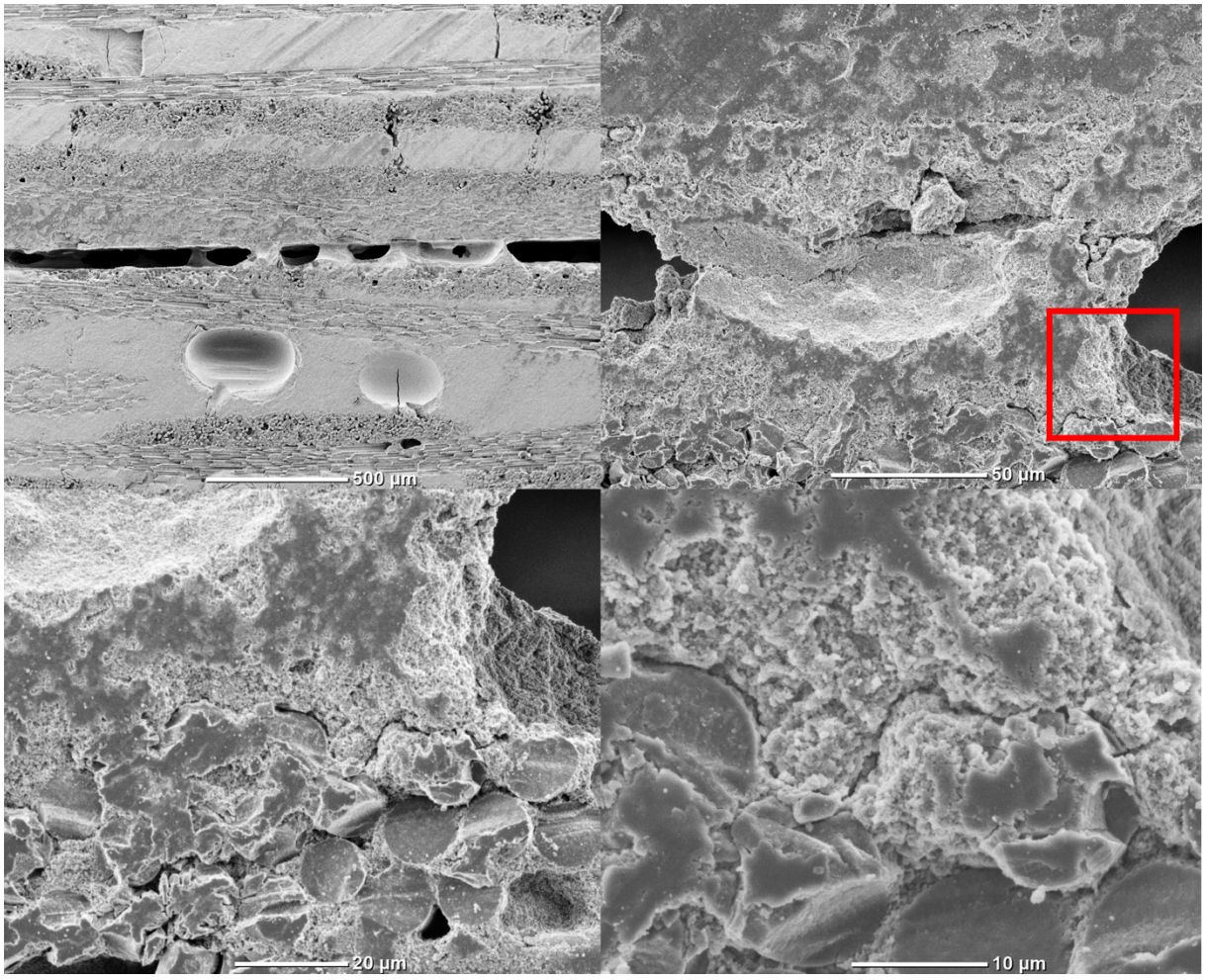

Figure 6-9 60wt.% joint continuous structure(left) progressively magnified

In fig. 9 a progressive magnification gives a better insight into the material structure, apart from the presence of some cracks, both the adhesion and the cohesion seem to be good. A perfect microstructure is not essential, also the provided OCMC as it

can be seen presents defects and cracks but still is able to withstand a considerable stress.

As it can be seen from the last picture, the space between the transversal section of the exposed fibers of the OCMC has been successfully infiltrated by the Al_2O_3 filled preceramic polymer.

Not satisfied with the results and seeing a big margin for improvements the suspension with the third value of filled powder was prepared.

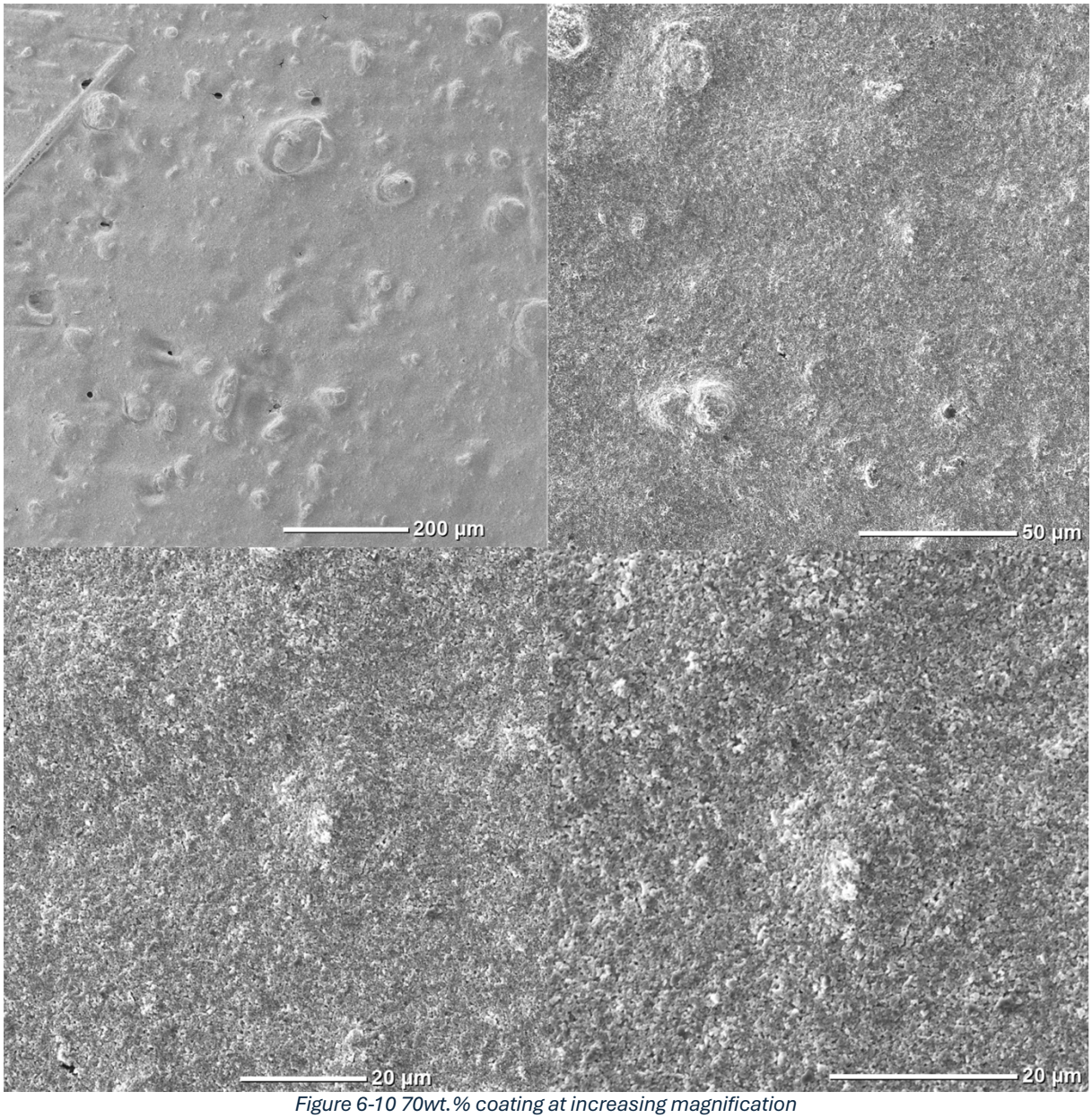

Figure 6-10 70wt.% coating at increasing magnification

From the top view pictures of the coating the difference from the previous coatings is hardly noticeable, this is due to the coating effectively resulting almost crack free even in the first, lowest filler concentration case. The first coating was performed by

using a coating spreader rod of 160 microns, meaning that the critical thickness was already higher in the first case. The application, since spreaders with higher thickness weren't available at the laboratory, proceeded for the successive percentages by spatula spreading. The effect of the increased concentration from literature should give an increase on the critical thickness but was not measured.

No visible cracks are present in the 70% samples where the thickness is comparable to the previous ones. even the on higher magnification ones.

The zone in which the coating gets thicker, corresponding to the ending of the cmc (between 200 and 300 micron thickness, precision related to the caliber used) cracks appear as shown in fig.11.

Moving to the joint sample, on the 70% big improvement were shown. The zones of continuity between the substrates are a lot more compared to the 50 and 60% samples.

What can be also noticed is that apart from the foreground structure most of the structure in the inside is not empty as observed in the lower concentration samples.

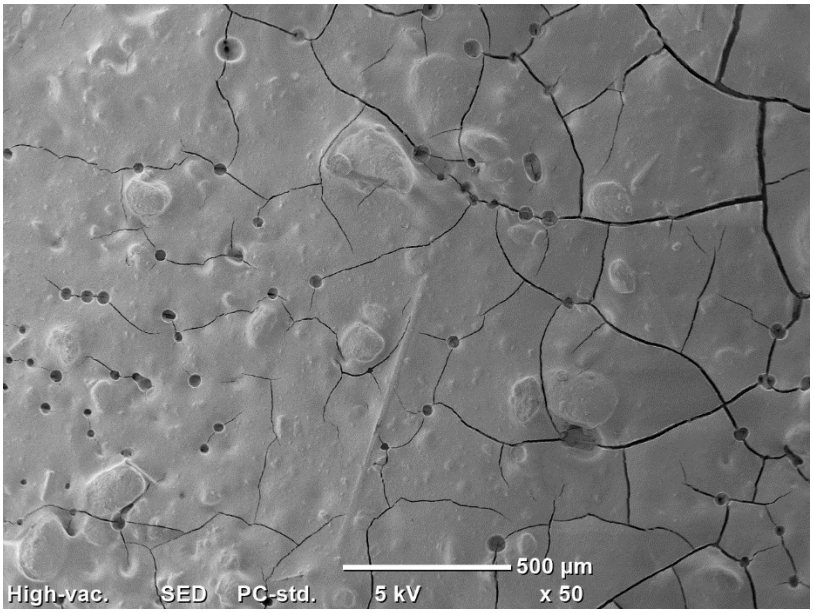

Figure 6-11 Presence of cracks on 70% coating sample

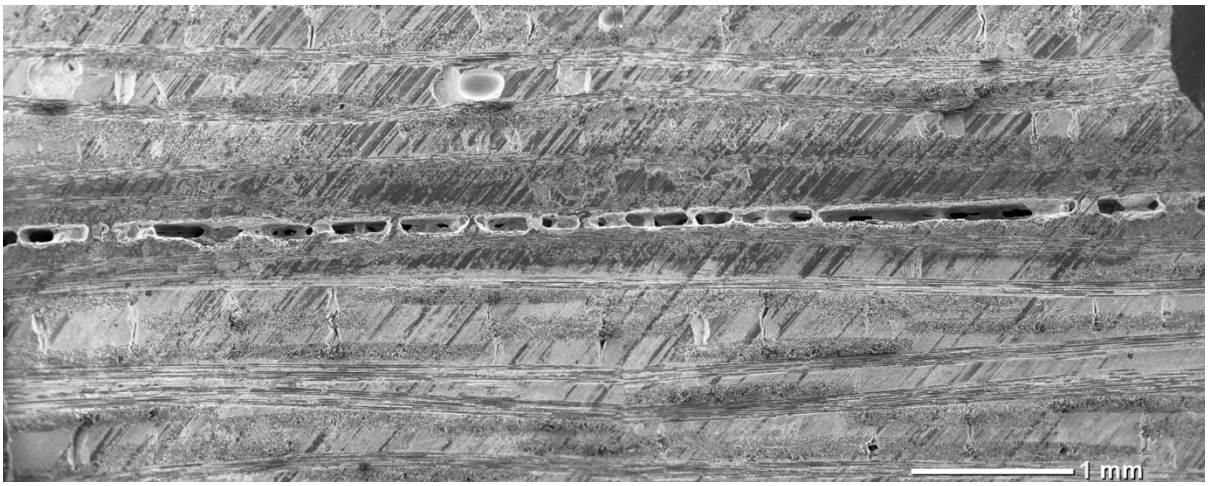

Figure 6-12 70wt. % joint sample full length

Higher magnification images reveal a more promising structure than anticipated. While the points of no connection on the section should be none to exploit the full potential of the material+fillers, what is positive is the full infiltration that is shown in the pictures below, it makes it impossible to distinguish the interface between the substrate and the joining material.

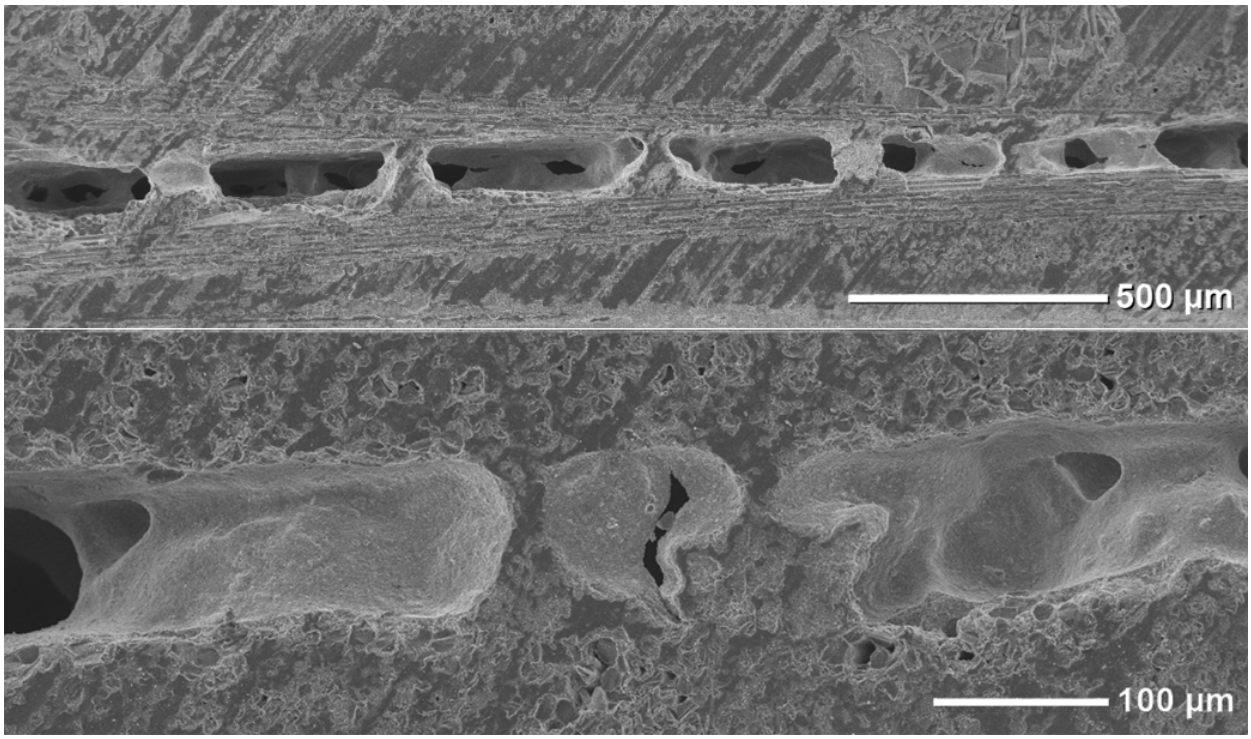

Figure 6-13 70wt.% joining sample at increasing magnification

Next the 80% samples were analysed, the coatings didn't show any difference from the previous ones and will not be shown. Instead, in the joint once again the increase in the percentage resulted in a lot more coverage of the joining material along the section observed.

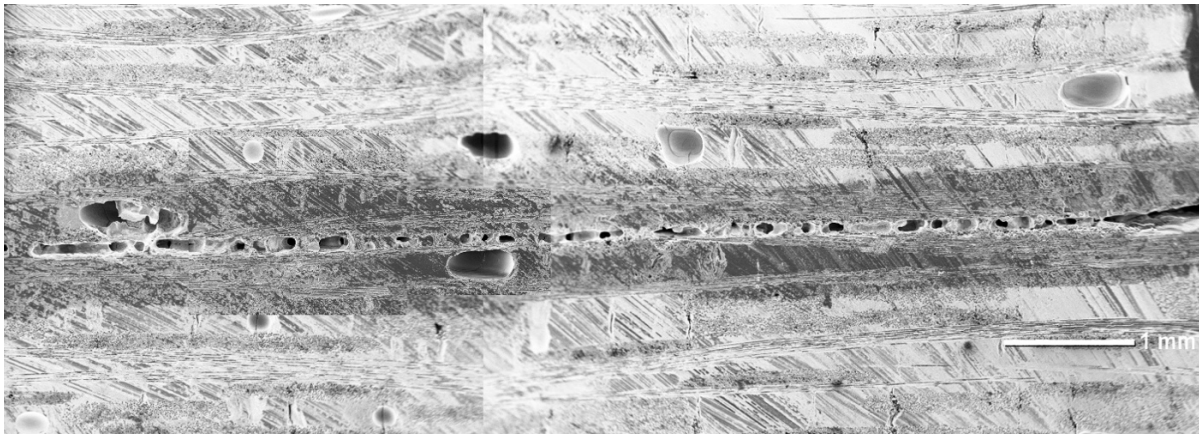

Figure 6-14 80wt. % joint sample full length

In most cases, the original surface of the CMC is no longer recognizable within the bridging structure between the substrates, as observed in the 70% samples. Although, the increase in particles resulted in an increase in brittleness, some cracks are showing compared to the previous one.

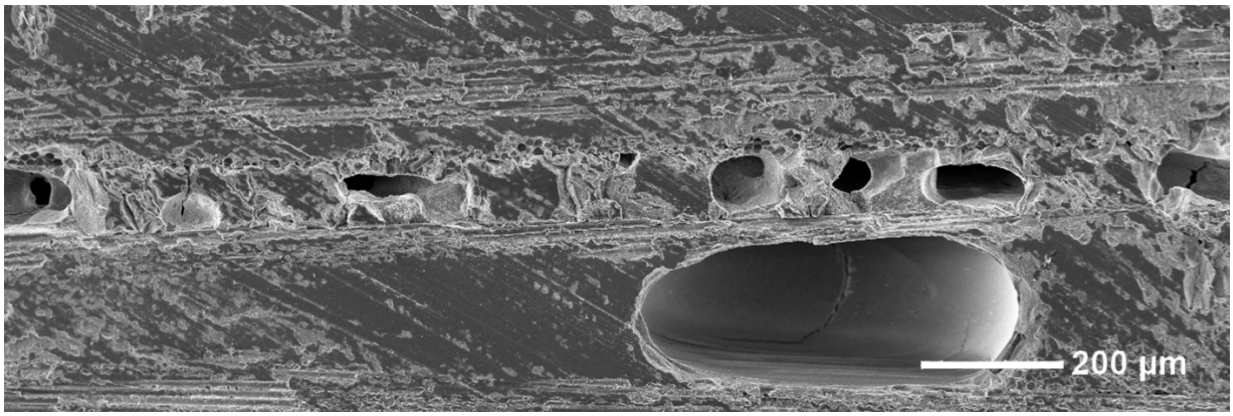

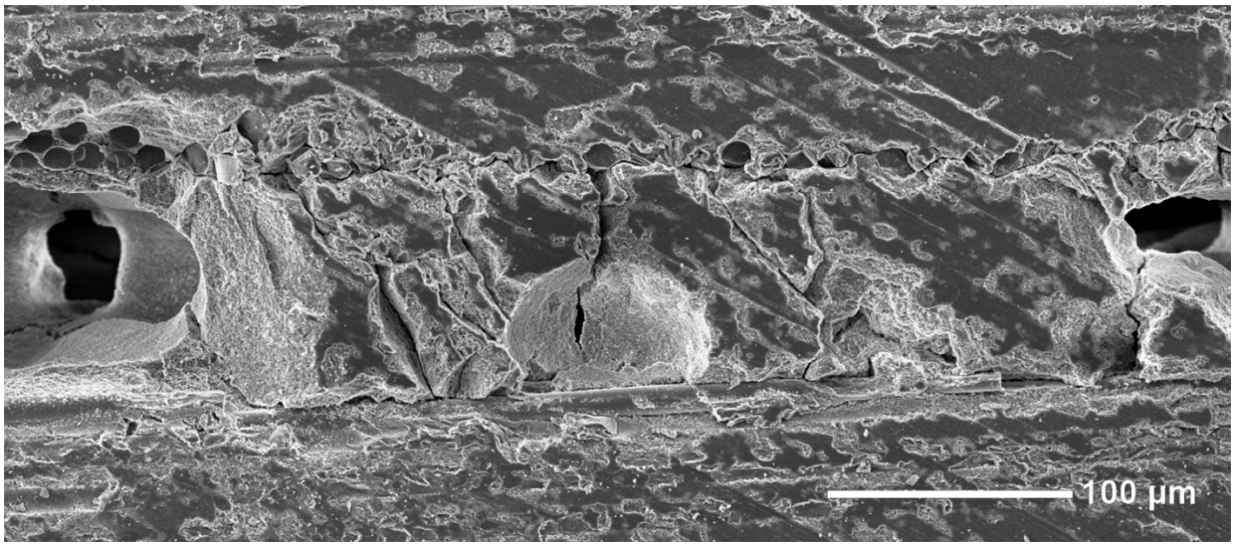

Figure 6-15 80wt.% joint at different magnifications

Looking at the higher magnifications, there seems to be a decreasing of the adhesion even if not noticeable in the less zoomed pictures. This drawback, could be related to the increase in viscosity due to the higher dispersion of powders, leading to a lower infiltration of the resin inside the material of the CMC. If this is related to the viscosity, going to higher values of viscosity so increasing again the concentration of dispersed powders, it would lead to an additional loss in adhesion.

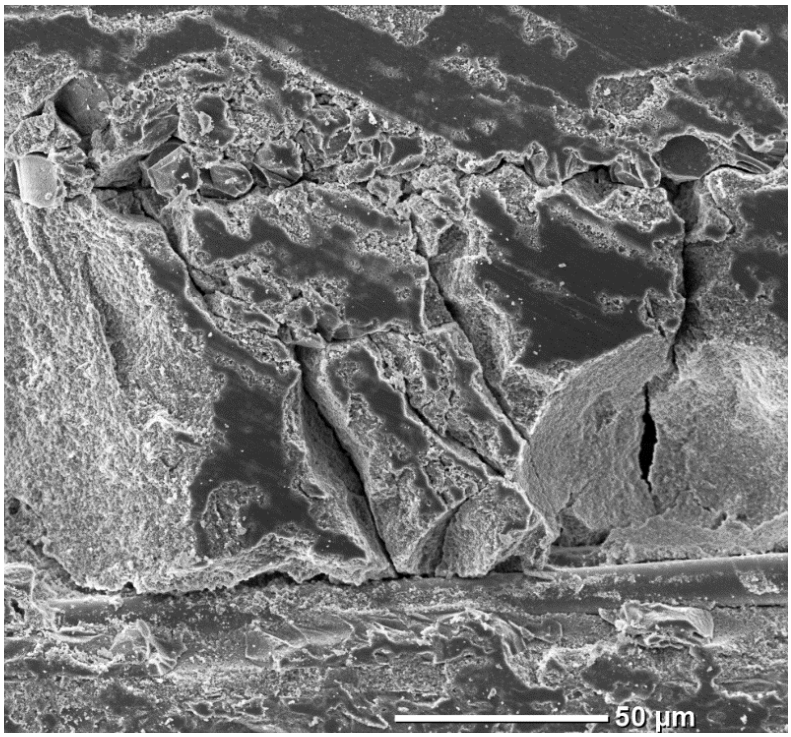

Figure 6-16 Some cracks showing in the 80wt.% sample at 500x magnification

The 90% samples, following the previous analysis, were prepared. The following image seem to confirm that the increase in viscosity resulting in a decrease of the resin infiltration and adhesion. The joint is composed by a material which seems almost separated from the CMC. The joining material density seems to be higher but little to no continuity between the material and the CMC is present.

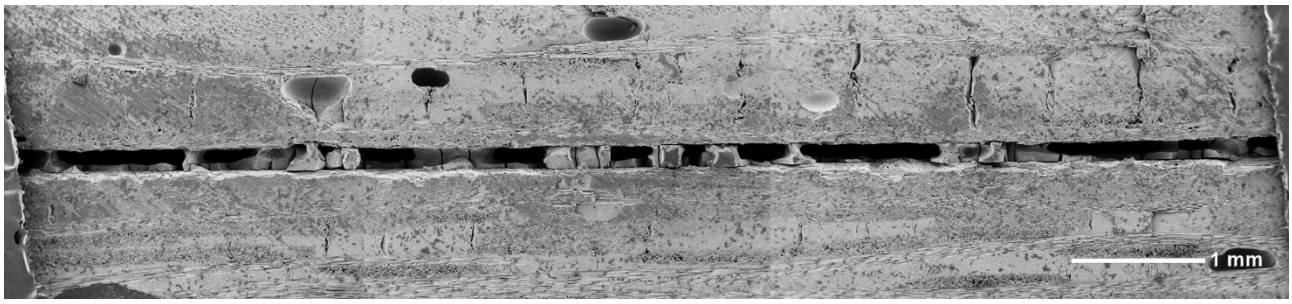

Figure 6-17 90wt.% sample full joint length

At higher magnification the phenomena is clearly visible, due to the worsening of the joint the peak in increase of strength following the incorporation of fillers described in literature will be assumed to be somewhere between the 70 and 80wt.% concentration.

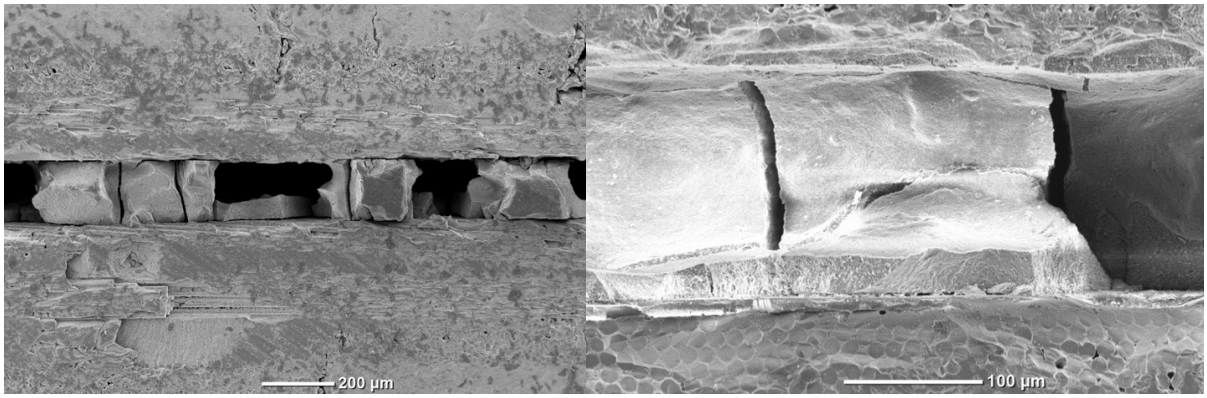

Figure 6-18 90wt.% sample at increasing magnification

6.1. Mechanical Tests

Once the morphological characterization of the samples was completed, the new samples using the two optimal filler concentrations (70% and 80%) identified in the previous chapter were prepared. These samples were then mechanically tested on the Zwick Roell Z050 coupled with the "Reversal cage" specimen grip.

For each filler concentration three equal samples were tested, on the 80% mixture the first specimen failed during the setup process, so it is not shown in the graph.

The test is a single lap offset; the testing speed is 0.5 mm/min. The area used to calculate the stress will be the design one so 12.5 mm x 25 mm. The results are reported in the following graph.

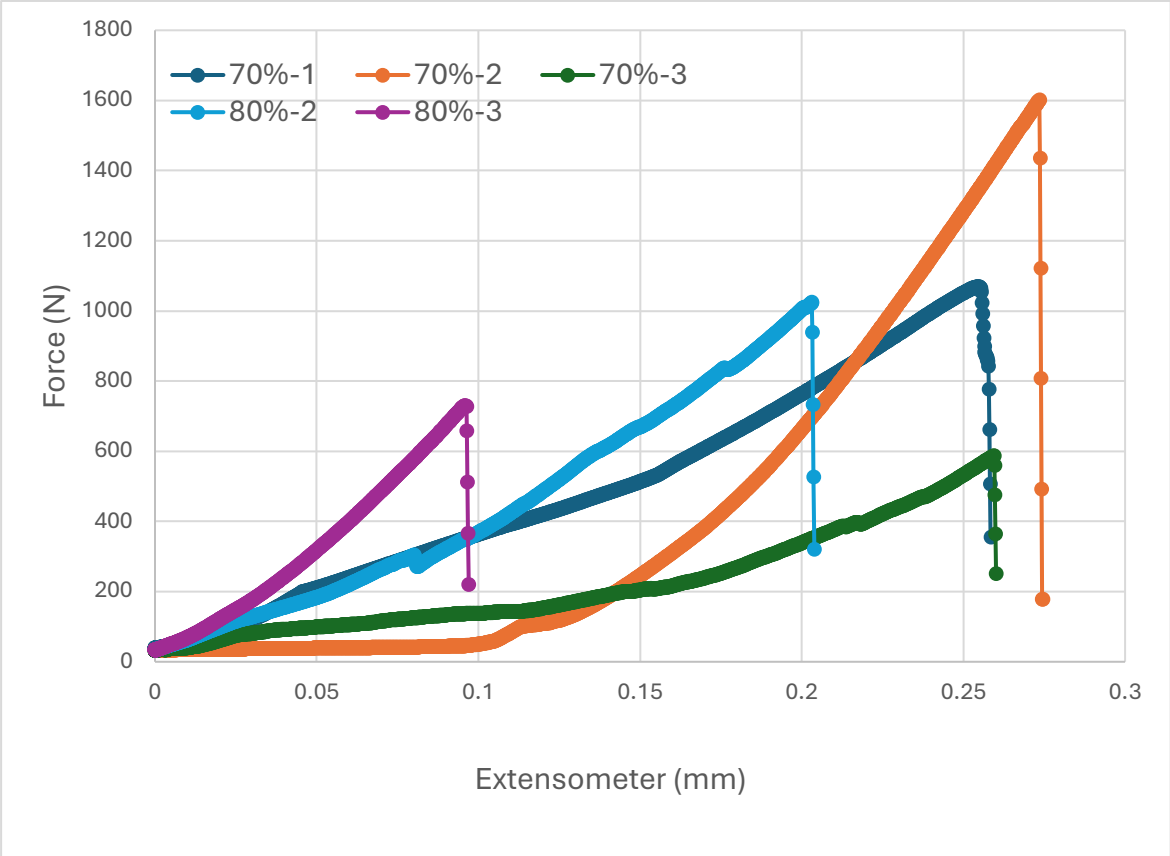

	Area	Max Force (N)	Max Stress (MPa)
80% sample	312,5	1025	3

70% sample	312,5	1603	5

Table 3 Sample maximum Force and Shear strength

After testing, a microscope analysis of the fracture surface was performed. The positive aspect is that in both cases (70% and 80%) the fracture was due to cohesion forces. Although, the problems related to the continuity being limited to a small part of the joining area resurfaced. In the following images can be noted that the surface fractured, involved in the joint is only a small percentage of the entire interested area. Interestingly, the failure modes differ between the two cases. In the left column (images A and C), the fracture occurs along a relatively planar surface, while in the right column, the fracture path is more irregular.

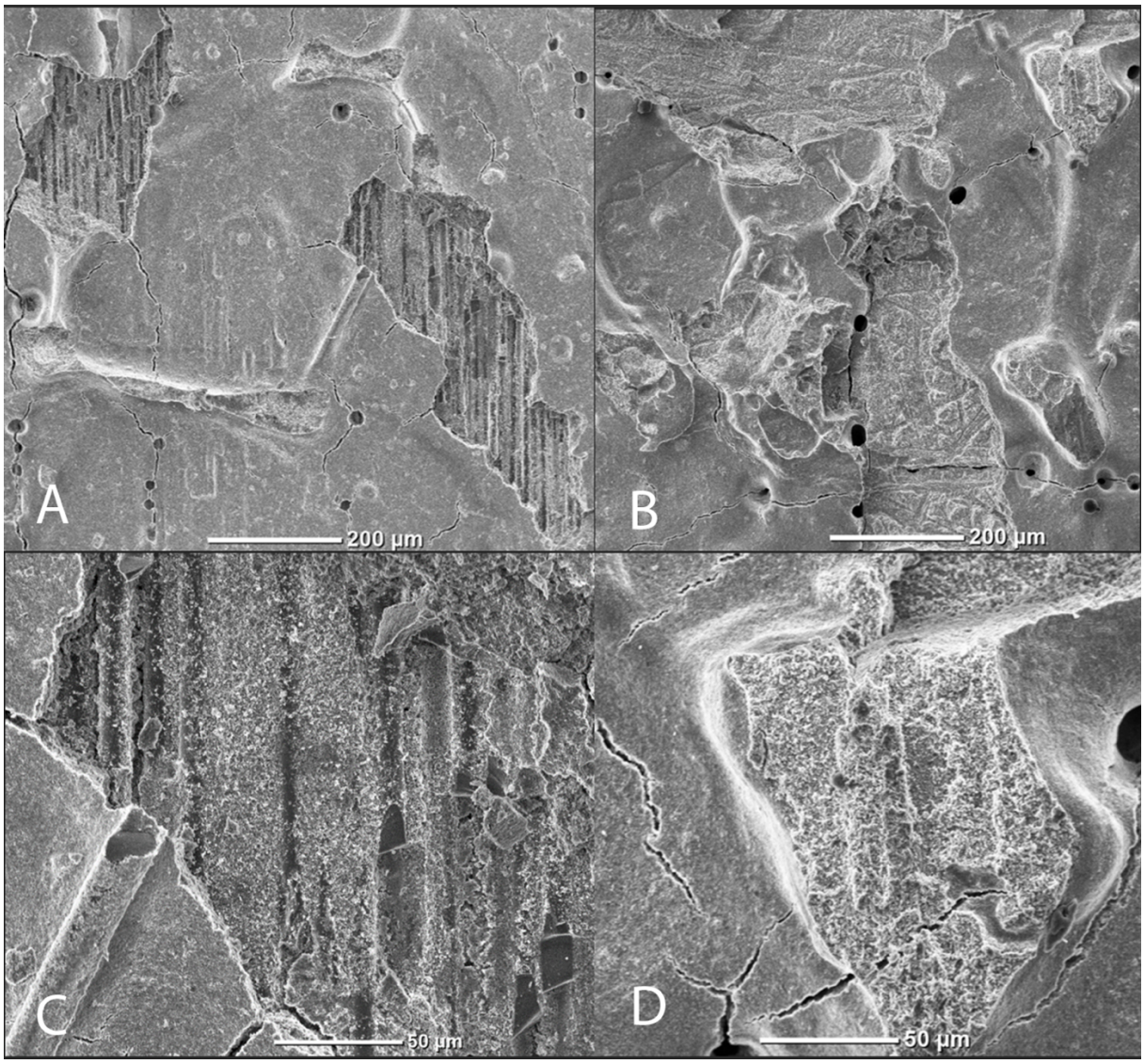

Figure 6-19 Microscope analysis of the fractured surfaces after mechanical test, A-C (70%) and B-D (80%) at 100x and 500x magnification

6.2. Impregnated fiber foils joint

To simulate the production process of the CMC and create a joint as similar as possible to the base material, the following experiment was conducted. Since dispersing fibers in the mixture was challenging, and their presence appeared low in the microscope images, the approach was to create a "sandwich" where the fiber foils are embedded in the polymeric precursor, as shown in the diagram.

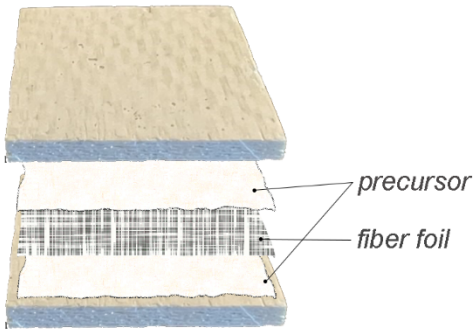

Figure 6-20 Joint experiment scheme

The joints were successfully prepared, enduring the thermal processes involved in ceramization. Subsequently, they were mechanically tested using the same methods as the other samples. The results are reported below, only 2 curves are shown, also in this case one of the samples broke during insertion in the cage:

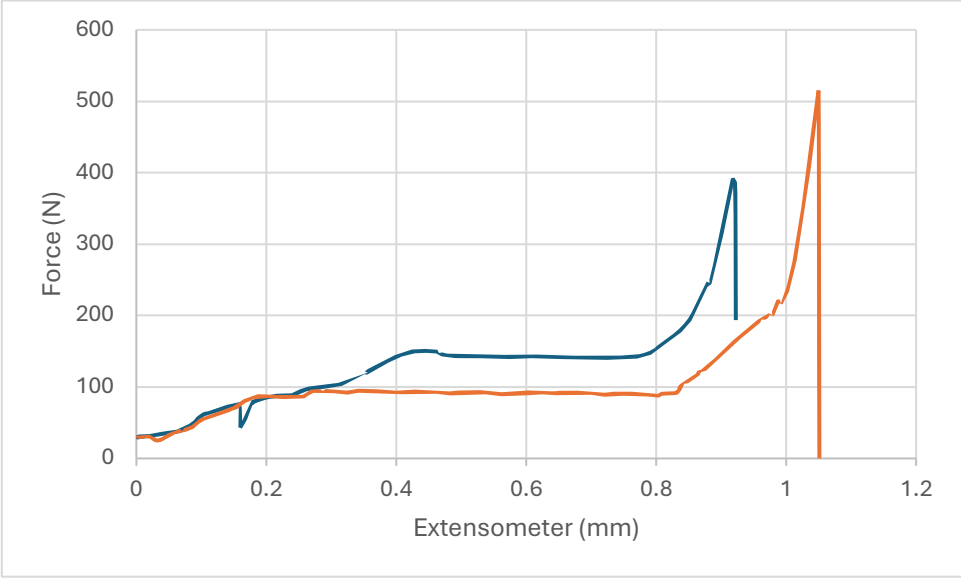

Sample #	Area (mm2)	Force(N)	Stress (MPa)
1	312,5	0	0
2	312,5	515.08	2
3	312,5	393.52	1

Table 4 Maximum force and shear strength for impregnated foil joint

The stress levels are well below the maximum registered with the previous method of joining but, unlike all the previous samples, the fracture did not result from breaking of the joining material. Instead, in both cases, there was a detachment of the material from the substrate, so the adhesion ended up being the problem here.

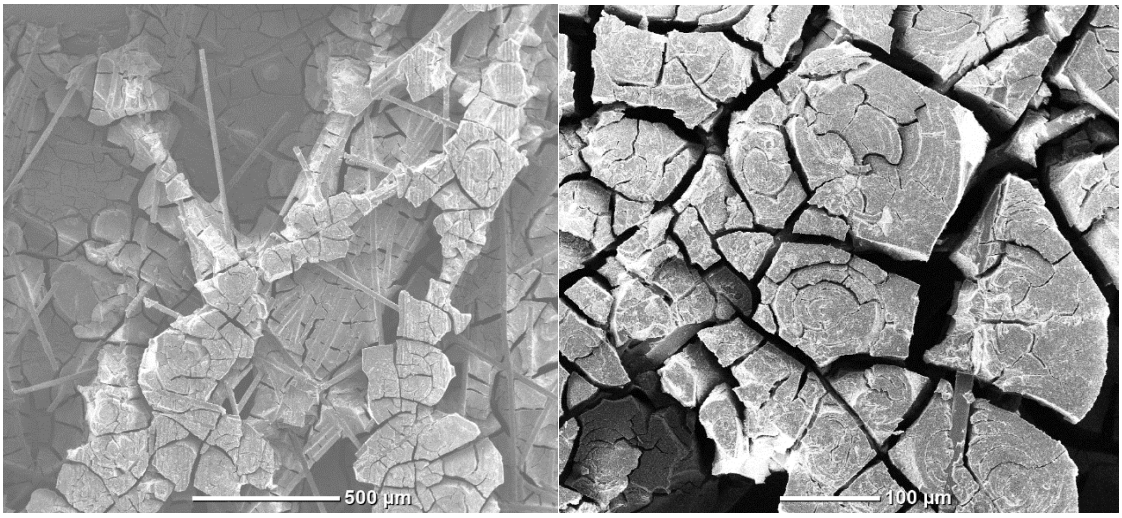

Figure 6-21 Impregnated fiber foils fracture surfaces after mechanical test

7 Conclusions

The increasing importance of Ceramic Matrix Composites (CMCs) in a wide range of high-performance applications, particularly in the energy, aerospace, and automotive industries, is driven by their ability to withstand extreme conditions that conventional materials cannot endure. These materials offer exceptional high-temperature stability, strength, and corrosion resistance, making them ideal for harsh environments.

Despite these advantages, the widespread adoption of CMCs is hindered by challenges in forming robust and reliable connections between the ceramic components. The development of effective joining techniques is therefore critical to enable their integration across a broader range of sectors and applications.

In the present work, a relatively novel method for fabricating ceramic joints using preceramic polymers was investigated. The approach involved a simple mixing and dispersion procedure using Durazane 1800, a commercial polysilazane, combined with alumina nanopowder and fiber inclusions. The prepared slurry subsequently underwent ceramic conversion through curing and pyrolysis. By varying the inclusion content, the quality of the joints was enhanced, with the primary objective being to determine the optimal amount of filler material needed to achieve maximum possible strength. Various joints with different percentages of fillers were produced, analyzed, and mechanically tested. The results showed that the maximum strength was achieved with a filler content corresponding to **70% of powder and 1% of fibers by weight of the resin**, which exhibited the highest shear strength in mechanical tests, about 5Mpa at ambient temperature, suggesting it as the optimal ratio for maximum joint performance.

However, despite substantial improvements, the fabricated joints remain far from being fully reliable, with low overall strength and considerable variation between samples with the same inclusion percentage. This indicates that other factors influencing consistency need to be addressed.

One critical observation was that increasing the particle content in the resin led to an increased incorporation of micro air bubbles into the preceramic slurry. These bubbles contributed to higher porosity in the final ceramic joints, which likely affected their strength. To minimize this issue, the use of a **vacuum disperser** could improve particle distribution

and reduce air bubble formation, thus enhancing the consistency and quality of the joints. Another possibility that can be investigated is the reduction of the porosity by re-infiltration of the preceramic polymer into the joint.

Additionally, the preliminary experiments with foil impregnation showed promising results. Though still at an early stage, this approach could improve the cohesion of the joining material above the strength values typically observed on the standard PDC joint. Enhancing adhesion through surface treatments could potentially lead to stronger and more reliable joints.

In conclusion, while the results offer valuable insights for improving ceramic joining technology, further research is required to optimize both the consistency and strength of the joints.

8 References

[1] M. Fischedick, J. Roy, A. Abdel-Aziz, A. Acquaye, J. Allwood, J.-P. Ceron, Y. Geng, H. Kheshgi, A. Lanza, D. Perczyk, L. Price, E. Santalla, C. Sheinbaum e K. Tanaka, «Industry. In: Climate Change 2014: Mitigation of Climate Change. Contribution of Working Group III to the Fifth Assessment Report of the Intergovernmental Panel on Climate Change.,» Cambridge University Press, 2014.

[2] M. Åhman, L. J. Nilsson e B. Johansson, «Global climate policy and deep decarbonization of energy-intensive industries. Climate Policy, 17(5),» 2016.

[3] J. M. Alwood, M. F. Ashby, T. G. Gutowski e E. Worrell, «Material efficiency: A white paper,» *Resources, Conservation and Recycling,* vol. 55, 2010.

[4] T. Konegger, O. Flores e J. Torrey, «Ceramics for Sustainable Energy Technologies with a Focus on Polymer Derived Ceramics,» in *Novel Combustion Concepts for Sustainable Energy Development* , 2014, pp. 501-533.

[5] D. O. Memon, «Symple Flying: What Are Ceramic-Matrix Composites & How Are They Used In Jet Engines?,» 2023. [Online]. Available: https://simpleflying.com/ceramic-matrix-composites-jet-engine-use-guide/.

[6] P. Wehrel, «Technological Level of CMC Components for Stationary Gas Turbines and Aero-Engines,» 2022.

[7] Q. Zeng e X. Chen, «Combustor tecnology of high temperature rise for aero engine,» 2023.

[8] P. Wehrel, R. Schöffler, C. Grunwitz, F. Carvalho, M. Plohr, J. Häßy e A. Petersen, «Performance and Emissions Benefits of Cooled Ceramic Matrix Composite Vanes for High-Pressure Turbines,» ASME. J. Eng. Gas Turbines Power, 2023.

[9] C. Spatz, N. Langhof, J. Schmidt e W. Krenkel, «CMC jackets for metallic pipes – A novel approach to prevent the creep deformation of thermo-mechanically loaded metals,» *Journal of the European Ceramic Society,* 2018.

[10] G. Gardiner, «Composites World:A new era for ceramic matrix composites,» 2023. [Online]. Available: https://www.compositesworld.com/articles/a-new-era-for-ceramic-matrix-composites.

[11] G. Aerospace, «GE Successfully Tests World's First Rotating Ceramic Matrix Composite Material for Next-Gen Combat Engine,» 2015. [Online]. Available: https://www.geaerospace.com/news/press-releases/defense-engines/ge-successfully-tests-worlds-first-rotating-ceramic-matrix-composite.

[12] A. Allison, «Joining Sub-Platform,» 2013. [Online]. Available: http://www.joining-platform.com/documents.html.

[13] E. H. P. e. al., «Ultrafast laser welding of ceramics,» *Science 365,* pp. 803-808, 2019.

[14] M. Ferraris e V. Casalegno, «Integration and Joining of Ceramic Matrix Composites,» in *Ceramic Matrix Composites: Materials, Modeling and Technology*, 2014, pp. 551-563.

[15] L. Snead, T. Nozawa, M. Ferraris, Y. Katoh, R. Shinavski e M. Sawan, «Silicon carbide composites as fusion power reactor structural materials,» *Journal of Nuclear Materials,* vol. 417, pp. 330-339, 2011.

[16] J. Zhang, Y. Yan, P. Li, B. Wang, P. Wang, Z. Zhong, J. Lin, J. Cao e J. Qi., «Unconventional joining techniques of ceramics by rapid heat sources: A review,» *Journal of the European Ceramic Society,* vol. 43, n. 14, pp. 5748-5762, 2023.

[17] M. Salvo, S. Rizzo, V. Casalegno, K. Handrick e M. Ferraris, «Shear and Bending Strength of SiC/SiC Joined by a Modified Commercial Adhesive,» *Int. J. Appl. Ceram. Technol.,* vol. 9, pp. 778-785, 2012.

[18] W. Lippmann, J. Knorr, R. Wolf, R. Rasper, H. Exner, A. Reinecke, M. Nieher e R. Schreiber, «Laser joining of silicon carbide—a new technology for ultra-high temperature resistant joints,» *Nuclear Engineering and Design,* vol. 231, pp. 151-161, 2004.

[19] D. King, J. Watts, K. Cissel, A. Kadhim, G. Hilmas e W. Fahrenholtz, «Solidification of welded SiC–ZrB2–ZrC ceramics,» *J. Am. Ceram. Soc.,* vol. 101, n. 9, pp. 4431-4439, 2018.

[20] Y. Zhang, J. Wu, Y. Zhou, X. Xu, K. Tian e Y. Liu, «Thermal shock resistance and oxidation resistance of MgAl2O4–Si3N4 ceramics for solar thermal absorber: the effects of TiO2 additive content,» *Ceram. Int.,* vol. 47, n. 17, pp. 25081-25088, 2021.

[21] D. Yushin, A. Smirnov, N. Solis Pinargote, P. Peretyagin e R. Torrecillas, «Modeling Process of Spark Plasma Sintering of Powder Materials by Finite Element Method,» *Materials Science Forum,* vol. 834, pp. 41-50, 2015.

[22] E. Y. Bormashenko, «Wetting of Real Surfaces,» *De Gruyter Studies in Mathematical Physics Series,* vol. 19, n. 1, 2013.

[23] «Johnson Matthey,» [Online]. Available: https://matthey.com/en/metal-joining.

[24] M. S. a. R. Asthana., «Brazing of advanced ceramic composites: issues and challenges,» *Ceram. Trans,* vol. 198, pp. 9-14, 2007.

[25] M. Singh., « Design, fabrication and characterization of high temperature joints in ceramic composites,» *Key Eng. Mat,* vol. 415, p. 164–165, 1999.

[26] M. Ferraris, S. De la Pierr, Y. Akram, C. Steinborn, G. Puchas e W. Krenkel, «High temperature creep behaviour of glass-ceramic joined Nextel 610™/Al2O3-ZrO2 composites,» *Journal of the European Ceramic Society,* vol. 42, n. 12, 2022.

[27] M. Singh, «Affordable, Robust Ceramic Joining Technology (ARCJoinT)». 1998.

[28] H. E. KHALIFA, C. P. DECK e C. A. BACK, «High durability joints between ceramic articles, and methods of making and using same». Brevetto US9132619B2, 2013.

[29] R. Riedel, G. Mera, R. Hauser e A. Klonczynski, «Silicon-Based Polymer-Derived Ceramics: Synthesis Properties and Applications-A Review,» *ournal of the Ceramic Society of Japan,* vol. 114, pp. 425-444, 2006.

[30] G. Barroso, Q. Li, R. K. Bordia e G. Motz, «Polymeric and ceramic silicon-based coatings – A review.,» *Journal of Materials Chemistry A.,* 2018.

[31] P. Colombo, G. Mera, R. Riedel e G. D. Sorarù, «Polymer-Derived Ceramics: 40 Years of Research and Innovation in Advanced Ceramics,» *ournal of the American Ceramic Society,* vol. 93, pp. 1805-1837, 2010.

[32] F. Kipping, «Organic Derivatives of Silicon. Saturated and Unsaturated Siliconhydrocarbons, Si4Ph8,» *J.Chem.Soc.,* vol. 119, pp. 830-847, 1921.

[33] H. ICHIKAWA, «Development of High Performance SiC Fibers Derived from Polycarbosilane Using Electron Beam Irradiation Curing-A Review,» *Journal of The Ceramic Society of Japan,* vol. 114, pp. 455-460, 2006.

[34] Zeigler, J. M. a. Fearon e F. W. G, «Silicon-Based PolymerScience, Advances in Chemistry Series,» *American Chemical Society,* vol. 224, 1990.

[35] M. Zeldin, Wynne e H. Allcock, «Inorganic and Organometallic Polymers, ACS Symposium Series,» *American Chemical Society,* vol. 360, 1988.

[36] F. Sarraf, S. Churakov e F. Clemens, «Preceramic Polymers for Additive Manufacturing of Silicate Ceramics. Polymers,» *Polymers,* vol. 15, n. 22, 2023.

[37] K. Okamura, «Ceramic fibres from polymer precursors,» *Composites,* vol. 18, p. 107–120, 1987.

[38] S. Yajima, Y. Hasegawa, K. Okamura e Matsuzawa, «Development of high tensile strength silicon carbide fibre using an organosilicon polymer precursor,» *Nature,* vol. 273, p. 525–527, 1978.

[39] Rocha, R. &. Greil, P. &. Bressiani, J. &. Bressiani e Ana., «Complex-Shaped Ceramic Composites Obtained by Machining Compact Polymer-Filler Mixtures,» *Materials Research-ibero-american Journal of Material,* vol. 8, 2005.

[40] Y.-W, K. a. C e B. Park, «Processing of Microcellular Preceramics UsingCarbon Dioxide,» *Comp. Sci. Tech,* vol. 63, p. 2371–2377, 2003.

[41] C. B. a. R. Riedel, «Rheological Investigations of a Polymeric Precursorfor Ceramic Materials: Experiments and Theoretical Modeling,» *J. Optoelectr.Adv. Mater.,* vol. 8, p. 561–567, 2006.

[42] «ceramicore,» [Online]. Available: http://www.ceramicore.com/.

[43] P. Greil, «Polymer Derived Engineering Ceramics,» *Adv. Eng. Mater.,* vol. 2, pp. 339-348, 2000.

[44] M. Labrousse, «Ex-polymer SiC Coatings with Al2O3 Particulates as Filler Materials,» 1993.

[45] Z. Z, B. RK e P. F., «Critical thickness of polymer-derived ceramic coatings with particulate fillers.,» *Int J Appl Ceram Technol,* p. 84–93, 2023.

[46] P. Greil, «Near Net Shape Manufacturing of Polymer Derived Ceramics,» *Journal of the European Ceramic Society,* vol. 18, n. 13, pp. 1905-1914, 1998.

[47] C. S. C. F. Sarraf F, «Preceramic Polymers for Additive Manufacturing of Silicate Ceramics,» *Polymers,* vol. 15, n. 22, 2023.

[48] R. Harshe, C. Balan e a. R. Riedel, «Amorphous Si(Al)OC Ceramic from Polysiloxanes:Bulk Ceramic Processing, Crystallization Behavior and Applications,» *J. Eur. Ceram. Soc,* vol. 24, pp. 3471-3482, 2004.

[49] N. J. a. F. Aldinger, «Fabrication and Characterization of Fully Dense Si–C–N Ceramics from a Poly(ureamethylvinyl)Silazane Precursor,» *J. Eur. Ceram. Soc.,* vol. 29, pp. 163-173, 2009.

[50] T. Isoda, H. Kaya, H. Nishii, O. Funayama e T. S. a. Y. Tashiro, «Perhydropolysilazane precursors to silicon nitride ceramics,» *J. Inorg. Organomet.,* vol. 2, n. 1, pp. 151-160, 1992.

[51] F. I. Hurwitz, P. Heimann e S. C. F. a. D. M. Hembree, «Characterization of the pyrolytic conversion of polysilsesquioxanes to silicon oxycarbides,» *Journal of Materials Science,* vol. 28, n. 24, pp. 6622-6630, 1993.

[52] P. Greil, «Active-Filler-Controlled Pyrolysis of Preceramic Polymers,» *J. Am. Ceram. Soc.,* vol. 78, n. 4, 1995.

[53] R. Riedel, A. Kienzle, W. Dressler, L. Ruwisch e J. B. a. F. Aldinger, «A silicoboron carbonitride ceramic stable to 2,000°C,» *Nature,* vol. 382, n. 796, 1996.

[54] J.He, M. Song, K.Chen, D.Kan e M.Zhu, «Polymer-Derived Ceramics Technology: Characteristics, Procedure, Product Structures, and Properties, and development of the Technology in High Entropy Ceramics,» *Crystals,* vol. 12, n. 9, 2022.

[55] R. P. Chaudhary, C. Parameswaran, M. Idrees, A. S. Rasaki, C. Liu, Z. Chen e P. Colombo, «Additive manufacturing of polymer-derived ceramics: Materials, technologies, properties and potential applications,» *Progress in Materials Science,* vol. 128, 2022.

[56] F. Zok, «Developments in Oxide Fiber Composites,» *Journal of the American Ceramic Society,* vol. 89, pp. 3309-3324, 2006.

[57] G. Puchas, S. Möckel e W. Krenkel, «Novel prepreg manufacturing process for oxide fiber composites,» *Journal of the European Ceramic Society,* vol. 40, n. 15, pp. 5930-5941.

[58] M. KGaA. [Online]. Available: https://www.merckgroup.com/en/brands/pm/durazane/durazane-product-finder.html?p=1.

[59] A. Qazzazie-Hauser, K. Honnef e T. Hanemann, «Crosslinking Behavior of UV-Cured Polyorganosilazane as Polymer-Derived Ceramic Precursor in Ambient and Nitrogen Atmosphere,» *Polymers,* vol. 13, 2021.

[60] R. Chavez, E. Ionescu, C. Balan, C. Fasel e R. Riedel, «Effect of ambient atmosphere on crosslinking of polysilazanes,» *J. Appl. Polym. Sci,* vol. 119, pp. 794-802, 2011.

[61] M. L. Leite, G. Barroso, M. Parchovianský, D. Galusek, E. Ionescu, W. Krenkel e G. Motz, «Synthesis and characterization of yttrium and ytterbium silicates from their

oxides and an oligosilazane by the PDC route for coating applications to protect Si3N4 in hot gas environments,,» *Journal of the European Ceramic Society,* vol. 37, n. 16, pp. 5177-5191, 2017.

[62] G. Motz, T. Schmalz, S. Traßl e R. Kempe, Oxidation behavior of SiCN materials. Design, processing and properties of ceramic materials from preceramic precursors, 2011.

[63] G. Barroso, M. Döring, A. Horcher, A. Kienzle e G. Motz, «Polysilazane-Based Coatings with Anti-Adherent Properties for Easy Release of Plastics and Composites from Metal Molds,» *Adv. Mater. Interfaces,* vol. 7, 2020.

[64] Almatis, «Reactive and Calcined Aluminas for Ceramics,» [Online]. Available: https://www.almatis.com/en/media/862/download?inline=1.

[65] 3M, «3M™ Nextel™ Ceramic fibers and textiles,» [Online]. Available: https://multimedia.3m.com/mws/media/1327055O/3m-nextel-technical-reference-guide.pdf.

[66] A. &. S. W. &. L. J. &. D. R. &. O. M. Tontisakis, «Evaluation of surface finish technology in the manufacture of Oxide-Oxide ceramic matrix composites.,» *Ceramics International.,* vol. 47, 2020.

[67] G. P. Marino, S. De La Pierre, M. Salvo, M. Ferraris e A. D. Lantada, «Modelling, additive layer manufacturing and testing of interlocking structures for joined components,» *Scientific Record,* 2022.